Theoretical Modelling, Design, and Testing of a Novel Low Pressure Spray Sprinkler for Travelling Agricultural Irrigation Systems

by
Michael John Ian Budler

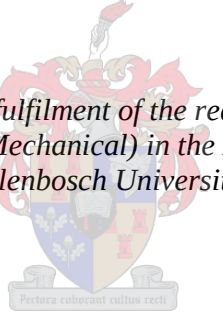

Thesis presented in partial fulfilment of the requirements for the degree of Master of Engineering (Mechanical) in the Faculty of Engineering at Stellenbosch University

Supervisor: Prof Hanno Carl Rudolf Reuter
Co-supervisor: Dr Michael Owen
Co-supervisor: Dr Eduard Hoffman

December 2017

DECLARATION

By submitting this thesis electronically, I declare that the entirety of the work contained therein is my own, original work, that I am the sole author thereof (save to the extent explicitly otherwise stated), that reproduction and publication thereof by Stellenbosch University will not infringe any third party rights and that I have not previously in its entirety or in part submitted it for obtaining any qualification.

Date: December 2017

Abstract

A novel, overhead spray sprinkler concept is developed for travelling irrigation systems including centre pivot and linear-move systems. The Powasave sprinkler is a low pressure spray sprinkler with the potential to reduce operating pressures in travelling irrigation systems by up to 35%, and produce a uniform spray droplet size. The core components of the Powasave sprinkler, and their functions, were discussed in this study and a theoretical model developed to simulate the spray characteristics beneath the sprinkler. The model was used to design a sprinkler prototype that was manufactured and installed on a centre pivot system in the Western Cape.

The application uniformity of the Powasave sprinkler prototype was evaluated in a series of distribution tests conducted beneath the centre pivot system. The distribution uniformity (DU) and coefficient of uniformity (CU) beneath the sprinkler prototype was evaluated and compared against two commercial spray sprinklers also installed on the centre pivot system: the Nelson D3000 Sprayhead sprinkler, and the S3000 Spinner sprinkler.

A comparison of the results show the Powasave sprinkler having a poor uniformity relative to the Sprayhead and Spinner sprinklers. Where the CU beneath the Powasave sprinkler was measured to be 64%, the CU measured beneath the Sprayhead and Spinner sprinklers were 77% and 94% respectively. Adjustments to the Powasave sprinkler design were recommended to improve the application uniformity to be more competitive with that of the Nelson sprinklers. Although the Powasave sprinkler concept has the potential to reduce operating pressure in travelling irrigation systems, it does not yet have the application uniformity attainable by the commercial spray sprinklers used in the industry.

Samevatting

'n Nuwe oorhoofse spuitbesproeier konsep word tans ontwikkel vir bewegende besproeiingstelsels, insluitende spilpunt- en lineêr-bewegende stelsels. Die Powasave besproeier is 'n laedruk spuitbesproeier wat die potensiaal het om operasionele druk in bewegende besproeiingstelsels tot en met 35% te verlaag, asook om 'n eenvormige sproei druppelgrootte te skep. Die kern komponente van die Powasave besproeier en hul funksies word in hierdie studie bespreek. 'n Teoretiese model is ontwikkel om die eienskappe van die sproeiwater onder die besproeier te simuleer. Hierdie model is gebruik om 'n prototipe te ontwerp vir 'n besproeier wat vervaardig en geïnstalleer is op 'n spilpuntstelsel in die Wes-Kaap.

Die toedieningseenvormigheid van die Powasave besproeier prototipe is geëvalueer met behulp van 'n reeks verspreidingstoetse wat onder die spilpuntstelsel uitgevoer is. Die toedieningseenvormigheid en koëffisiënt van eenvormigheid onder die besproeier prototipe is geëvalueer en vergelyk met twee kommersieel beskikbare besproeiers wat ook op die spilpuntstelsel geïnstalleer is: die Nelson D3000 *Sprayhead* besproeier en die S3000 *Spinner* besproeier.

'n Vergelyking van die resultate toon dat die Powasave besproeier oor swak eenvormigheid beskik in verhouding tot die Sprayhead en Spinner besproeiers. Die koëffisiënt van eenvormigheid, gemeet onder die Powasave besproeier, was 64%, waarteenoor die koëffisiënt van eenvormigheid, soos gemeet onder die Sprayhead en Spinner besproeiers, onderskeidelik 77% en 94% was. Die aanbeveling is derhalwe dat die ontwerp van die Powasave besproeier aangepas word om die toedieningseenvormigheid te verbeter en sodoende meer kompeterend te wees met die Nelson besproeiers. Alhoewel die Powasave besproeier konsep die potensiaal het om operasionele druk te verlaag in bewegende besproeiingstelsels, beskik dit nog nie oor die toedieningseenvormigheid wat bereik kan word deur die kommersiële besproeiers in die bedryf nie.

Acknowledgements

I would like to thank the following people who made this study possible:

My parents, for the love and support, and the opportunity to achieve what I have

My supervisor, Prof Reuter, for the wealth of knowledge you so freely gave throughout the project.

My co-supervisor, Dr Hoffman, for so willingly providing your expertise and the use of your equipment in the field work

My co-supervisor, Dr Owen, for the useful feedback and direction provided in the last few days of the study

The mechanical engineering workshop personal, for the manufacturing and advice

The Elsenburg agricultural research farm for their assistance in the field work and affording us the opportunity to make use of their equipment.

Table of contents

List of figures

List of tables

Nomenclature

A	area
C_d	drag coefficient
d	droplet diameter
d_{32}	Sauter mean droplet diameter
E_a	application efficiency
E_c	conveyance efficiency
ET	crop water use
E_{wu}	water use efficiency
F	force
G_w	water mass flux
g	gravitational acceleration
h_L	pressure head loss
ΔH	differential pressure head
k	number of virtual compartments along a spray plane
k_f	friction loss coefficient
k_o	orifice loss coefficient
k_{vc}	contraction coefficient
m	mass
n	number of collectors in control area or distribution test
n_{or}	number of orifice nozzles in an orifice set
n_{os}	number of orifice sets along a sprinkler pipe
P	pressure
r	radial direction
Re	Reynolds number
S	distance or displacement
S_{sc}	scatter bandwidth of an orifice nozzle trajectory stream
S_{sp}	length of spray plane
t	time
t_s	timer setting
t_w	orifice nozzle wall thickness
Δt	differential time period
u	velocity
V	volume
$\overline{\mathrm{V}}$	average volume
$\dot{\mathrm{V}}$	volume flow rate
Y_g	crop yield per unit area
z	elevation

Subscripts:

a	air
b	buoyancy

c	collector
d	droplet
dr	drag
f	field
g	gravity
irr	irrigation/irrigated
LQ	lowest quarter
max	maximum
nel	Nelson sprinkler
or	orifice nozzle
os	orifice set
ps	Powasave sprinkler
rz	plant root zone
res	resultant
s	source
sr	spray range
st	stop
sw	spray width
t	total
tr	travel
vc	virtual compartment
w	water

Greek Symbols

α	orifice nozzle trajectory angle
ε	volume flow rate fraction
θ	circumferential direction
μ	dynamic viscosity
ρ	density
ζ	ratio of pivot travel velocity and orifice set outlet circumferential spray width

Abbreviations

AAD	average application depth
AAR	average application rate
AR	application rate
CU	Coefficient of uniformity
DU	distribution uniformity
IAR	instantaneous application rate
LEPA	low energy precision application
LQD	lowest quarter application depth
OSM	orifice set model
SDTM	single droplet trajectory model

1 Introduction

1.1 Overview

Agriculture is an important primary activity in the modern economy. With a growing global population, there is increased pressure on the agricultural sector to produce more food to meet the global demand. Developing technologies in the agricultural sector have enabled the large scale production of food, and allowed farmers to radically improve crop yields. Advances in irrigation technology in particular, have played a pivotal role in facilitating these increased yields.

Modern precision irrigation systems like the centre pivot system, linear-move irrigation system, and drip irrigation system have largely replaced the conventional irrigation methods, which were labour intensive and water inefficient. Today, one of the more popular overhead irrigation systems used in the industry is the centre pivot system. The centre pivot is a reliable, automated irrigation system capable of irrigating large areas with a high application uniformity. It is water efficient and not labour intensive.

The purpose of this document is to investigate the application uniformity of a novel, low pressure spray sprinkler concept designed to be used on centre pivot irrigation systems. The new sprinkler concept, called Powasave, has the potential to reduce operating pressures in the centre pivot system while simultaneously producing a more uniform water droplet, and spray distribution.

1.2 Background

The Powasave sprinkler concept was developed at Stellenbosch University, and originated from research conducted by Roux (2012) that looked to improve the efficiency of heat transfer in cooling tower systems. The original spray sprinkler concept, on which the Powasave sprinkler is based, was proposed by Roux (2012) as an alternative solution to the existing spray sprinklers used in cooling towers. The primary issues that Roux (2012) identified with the existing spray sprinklers were as follows: (1) the existing spray sprinklers produced a non-uniform application of water across the packing fill in the cooling tower as a result of the overlapping circular spray zones of consecutive spray sprinklers; (2) the existing spray sprinklers produced a large droplet size distribution, with very small droplets being swept away by the updraft of air through the tower; and (3) the sprinklers required a relatively large operating pressure to function optimally. All three these factors impacted on the efficiency of heat transfer in the cooling tower system.

To address these issues, Roux (2012) introduced a novel sprinkler concept that he proposed could provide a near uniform water distribution, required less operating pressure, and produced a more uniform droplet size. In addition, the spray zone of the sprinkler was rectangular, and therefore no overlapping of consecutive spray sprinklers was necessary to achieve a uniform water distribution.

The proposed sprinkler concept comprised a length of pipe into which holes were carefully machined with specific diameters and orientations on the pipe circumference. The volume flow rate and spray distribution profiles of the sprinkler

could be manipulated by adjusting the diameters of the holes, and the trajectory angles relative to the horizontal. Furthermore, the spray characteristics of a jet-stream of water emitted from an orifice are well documented, and can be modelled using fluid dynamic relations.

The sprinkler concept proposed by Roux (2012) was then adapted by Budler (2014) to fit travelling irrigation systems; in particular, the centre pivot irrigation system. Centre pivot irrigation systems, like cooling tower systems, require a uniform application of water beneath the sprinkler package. In addition, spray sprinklers with a large droplet size distribution are susceptible to wind drift and evaporation losses, and may perpetuate soil surface crusting. A more uniform droplet size would mitigate these effects. The reduced operating pressures of the sprinkler concept would also reduce the pumping costs associated with irrigation.

A feasibility study was conducted by Budler (2014) in which a theoretical model of the adapted sprinkler concept was developed, and used to simulate the composite application rates beneath the sprinklers, the kinetic energies of the sprinkler droplets, the composite specific powers, and the operating power requirements of a centre pivot system fitted with a sprinkler package consisting of the adapted sprinkler concept. These parameters where then compared against those of commercial spray sprinklers used on centre pivot systems. It was concluded that the sprinkler concept had the potential to perform as well as the commercial spray sprinklers for the parameters investigated; and would do so at a reduced operating pressure.

Hence, the Powasave sprinkler concept is born. Powasave is now a patent pending overhead spray sprinkler designed to be used on overhead travelling irrigation systems (Patent application number: 2014/08443). This paper looks to build on the work by Budler (2014) in validating the Powasave sprinkler as a viable overhead spray sprinkler concept to be used on travelling irrigation systems. This will be achieved by manufacturing a number of Powasave sprinkler prototypes and evaluating their water distribution uniformity while operating in the field installed on a working centre pivot system. The sprinklers' performance will be compared against other commercial sprinklers operating on the same centre pivot system, under the same field conditions.

1.3 Motivation

Fresh water is increasingly becoming more of a valuable commodity. With increasing pressure on fresh water reserves, consumers are forced to use water more efficiently. The agricultural industry is the single largest consumer of fresh water, responsible for up to 87% of the world's annual fresh water consumption. It is therefore a responsibility of the industry to use this water as efficiently as possible.

By reducing water losses, and improving application uniformities of centre pivot irrigation systems, there is enormous potential to save significant amounts of water. Moreover, more efficient irrigation systems will allow farmers to better irrigate crops, utilise limited fresh water reserves more sparingly, and potentially increase crop yields off the same amount of water. Not only are there huge

environmental incentives to improve the efficiency of irrigation systems, but also economic incentives that will reflect in the bottom line of the industry.

1.4 Objectives

The objectives of this investigation are presented as follows:

- Develop a theoretical model to simulate the flow rate and distribution profile of a Powasave sprinkler.
- Use the model to design seven Powasave sprinkler prototypes that will replace seven commercial sprinklers on an existing centre pivot system.
- Measure the water distribution uniformity beneath the Powasave sprinklers while operating on the centre pivot system in the field, and compare the results with two commercial spray sprinklers also installed on the centre pivot system.

1.5 Study outline

The study will begin with a brief overview of centre pivot irrigation systems and their operation in Chapter 2. Two commercial spray sprinklers, the Nelson Sprayhead sprinkler and Spinner sprinkler, are presented and briefly discussed. These two sprinklers are used as the comparisons against which the performance of the Powasave sprinkler is compared.

The relevant literature is then presented with respect to the evaluation of the distribution uniformity (DU) and coefficient of uniformity (CU) beneath a spray sprinkler, or sprinkler package installed on a centre pivot system. These efficiency indicators provide a measure of the application uniformity beneath a spray sprinkler.

In Chapter 3, the Powasave sprinkler concept is presented, and each component of the sprinkler is discussed as it pertains to centre pivot systems. In chapter 4, the Powasave sprinkler model is developed which is used to design seven sprinkler prototypes for specific operating requirements on a centre pivot system.

Chapter 5 presents the experimental work; which details the water distribution measurements taken to evaluate the DU and CU beneath the different sprinklers. Details of the manufactured Powasave sprinkler prototypes and Nelson sprinklers installed on the test centre pivot system are discussed. The experimental procedures, apparatus, measuring equipment, and data processing procedures are all outlined.

Chapter 6 presents the results of the water distribution measurements, and the evaluated DU and CU indicators for each sprinkler type. Finally, Chapter 7 provides a discussion of the results, in which a number of observed phenomena are discussed regarding the distribution profiles measured beneath the different sprinklers, and the methods used to measure the distribution profiles.

2 Literature study

2.1 Overview of centre pivot irrigation systems

2.1.1 General assembly and operation

The centre pivot irrigation system is an overhead sprinkler systems that can irrigate circular areas anywhere from 2 Ha to 200 Ha (Agrico, 2016). A centre pivot consists of a series of suspended radial supply pipes, or spans, each supported by a network of under-trussing rods and A-frame towers which rotate about a central pivot tower, as shown in Figure 2-1. Spray sprinklers are attached to outlets intermittently spaced along the radial supply pipe.

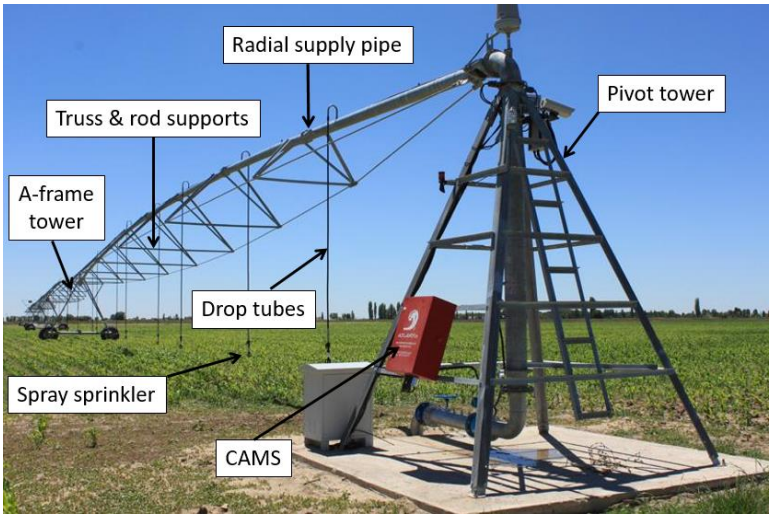

Figure 2-1: Centre pivot irrigation system (Atlantis Engineering, 2012)

Attached to the central pivot tower is the computer aided management system (CAMS) which controls the operation and movement of the centre pivot system. Water is pumped from a source through the pivot tower and into the radial supply pipes.

The radial supply pipes convey water across the field from the pivot tower to the outer spans. Span lengths are dependent on the diameter of the supply pipe and typically range in length from 24 m to 67 m (Reinke Manufacturing Company, Inc, 2016) (Agrico, 2016). To reduce both operating costs and capital inlay costs, the radial supply pipes are often telescoped; where larger diameter pipes are used near the central tower where the flow rates are largest, and smaller diameter pipes are used on the tail spans where the flow rates are the smallest (New & Fipps, 2000). A key functional feature of a centre pivot system is its ability to operate over uneven terrains. The series of suspended radial spans are thus connected in such a manner as to allow for three degrees of motion between consecutive spans.

The under-trussing framework provides structural support for the radial supply pipes and distributes the weight of the suspended sections to the A-frame towers either end of the span. Each A-frame tower is equipped with a centre drive motor and gearbox assembly that drives two wheels positioned on the outer ends of the

tower base. Attached to each tower is a control box which regulates the power supply to the drive assembly.

The rate at which the centre pivot moves about the field is governed by the timer setting on the CAMS at the control panel on the pivot tower. The timer setting determines the percentage of a 60 second cycle that the end tower is in motion. For example, a timer setting of 50% will cause the end tower to move for 30 seconds of a cycle and remain stationary for the other 30 seconds.

As the end tower moves about the field, the inner towers move to maintain radial alignment between spans. The movement of the inner towers is managed by an alignment system which consists of a yoke and control arm mounted at the flexible join between supply pipe spans. The control arm operates a set of micro-switches in the control box mounted on the A-frame tower, which regulate the power supply to the drive assembly. At a pre-set angle of misalignment, the micro-switches in the control box activate the power supply to the drive assembly, and the inner tower moves to maintain alignment with the outer tower.

It must be noted that all the A-frame towers of a centre pivot system travel at the same speed when in motion; this is because all the towers are fitted with the same centre drive system. What differentiates the rate of motion of the inner towers from that of the outer tower is the alignment system.

An end-boom is often suspended beyond the last A-frame tower. The end-boom pipe can be anything from 1 m to 13 m in length (Reinke Manufacturing Company, Inc, 2016). End booms can also be fitted with end gun sprinklers and booster pumps to increase the irrigated area under the pivot.

2.1.2 Spray sprinklers

The sprinkler package installed on a centre pivot system is the most important factor in determining the effectiveness of the system. The selection of an appropriate sprinkler package is determined by a number of factors including the soil properties and infiltration rate, field topography, local weather conditions, and the type of crop to be irrigated. The correct sprinkler package should have an application rate that is suitable for the soil properties of the field, should apply water uniformly over the field, and should be resistant to wind drift and droplet evaporation events.

There are various types of spray sprinklers on the market today that produce spray patterns suitable for various irrigation applications. However, in this study only two spray sprinklers will be discussed. These are the Nelson D3000 Sprayhead sprinkler, and the Nelson S3000 Spinner sprinkler manufactured by the Nelson Irrigation Corporation. The Nelson range of spray sprinklers are a popular choice of sprinkler, and leading suppliers of centre pivot systems, like Agrico, have opted to only supply this range of sprinklers with their centre pivot systems. These two Nelson sprinklers are also installed on the working centre pivot system that was used to test the Powasave sprinkler prototypes. Therefore, these two Nelson sprinklers are used as a benchmark against which the novel Powasave sprinkler is compared.

Figure 2-2 shows the Nelson D3000 Sprayhead sprinkler and the S3000 Spinner sprinkler assemblies. Each sprinkler assembly consists of a 3TN nozzle, sprinkler body, impact plate, and cap assembled to form a compact sprinkler unit.

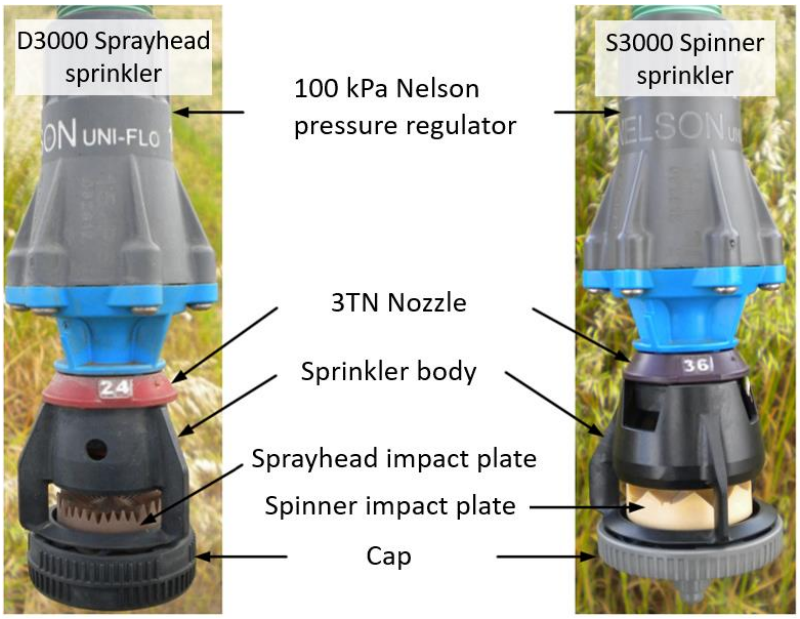

Figure 2-2: Nelson D3000 Sprayhead sprinkler & the Nelson S3000 Spinner sprinkler

The size of the nozzle diameter governs the volumetric flow rate through the sprinkler for a given operating pressure. The flow rate through consecutive sprinklers along a centre pivot system can easily be changed by inserting different sized nozzles.

The distribution profiles of the Nelson sprinklers are determined by the characteristics of the impact plates. The D3000 Sprayhead sprinkler has a stationary impact plate with 33 medium depth grooves generating discrete water trajectories at angles of +9°, +4°, and -3° to the horizontal (Nelson Irrigation Corporation, 2016). The S3000 Spinner sprinkler, on the other hand, has a rotating impact plate with multiple trajectories producing a spray canopy during operation. On centre pivot installations, the Nelson sprinklers are designed to have an overlap factor of 2 to 4 to achieve a good application uniformity (King, et al., 2000).

Each sprinkler installed on a centre pivot system is usually fitted with a pressure regulator. This is to ensure the volume flow rate and spray distribution profile through each sprinkler remains constant for pressure fluctuations induced in the radial supply pipe. Pressure fluctuations in the radial supply pipe are caused by friction losses in the piping network, elevation differences across the field, or pump surges.

2.2 Irrigation efficiency

The performance evaluation of an irrigation system is critical in gauging how effectively water is being utilized in producing a crop. Such an evaluation should assess the system in performing its function of distributing water from a source to

a field, how uniformly that water is distributed over the field, and how effectively the irrigated water is converted into crop yields.

Rogers *et al* (1997) define irrigation efficiency as the fraction of water delivered to the field that is used "beneficially". The term 'beneficial' is loosely defined and accommodates irrigation events with objectives other than simply satisfying crop water requirements in the plant root zone. Other 'beneficial' uses of irrigation water may include crop cooling, salt leaching, application of fertilizers and pesticides, or frost protection (Howell, 2003).

In each case the objective of the irrigation event is different and will affect how the irrigation efficiency is calculated. For example, water evaporation off the crop foliage is considered a loss when the objective of the irrigation event is to satisfy crop water requirements in the plant root zone, but is not considered a loss when the objective of the irrigation event is to cool the crop.

Irrigation efficiency is, however, well defined when the primary objective of the irrigation event is to satisfy crop water requirements. Measuring irrigation efficiency is a difficult and expensive task. The industry has, therefore, defined a number of efficiency indicators to assess the various aspects of an irrigation event to simplify the process of approximating the irrigation efficiency. The more indicators one is able to measure, the better the effectiveness of the irrigation system is understood.

Rogers *et al* (1997) and Howell (2003) present a number of efficiency indicators to assess the effectiveness of an irrigation system. These indicators, discussed in the following sections, reflect the irrigation system performance, the uniform distribution of water, and the response of the crop to the irrigation events.

2.2.1 Conveyance efficiency & water application efficiency

The performance of an irrigation system is reflected by the conveyance efficiency and water application efficiency (Howell, 2003). Conveyance efficiency (E_c) is the volume fraction of the total water diverted from the source (V_s) that reaches the field (V_f)*:*

$$E_c = 100\left(\frac{V_f}{V_s}\right) \tag{2.1}$$

This indicator is primarily of concern when water is conveyed using open channels or ditches. Most overhead spray sprinkler systems today make use of closed conduits to convey the water, and hence losses between the source and field are considered negligible.

Water application efficiency (E_a) is the fraction of the water delivered to the field that is made available in the plant root zone (V_{rz}):

$$E_a = 100\left(\frac{V_{rz}}{V_f}\right) \tag{2.2}$$

Water delivered to the field that does not reach the root zone is considered a loss, and reduces the application efficiency. For overhead sprinkler irrigation systems water losses may include wind drift, evaporation, foliage interception, runoff, and deep soil percolation (Howell, 2003). Figure 2-3 illustrates the typical water losses associated with overhead sprinkler irrigation systems fitted with different sprinkler packages; including impact sprinklers, spray sprinklers, and low energy precision application (LEPA) sprinklers.

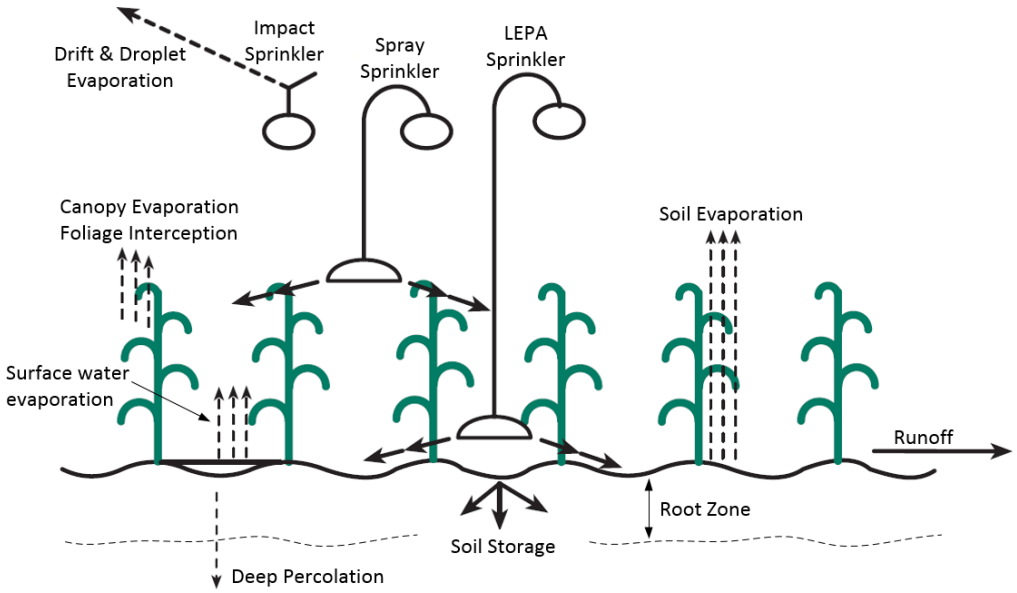

Figure 2-3: Irrigation water losses, adapted from Rogers et al. (1997)

The centre pivot irrigation system is one of the more efficient overhead irrigation systems on the market, capable of application efficiencies ranging between 70% - 95% (Rogers, et al., 1997). Having a high application efficiency, however, does not necessary mean that plants in the field won't experience water stress (Rogers, et al., 1997). This may be so for two reasons: (1) insufficient water may have been applied to meet crop water requirements, and (2) water may not have been uniformly applied resulting in some plants experiencing less watering than others.

Consider the irrigation events A and B illustrated in Figure 2-4. Both irrigation events boast a high application efficiency (E_a = 100%), which merely indicates that all the irrigated water penetrates the soil surface and is made available in the plant root zone. However, portions of the field still experience water stress due to insufficient water being applied to satisfy the soil moisture deficit in the root zone, and because the water was not uniformly applied across the field. The uniform application of a sufficient amount of water is essential in achieving an effective irrigation event.

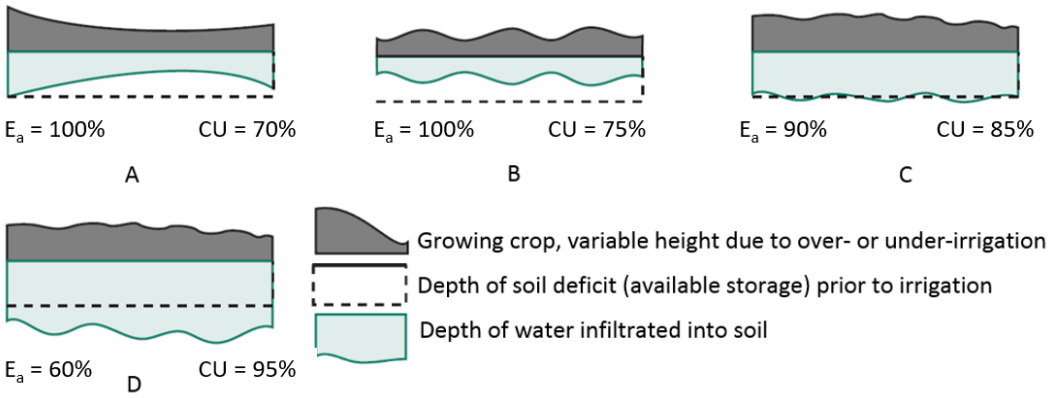

Figure 2-4: Application efficiency and coefficient of uniformity (CU) of various sprinkler irrigation events, adapted from Rogers, et al. (1997)

The parameter used to gauge the degree of uniformity with which water is applied to the field surface is termed the coefficient of uniformity (CU), and will be discussed in Section 2.2.2. A poor CU indicates over- and under-watering in various regions of the field, which can significantly reduce crop yields in those regions.

The effectiveness of an irrigation event is not only determined by the efficiency of the irrigation system in conveying and applying an even distribution of water, but also relies on the effective management of the system in terms of scheduling irrigation events. Irrigating too regularly may result in water leaching below the effective root zone of the plants, while insufficient irrigation will leave the plants short of water and susceptible to water stress.

Poor irrigation scheduling can severely impact on the application efficiency. Consider irrigation event *D* in Figure 2-4, in which over-watering has occurred. Excess water is unable to be retained in the root zone, and is lost as it infiltrates below the effective reach of the plants; reducing the application efficiency of the irrigation event. Good irrigation scheduling should aim to sufficiently meet the plant moisture requirements while minimizing water losses due to deep soil percolation.

The ideal conditions of an irrigation event are shown by event *C* in Figure 2-4. Sufficient water has been applied to meet soil moisture deficits, and the water has been more uniformly applied over the field. Small non-uniformities in the distribution of the water reduce the application efficiency somewhat, as water infiltrates below the root zone in localised regions of the field.

A good application efficiency, therefore, is achieved by the effective management of an efficient irrigation system. A key characteristic of an efficient irrigation system is a uniform application of water.

2.2.2 Coefficient of uniformity

The critical component of the centre pivot system in achieving high application efficiencies is the sprinkler package; the performance of which is best characterised by the coefficient of uniformity (CU). The CU is a measure of how

uniformly water is distributed over a field. It is indicative of how equitably the irrigated water is made available to each of the plants in the field.

The CU beneath a sprinkler is typically measured at the soil surface by placing collectors at selected intervals in the spray area of the sprinkler and recording the volume of water caught in each collector.

The CU is a statistical property describing the distribution of the irrigated water over the spray area. It is a measure of the deviations of the applied water volume in each collector (V_i) from the average applied water volume ($\bar{V}$), as a fraction of the total volume of water applied over the control area, and is defined as follows (Howell, 2003):

$$CU = 100\left[1 - \frac{\sum_{i=1}^{n}|V_i - \bar{V}|}{\sum_{i=1}^{n} V_i}\right] \tag{2.3}$$

where n is the total number of collectors in the control area. A high CU indicates good water application uniformity.

When each collector represents the same proportion of the spray area, then the CU is evaluated using equation (2.3). However, when the proportion of land area represented by each collector varies over the control area, the CU is calculated by weighting the volume caught in each collector by the proportional area represented by that collector.

On a centre pivot system, the annular spray area under consecutive sprinklers increases as one moves away from the pivot tower. Therefore, when collectors are positioned radially beneath a centre pivot system, each successive collector is representing a larger proportion of the total irrigated land area. In such a case the volume of water caught in each successive collector is weighted by the larger proportion of the land area it represents. The CU for centre pivots is given by the Heerman and Hein formula (Howell, 2003):

$$\mathrm{CU_H} = 100\left[1 - \frac{\sum_{i=1}^{n} S_i\left|V_i - \bar{V}_p\right|}{\sum_{i=1}^{n} S_i V_i}\right] \tag{2.4}$$

where S_i is the distance of the i^{th} collector from the pivot tower, and $\bar{V}_p$ is the weighted average volume of water recorded in all n collectors, given by:

$$\bar{V}_p = \frac{\sum_{i=1}^{n} V_i S_i}{\sum_{i=1}^{n} S_i} \tag{2.5}$$

Centre pivot irrigation systems equipped with pressure-regulated, low pressure sprinkler packages are capable of attaining CU values of 90% to 95%, and a CU value of 85% is considered the minimum below which a sprinkler package needs updating (King, et al., 2000).

2.2.3 Distribution uniformity

A parameter often used in conjunction with the CU is the distribution uniformity (DU). When the CU is poor, the DU is used to measure the severity of the non-uniformity. The DU indicates how severe the under-watering is in the least-watered regions of the field. Usually the DU is quoted for the least-watered quarter of the irrigated area (Howell, 2003). In that case, the DU is the average depth of water received by the least-watered quarter of the field as a fraction of the average depth of water received over the entire field:

$$\mathrm{DU} = 100\left(\frac{\mathrm{LQD}}{\mathrm{AAD}}\right) \tag{2.6}$$

where LQD is the lowest-quarter application depth, and AAD is the average application depth.

Average application depth

The average application depth (AAD) is the average depth of water applied to a spray area for a given irrigation event, typically expressed in millimetres. It is defined as the average volume of water ($\bar{V}$) applied over a spray area (A):

$$\mathrm{AAD} = \left(\frac{\bar{V}}{A}\right) \tag{2.7}$$

The AAD underneath a sprinkler, or set of sprinklers, is measured by sampling the application depth at selected intervals in the spray area of the sprinkler. This is done by placing collectors at selected intervals in the sprinkler spray area and recording the volume of water caught in each collector. The AAD is then calculated from equation (2.7) where $\bar{V}$ is the average volume of water caught by the collectors, and *A* is the inlet catchment area of a collector.

Equation (2.7) is applicable when each collector represents the same proportion of the spray area under consideration. When measuring the AAD underneath a centre pivot system, where the annular areas represented by each collector increase along the length of the centre pivot, the average applied water volume in equation (2.7) needs to be calculated using equation (2.5).

Lowest-quarter application depth

The lowest-quarter application depth (LQD) is the average depth of water applied to the least watered quarter of a spray area. The LQD, measured over a spray zone, is given by the average volume of water measured in the collectors making up the lowest quarter of all the volume measurements taken over the spray area, divided by the inlet area of a collector:

$$\mathrm{LQD} = \frac{\bar{V}_{LQ}}{A_c} \tag{2.8}$$

where $\bar{V}_{LQ}$ is the average volume of the lowest quarter of the collector volume measurements, and A_c is the collector inlet area. When each collector represents the same proportion of the spray area, then the LQD is evaluated using equation (2.8). For centre pivot irrigation systems, the average lowest-quarter applied volume is given by:

$$\bar{V}_{LQ} = \frac{\sum_{i=1}^{n_{LQ}} V_i S_i}{\sum_{i=1}^{n_{LQ}} S_i} \tag{2.9}$$

Where n_{LQ} is the number of collector volume measurements making up the lowest-quarter values. The selection of the lowest-quarter volumes measured beneath a centre pivot system is discussed further in Appendix A.

2.2.4 Water use efficiency

Howell (2003) suggests that irrigation efficiency can be more completely understood when the response of the crop to the irrigation events is quantified. Howell (2003) presents water use efficiency (E_{wu}) as a parameter to describe irrigation effectiveness in terms of crop yield:

$$E_{wu} = \frac{Y_g}{ET} \tag{2.10}$$

where Y_g (g·m^{-2}) is the economic crop yield per unit area, and ET (mm) is the crop water use. The water use efficiency indicator, expressed in (kg·m^{-3}), provides a measure of the gross crop mass harvested off the field as a fraction of the total water volume irrigated.

Although crop yields are significantly affected by the application efficiency and distribution efficiency of the irrigation system, these are not the only factors affecting the crop yield. Other factors may include soil conditions, weather conditions, crop health, pest invasions, and irrigation scheduling management. These factors are independent of the irrigation system itself, and will be unique to the environment where the irrigation system is installed. The water use efficiency indicator is therefore not only a measure of the application efficiency of the irrigation system, but also a measure of the efficient management of the irrigation system.

2.3 Summary

The effectiveness of an irrigation system in maximising crop yields and minimizing water losses, is very much dependant on the effective management of an efficient irrigation system. The efficiency of an irrigation system is gauge by the conveyance efficiency and application efficiency. For modern overhead sprinkler irrigation systems, closed conduits are used to convey the irrigated water, and therefore conveyance efficiencies are usually very good.

The application efficiency is the measure of the effectiveness of a system in making the water delivered to the field available in the crop root zone. A good application efficiency maximises the potential for the crop to use the irrigated water.

To maximise crop yield, however, the irrigated water should be uniformly applied over the field. This requires a sprinkler system with a good application uniformity; which is best quantified by the distribution uniformity (DU) and the coefficient of uniformity (CU). Centre pivot systems are one of the more efficient overhead irrigation systems on the market, capable of high application efficiencies and uniformities.

Although irrigation effectiveness cannot be fully quantified by a single indicator, the application uniformity is one of the more influential characteristics of a sprinkler irrigation system; affecting both the application efficiency of the system and ultimately the crop yield.

The application uniformity of a novel, overhead spray sprinkler is the focus of this study. All the relevant theory was presented in this chapter regarding the evaluation of the DU and CU beneath a sprinkler package installed on a centre pivot system.

3 Powasave sprinkler

The Powasave sprinkler concept has the potential to reduce operating pressures in centre pivot systems while producing a uniform droplet size. Roux (2012) also showed the Powasave sprinkler capable of producing a near uniform water distribution while operating in cooling tower systems. In this study, the distribution uniformity of the Powasave sprinkler is tested on a travelling centre pivot irrigation system, and evaluated against the Nelson D3000 Sprayhead sprinkler and S3000 Spinner sprinkler. The functional features of the primary components of the Powasave sprinkler are presented and discussed in this chapter.

3.1 Sprinkler description

The Powasave sprinkler package consists of horizontal sprinkler assemblies fixed at the outlets of the radial supply pipe of a centre pivot system, as shown in Figure 3-1. The main components of the Powasave sprinkler include a sprinkler pipe, orifice set, pressure regulator assembly, and support structure.

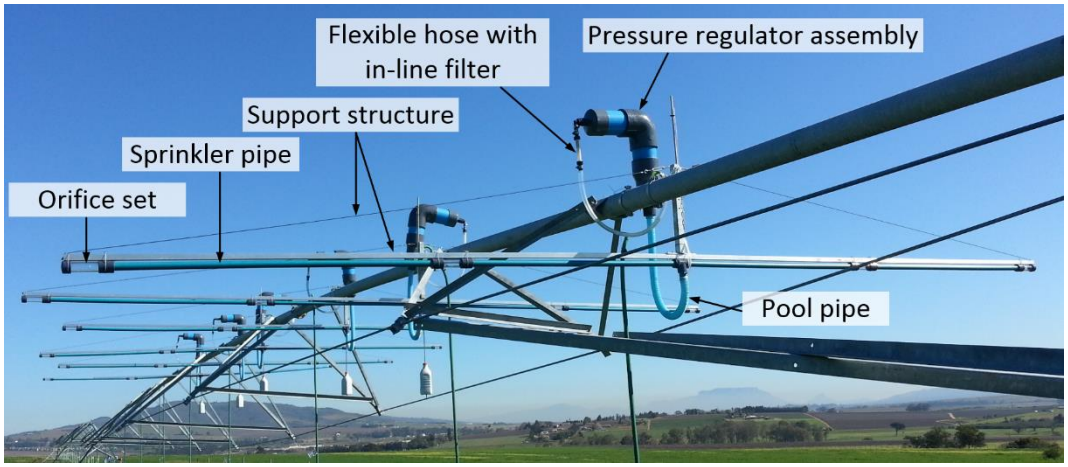

Figure 3-1: Powasave sprinkler assemblies installed on a segment of a centre pivot system

The four primary components of the Powasave sprinkler serve the following functions:

(1) The sprinkler pipe delivers water diverted from the radial supply pipe of the centre pivot to orifice set outlets distributed along the length of the sprinkler pipe
(2) The orifice set outlets distribute the supplied water over a specified spray area on the ground beneath the sprinkler pipe
(3) The pressure regulator assembly regulates the pressure inside the sprinkler pipe to a predetermined water head, and dissipates excess pressure energy in the radial supply pipe caused by field elevation differences or pump surges
(4) The support structure fixes the sprinkler pipe assembly and pressure regulator to the main radial supply pipe of the centre pivot system, and provides support to the sprinkler pipe lengths extending perpendicularly from the centre pivot radial supply pipe

Each of the Powasave sprinkler components are discussed in more detail in the following sections.

3.1.1 Sprinkler pipe

The sprinkler pipe comprises a length of PVC pipe, closed at it ends, with a water inlet to the interior of the pipe in the form of a tee located at its centre, as illustrated in Figure 3-2. Multiple orifice set outlets are distributed along the length of the pipe through which water is irrigated.

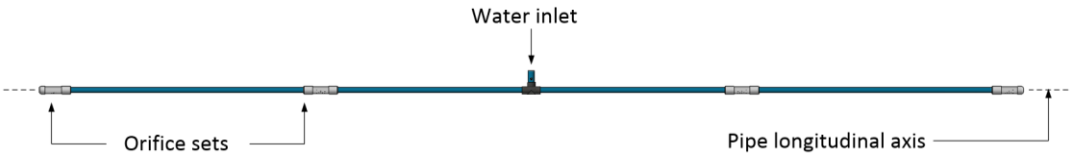

Figure 3-2: Powasave sprinkler pipe fitted with 4 orifice set outlets

The function of the sprinkler pipe is to carry water diverted from the radial supply pipe of the centre pivot system to orifice sets suspended some distance away. When selecting an appropriate sprinkler pipe diameter, there are two opposing parameters that need to be considered: (1) the friction losses incurred in the pipe, and (2) the weight of the water in the pipe that needs to be supported by the centre pivot system. Figure 3-3 illustrates the relationship between the two parameters for a 1 m length of smooth PVC pipe at an average flow velocity of 1 m/s.

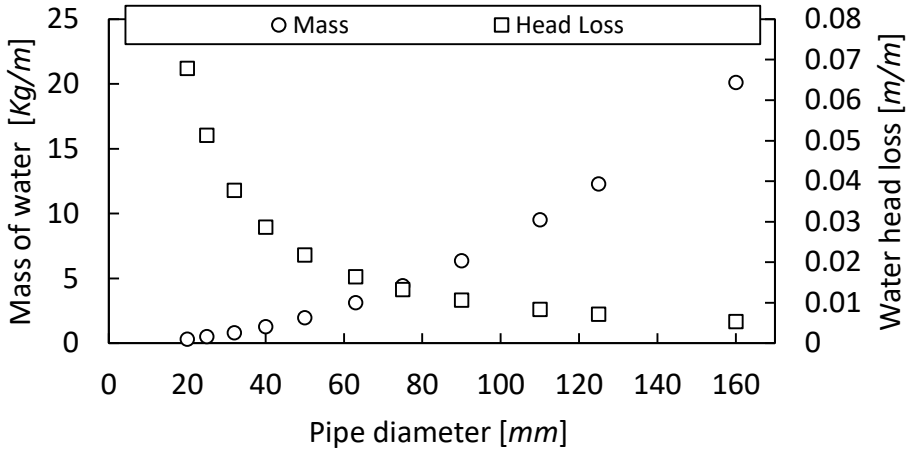

Figure 3-3: Water mass and head loss in a 1 m length of smooth PVC pipe for an average flow velocity of 1 m/s (Budler, 2014)

A smaller diameter pipe carries a smaller water mass but incurs a larger pressure head loss, while a larger diameter pipes carries more water mass but incurs a smaller pressure head loss. The diameter of the sprinkler pipe should be selected to produce the least amount of pressure drop between consecutive orifice set outlets along the sprinkler pipe, while keeping the additional water mass to be supported by the centre pivot to a minimum.

Significant pressure losses between orifice set outlets will alter the distribution characteristics of downstream orifice sets, which may compromise the ability of the sprinkler to apply a uniform water distribution. A suitable trade-off is to be made

taking into account the maximum expected flow rates through the sprinkler pipe and the length of the sprinkler pipe.

3.1.2 Orifice set

An orifice set consists of multiple orifice nozzles in which each nozzle takes the form of a hole machined through the sprinkler pipe wall such that the axis of the hole is radial to the longitudinal axis of the pipe, as shown in Figure 3-4.

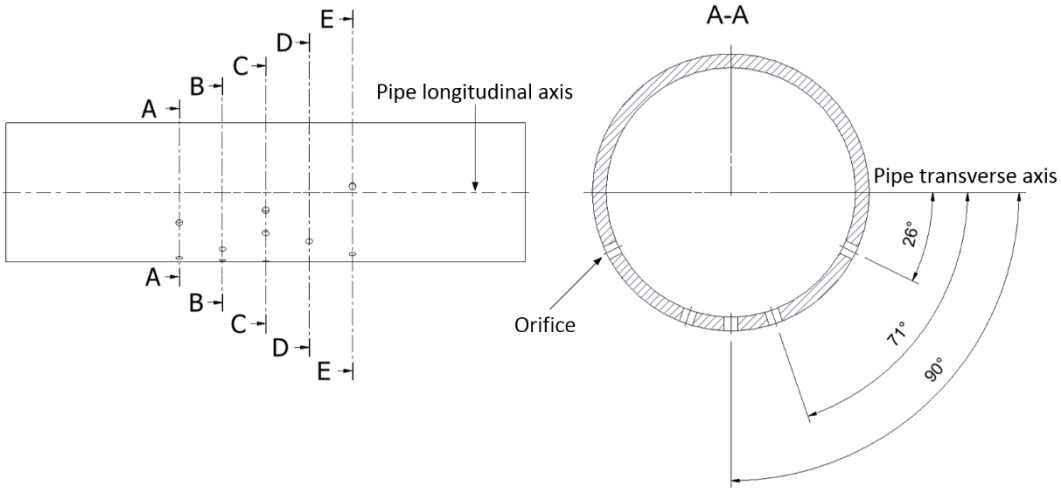

Figure 3-4: An orifice set consisting of 21 holes with a 1.6 mm *diameter spaced along 5 cross-sectional planes*

The axes of the holes extend in various angular directions relative to the transverse axis of the pipe. The diameters of the holes may range from 0.75 mm to 2 mm. During operation, each orifice nozzle provides a jet of water which breaks up into droplets during flight.

The holes of an orifice set may be machined on several cross-sectional planes spaced along the pipe longitudinal axis, as indicated by planes A – E in Figure 3-4. The reasons are: (1) the number of holes that can be machined in the circumference of the pipe in a single plane are restricted by the size of the holes and available space on the pipe circumference; (2) too many holes machined in a single plane may weaken the structural integrity of the pipe; and (3) it was observed that the jet streams of holes spaced too closely together tend to coalesce, or cross over each other, which may alter the desired spray distribution pattern.

By distributing the holes over a number of cross-sectional planes, less holes are required in a plane, and the holes can therefore be spaced farther apart to avoid crossover of jet-stream trajectories. Several orifice set prototypes were machined where the spacing between consecutive cross-sectional planes was set to 2.5 mm, 7.5 mm, and 12.5 mm. It was observed that a spacing of 12.5 mm between consecutive planes was sufficient to avoid water streams interfering with each other. It was also noted that trajectory angles between orifice nozzles in a single plane should not be within 10° of each other to avoid streams coalescing.

The orifice set serves the function of uniformly distributing a supplied volume of water over a specified radial spray width on the field. The required spray width is

generally determined by the distance between outlets on the radial supply pipe of the centre pivot, which can be anywhere between 2.2 m and 3.5 m. The desired water volume is applied over the selected radial spray width by engineering the trajectory streams of the orifice nozzle to apply equal volumes of water at equi-spaced intervals along the spray width. The more orifice nozzles in the orifice set, the smaller the intervals between the trajectory streams.

The volume flow rate through an orifice nozzle is governed by the orifice diameter, the pressure head in the sprinkler pipe, and the sprinkler pipe wall thickness. The volume flow rate through an orifice set is then the sum of the flow rates through each orifice nozzle. The trajectory profile and spray range of an orifice nozzle is determined by the orifice diameter, trajectory angle on the pipe circumference, the pressure head inside the sprinkler pipe, and the nozzle elevation above the soil surface.

Figure 3-5 shows the modelled distribution profile of an orifice set consisting of 21 orifice nozzles, each with a diameter of 1.6 mm, operating under a pressure head of 0.5 m at a sprinkler pipe elevation of 3 m. Discrete water jets apply water at generally equi-spaced intervals over a spray width of 3.5 m at a target spray plane located 3 m beneath the sprinkler pipe. The distribution profile is generated using the Powasave sprinkler model discussed in Chapter 4.

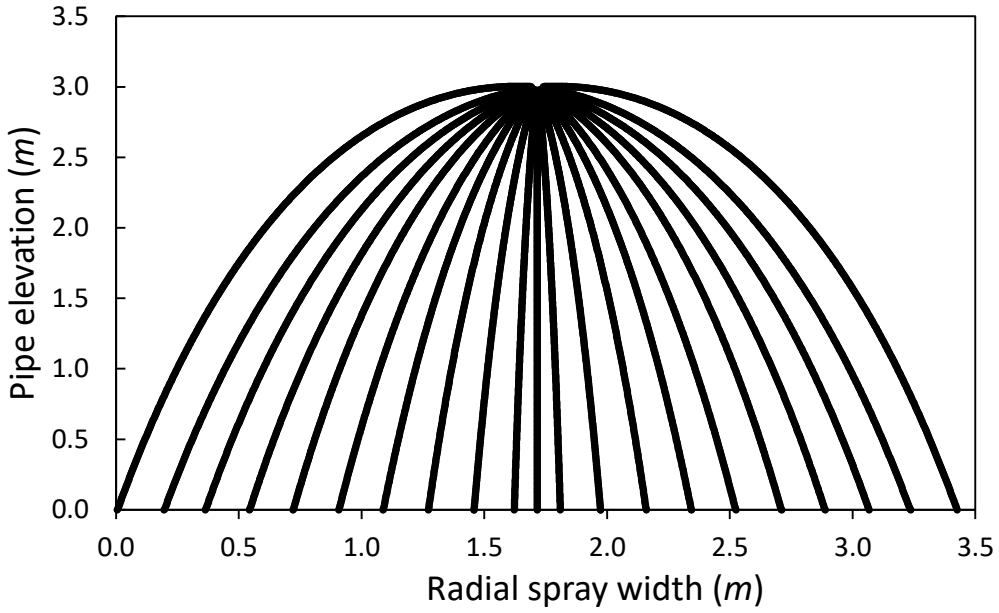

Figure 3-5: Radial spray distribution profile of an orifice set comprised of 21 orifice nozzles with a diameter of 1.6 mm, operating at a pressure head of 0.5 m and elevation of 3 m

Where commercial spray sprinklers, like the Nelson sprinklers, require the spray zones of consecutive sprinklers to overlap to achieve a good uniformity, the Powasave sprinklers can, in theory, be designed to provide a good uniformity with very little overlap. Consequently, the application rates over the length of the pivot can be more precisely adjusted for due to the smaller annular bands covered by the Powasave sprinklers.

3.1.3 Pressure regulator assembly

The pressure inside the main radial supply pipe of a centre pivot system varies from the inlet at the pivot tower to the end nozzle on the outer tower due to friction losses and momentum transfer in the piping network. Furthermore, pressure fluctuations may be induced in the supply pipe due to undulations in the field topography or pump surges. The pressure variation in the radial supply pipe of the centre pivot necessitates the use of a pressure regulator in the Powasave sprinkler assembly to regulate the pressure in the sprinkler pipe to that specified for the correct operation of the orifice set outlets. Pressure fluctuations experienced in the sprinkler pipe may affect the flow rates and spray distribution profiles beneath the sprinkler.

The pressure regulator should therefore be capable of dissipating excess energy in the supply pipe at high pressure regions, but incur a minimal energy loss at low pressure regions in the supply pipe. In addition, the pressure regulator should maintain a constant pressure in the sprinkler pipe for various supply line pressures, be robust, reliable, and resistant to clogging.

Figure 3-6 shows a pressure regulator assembly consisting of a vertical PVC pipe reservoir, and a horizontal PVC pipe housing a float valve fixed into the end cap.

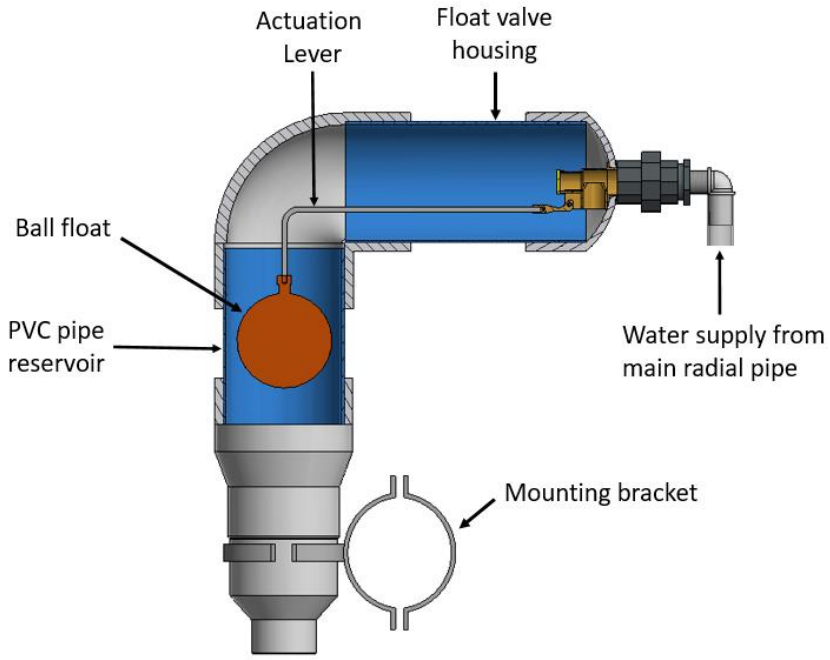

Figure 3-6: Pressure regulator concept

Water is supplied to the inlet of the float valve from the main radial supply pipe of the centre pivot system. An actuation lever, bent through 90°, positions the ball float in the reservoir portion of the assembly. The float actuates the valve by action of the water level in the reservoir. As the water level rises in the reservoir, the action of the ball float throttles the incoming water through the valve. As the water level in the reservoir falls the valve is opened and the flow rate through the valve

increases. The pressure in the sprinkler pipe is governed by the head of water stored in the reservoir above the sprinkler pipe inlet.

Care should be taken to select a float valve that has sufficient volume flow capacity at the required operating pressures to meet the flow requirements through the sprinkler pipe. If the float valve is undersized, an insufficient amount of water will be supplied through the valve to meet the flow through the orifice sets and build up the necessary water head in the reservoir pipe.

For a given pressure at an outlet along the radial supply pipe of a centre pivot system, a flow equilibrium will be achieved between the inlet flow through the valve and the outlet flow through the orifice sets. This flow equilibrium will fix the water level in the reservoir. To ensure the pressure head in consecutive Powasave sprinklers installed along the radial supply pipe are essentially the same, the fluctuation of the water level in the pressure regulator reservoir should be kept to a minimum for different supply line pressures. This can be achieved by using a broad cylindrical float that will provide an actuation force linearly proportional to the water level in the reservoir. Large pressure fluctuations in the radial supply pipe are thereby reflected as small changes in the water level in the reservoir.

The water held in the reservoir also acts as a damper on pressure surges experienced in the radial supply pipe. Pressure surges will temporarily increase the inlet flow through the float valve into the reservoir. The increased flow, however, is absorbed by the volume of water held in the reservoir and reflected as a smaller change in water level; hence reflecting a small change in the pressure head in the sprinkler pipe.

3.1.4 Support structure

A support structure is required to attach the sprinkler pipe and pressure regulator assembly to the centre pivot system, and provide structural support to the sprinkler pipe segments extending out from the radial supply pipe of the pivot.

Key functional requirements of the support structure are: (1) preventing rotation of the sprinkler pipe in the horizontal plane about the central inlet T-piece to keep the sprinkler pipe perpendicular to the radial supply line, and maintain proper orifice set alignment relative to the ground; and (2) providing rotational freedom in the vertical plane to ensure the sprinkler pipe remains horizontal during operation.

Furthermore, the support structure should be lightweight, yet strong and rigid enough to support the loadings experienced during operation, including those induced by weather elements such as wind, rain, and sunlight.

3.2 Installation on centre pivot system

A Powasave sprinkler pipe installation on a centre pivot system is shown in Figure 3-7. The sprinkler pipe is suspended, in a horizontal fashion, from the main radial supply pipe such that the longitudinal axis of the sprinkler pipe is perpendicular to that of the radial supply pipe of the centre pivot, and tangential to the direction of movement of the pivot.

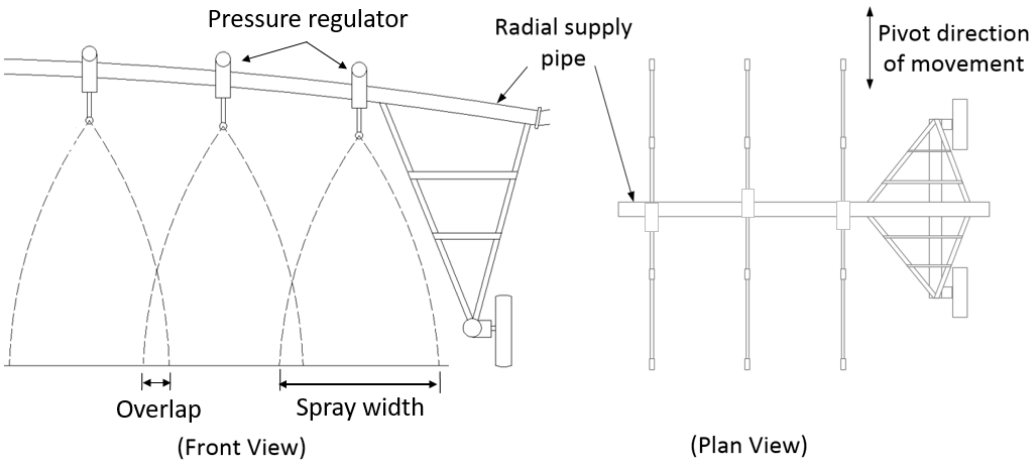

Figure 3-7: Powasave sprinkler installation on a centre pivot system

It is essential that the Powasave sprinkler remain horizontal during operation to ensure there are no pressure fluctuations in the sprinkler pipe due to elevation differences at its ends which may occur when the centre pivot A-frame towers move up or down a slope, as indicated in Figure 3-8. The sprinkler pipe should therefore be free to rotate in the vertical plane coincident with the longitudinal axis of the pipe.

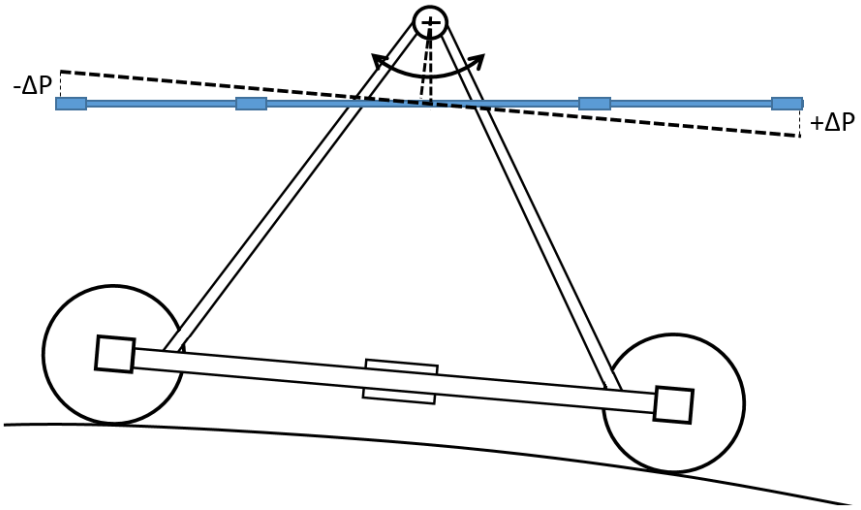

Figure 3-8: Sprinkler pipe rotates to remain horizontal during operation

Since the operating pressure head in the sprinkler pipe is typically less than 1 m, any elevation difference between the ends of the sprinkler pipe will induce a pressure gradient in the pipe, and alter the flow rates and spray pattern through each of the orifice sets. Figure 3-8 illustrates the pressure differential that would occur at the ends of the sprinkler pipe if it were fixed to the pivot, and not able to freely rotate.

However, because the sprinkler pipe remains horizontal during operating, the elevation of the orifice sets above the ground may vary as the centre pivot system climbs or descends an incline in the field. This will have the effect of changing the radial spray width of the individual orifice sets. Consecutive Powasave sprinklers

installed on a centre pivot are required to have sufficient spray overlap to accommodate the most severe incline angles in the field.

Each Powasave sprinkler irrigates an annular band about the pivot tower as shown in Figure 3-9. A key feature of the Powasave sprinkler package is the increasing sprinkler pipe lengths at distances farther from the pivot tower. Sprinklers farther from the pivot tower irrigate a larger annular area while travelling at a greater tangential velocity than sprinklers positioned closer to the pivot tower. In order to apply the same volume of water per unit area at the increased travelling speeds, the sprinklers are required to have a larger volume flow rate.

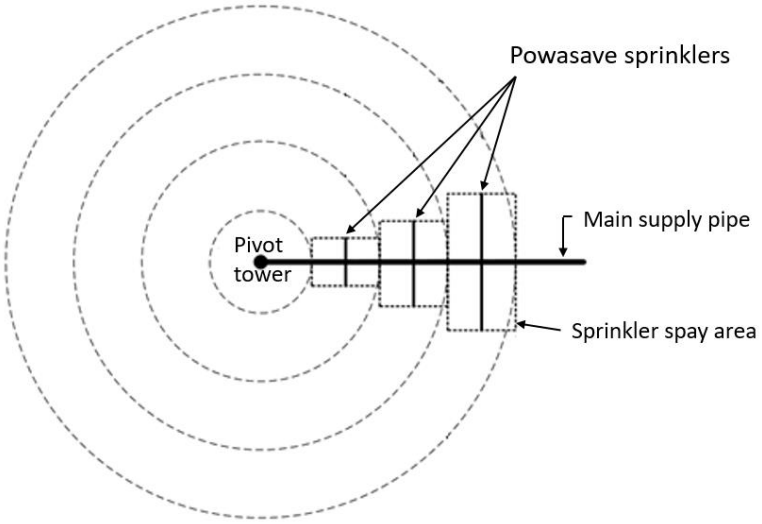

Figure 3-9: Annular spray bands of consecutive Powasave sprinklers installed on a centre pivot system

However, increasing the sprinkler volume flow rate without increasing the area over which this water is distributed will increase the application rates. Application rates exceeding the infiltration rates of the soil will result in water runoff at the soil surface; hence reducing the application efficiency of the sprinkler system.

Therefore, to achieve a uniform water distribution over the field while simultaneously keeping application rates at acceptable levels, the length of the sprinkler pipes increase with increasing distance from the pivot tower. Increasing the length of the sprinkler pipe increases the area over which the water is irrigated, in turn reducing the application rates.

3.3 Orifice set features

The core component of the Powasave sprinkler is the orifice nozzle. The configuration of each orifice nozzle determines the drop size and trajectory path of each droplet of water irrigated beneath the sprinkler.

3.3.1 Orifice nozzle droplet size

Roux (2012) conducted an investigation of the droplet diameter (d_d) produced by a single orifice nozzle for varying nozzle pressures, trajectory angles, nozzle elevations, and wall thicknesses. The droplet diameter measurements are

presented in terms of the Sauter mean droplet size diameter defined as, *"a uniform droplet diameter for a monodisperse droplet distribution that is representative of a polydisperse droplet distribution having similar heat and mass transfer and pressure drop characteristics".* The Sauter mean droplet diameter (d_{32}) is defined by:

$$d_{32} = \frac{\sum {d_d}^3}{\sum {d_d}^2} \tag{3.1}$$

By photographing the water stream produced by an orifice nozzle against a sand blasted glass screen illuminated by 100 W tungsten halogen backlights and using image processing software, Roux (2012) was able to determine the Sauter mean droplet diameter of the water droplets emitted by an orifice nozzle.

The findings are presented in Figure 3-10, showing the Sauter mean droplet diameter produced by an orifice nozzle for varying pressure head, spray angles, nozzle height, and orifice wall thickness.

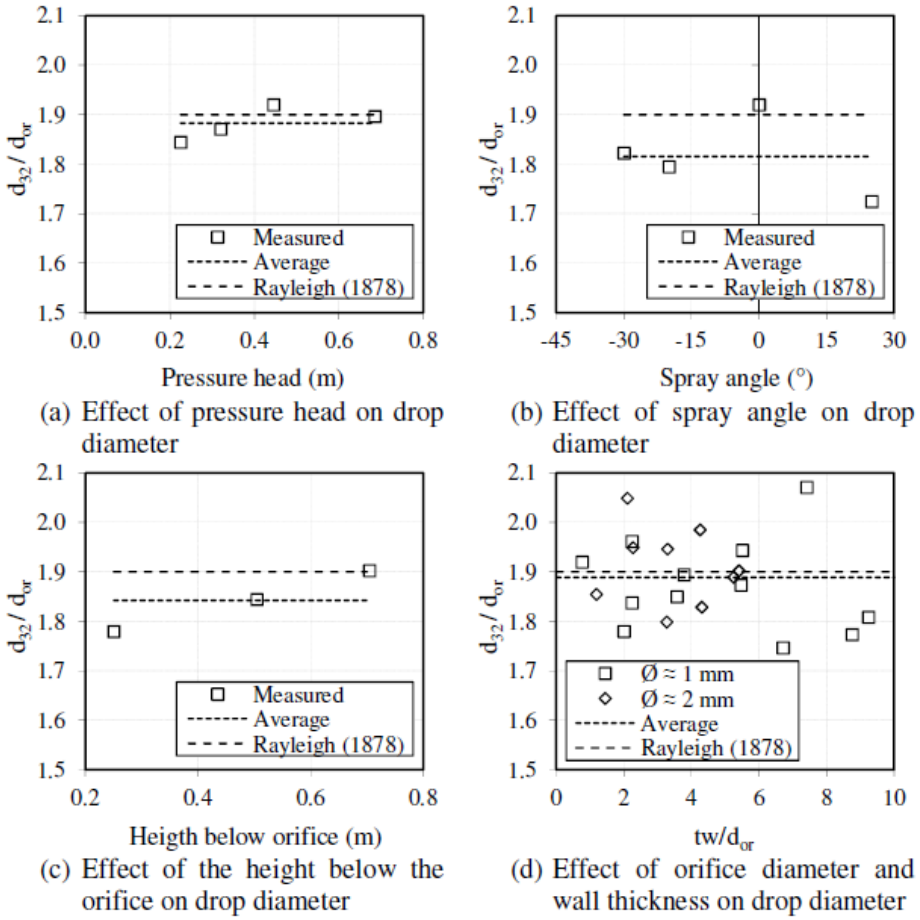

(a) Effect of pressure head on drop diameter

(b) Effect of spray angle on drop diameter

(c) Effect of the height below the orifice on drop diameter

(d) Effect of orifice diameter and wall thickness on drop diameter

Figure 3-10: Sauter mean droplet diameters produced by an orifice nozzle for varying pressure heads, spray angles, orifice nozzle elevation, and orifice wall thickness (Roux, 2012)

The results show that a direct correlation exists between the Sauter mean droplet diameter and the orifice nozzle diameter (d_{or}). Regardless of the nozzle pressure,

spray angle, wall thickness, or elevation, the relationship between the Sauter mean droplet diameter and the orifice nozzle diameter is given by $d_{32}/d_{or} \approx 1.9$. This correlates well with the findings of Rayleigh (1878) stating that the droplet diameter produced by an orifice nozzle is approximately $d_d/d_{or} \approx 1.9$.

The relationship between the orifice nozzle diameter and the resultant droplet diameter allow for the selection of a suitable droplet size that best fits an irrigation circumstance. A Powasave sprinkler can therefore be designed to emit a droplet size that will minimise soil crusting effects and water losses due to wind drift and evaporation.

Furthermore, images taken by Roux (2012) of the jet streams produced by the various orifice nozzles that were tested, show the resultant droplet diameters to be fairly uniform in size, as shown in Figure 3-11.

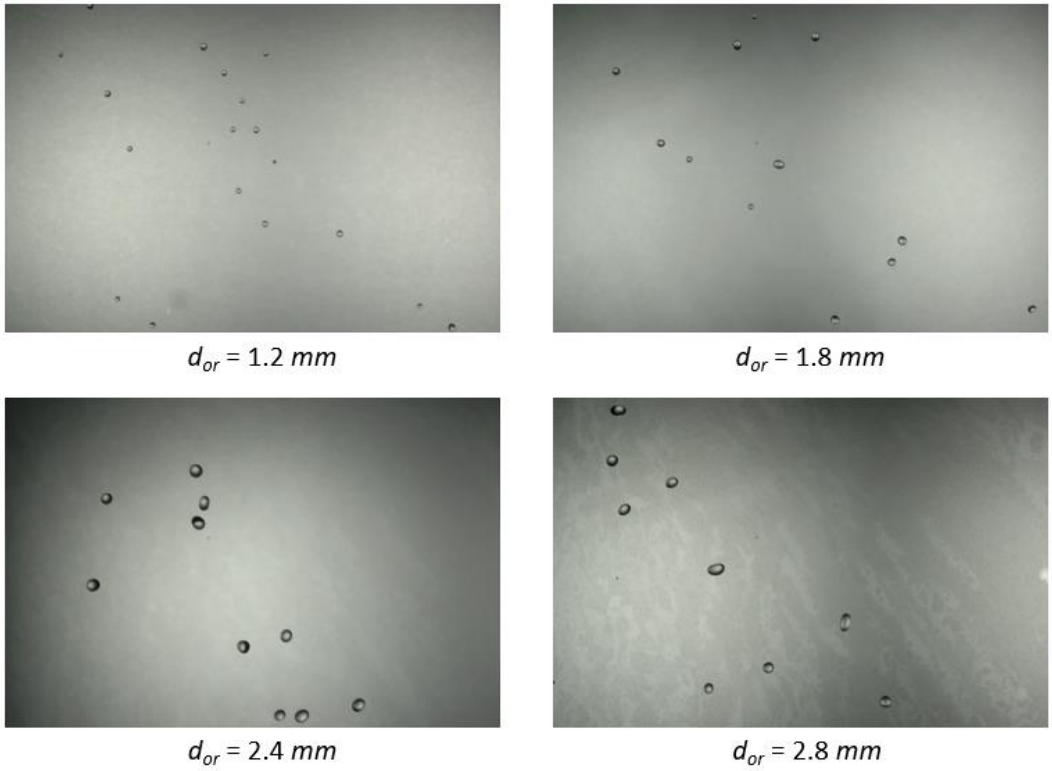

Figure 3-11: Droplet diameters produced by various orifice nozzle diameters for a fixed pressure head of 0.5 m, a trajectory angle of α = 0°, and a nozzle elevation of 0.5 m (Roux, 2012)

3.3.2 Reduced operating pressures

An economic advantage of the Powasave sprinkler is the reduced operating pressure requirements relative to other commercial sprinklers on the market. Most commercial sprinklers apply water to the ground by accelerating water through a single nozzle onto an impact plate which breaks up the jet of water into discrete streamlets, or droplets, and further accelerates these streamlets through an angle of 90° or more, as illustrated in Figure 3-12.

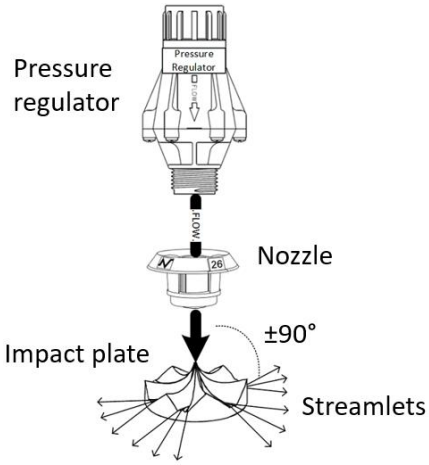

Figure 3-12: Commercial sprinkler pressure regulator, nozzle, and impact plate

Significant energy is required to realise the momentum changes of the water as it is accelerated through the nozzle and off the impact plates, and to provide sufficient kinetic energy to the droplets to travel the throw distances common to these kinds of sprinklers. The Nelson S3000 Spinner sprinkler requires 100 kPa to achieve a throw diameter of 12 m.

Powasave sprinklers, on the other hand, do not require the energy to project the droplets large distances, nor are there any significant momentum changes that occur across the orifice nozzles. The sprinkler pipe transports the water from the radial supply pipe, incurring minimal energy loss, to the orifice sets at which point the water droplets only require sufficient kinetic energy to travel half the distance between consecutive outlets on the main radial supply pipe, typically about 3.35 m.

The energy loss incurred across an orifice set is that incurred across the individual orifice nozzles, and are attributed to three factors: (1) an entry loss as the water in the sprinkler pipe enters the orifice nozzle (k_o); (2) a loss due to vena contracta effects occurring at the nozzle mouth (k_{vc}); and (3) the friction losses (k_f) incurred along the orifice wall as the water passes through the orifice nozzle, as illustrated in Figure 3-13.

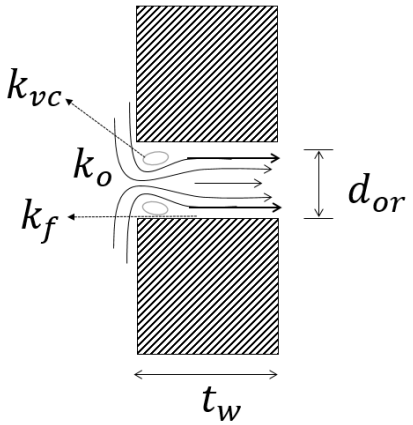

Figure 3-13: Losses through an orifice nozzle

An orifice nozzle with a trajectory angle of α = 0°, at an elevation of 3 m, requires only 0.5 m water head (4.9 kPa) to achieve the throw distance necessary to cover the radial spray width between consecutive sprinklers installed 3.35 m apart on a centre pivot system. A significant reduction in the required end sprinkler pressure will decrease the centre pivot system pressure requirements and reduce the operational costs of irrigating.

The 'low' pressure commercial sprinkler packages on the market today require a minimum sprinkler operating pressure of 100 kPa. Packages fitted with pressure regulators require an additional 40 kPa to function optimally, thereby increasing the minimum requirements to 140 kPa. Powasave sprinklers, on the other hand, can be designed to operate at pressures under 1 m water head (10 kPa), thereby reducing the end pressure requirements of a centre pivot system by over 90% (Budler, 2014). The actual pressure reductions over the length of the centre pivot machine are, however, diluted by the losses in the piping network, but may still be substantial.

A centre pivot design provided by Agrico for a 31.8 Ha system delivering an average application depth of 5.2 mm of water per pass on a level field in the town of Lichtenburg in the North West province of South Africa, has a system pressure breakdown shown in Table 3-1.

Table 3-1: Comparison of centre pivot system pressure requirements for Nelson and Powasave sprinkler packages

System pressure component	**Pressure loss (kPa)**	
	Nelson Sprinkler Package	**Powasave Sprinkler Package**
Elevation of water	34	34
Friction in machine pipe network	88	88
Loss across pressure regulator	40	40
Minimum end sprinkler pressure	100	10
Total	**263**	**172**

Fitted with a Nelson sprinkler package, the centre pivot system requires a minimum end sprinkler pressure of 100 kPa, and a total pressure of 263 kPa at the pivot tower to function optimally. If the same centre pivot system was fitted with Powasave sprinklers, and assuming a pressure regulator assembly is fitted with similar pressure drop characteristics as those installed on the Nelsons sprinklers, the required end sprinkler pressure can be reduced to 10 kPa and the system pressure reduced to 172 kPa; which is a 35% reduction in the required operating pressure at the pivot tower.

It must be noted, however, that the centre pivot system pressure requirements are not the only components contributing to the overall pumping power demands. Additional piping losses, and water elevation potential energy, are required of the pump to convey the irrigation water from a source to the centre pivot machine. As these energy requirements increase, the pressure savings achieved on the pivot form a smaller fraction of the overall pumping requirements.

4 Powasave sprinkler modelling

A theoretical model is developed to simulate the Powasave sprinkler spray characteristics. Three elements of the sprinkler are modelled: (1) the spray trajectory and volume flow rate of a single orifice nozzle, (2) the distribution profile and flow rate of an orifice set consisting of a number of single orifice nozzles, (3) the application rate under a single sprinkler pipe consisting of a number of orifice sets. The relevant model theory and evaluations are presented in this chapter.

4.1 Single orifice nozzle

The fluid mechanic characteristics of a single orifice nozzle are the foundation on which an orifice set is modelled. In this section a single droplet trajectory model (SDTM) is developed, following a similar approach implemented by Roux (2012), Reuter (2010), Viljoen (2006) and Xiaoni *et al*. (2006), to simulate the trajectory profile of a droplet in motion emitted from a single orifice nozzle.

4.1.1 Single droplet trajectory model

In developing the model theory, a co-ordinate system is necessary that remains true for any sprinkler installed along the length of the centre pivot radial supply pipe. A local, travelling co-ordinate system is defined that moves with the centre pivot supply pipe about the field, as shown in Figure 4-1. The system is defined such that: (1) the radial direction, r, is coincident with that of the radial supply pipe of the centre pivot system; (2) the circumferential direction, θ, is coincident with the tangential line intersecting the radial direction at right angles; (3) the elevation, z, is coincident with the vertical plane in which gravity acts; and (4) the radial, circumferential, and elevation directions remain at right angles so that $r \perp \theta \perp z$.

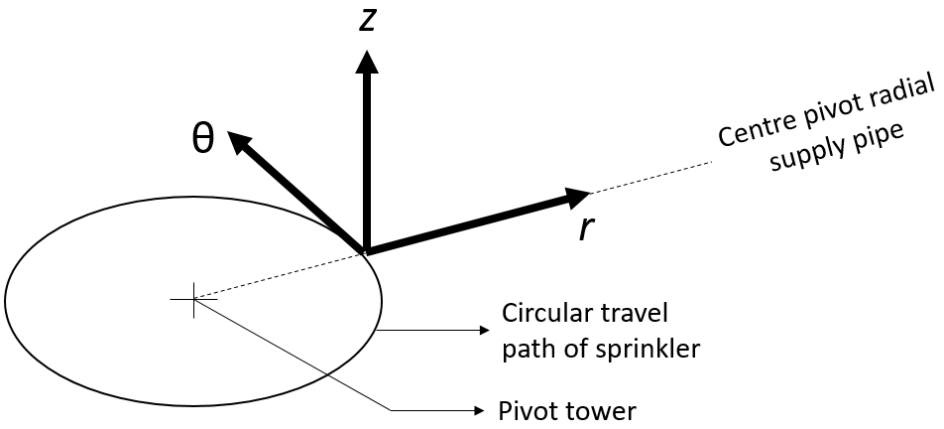

Figure 4-1: Local travelling co-ordinate system

Figure 4-2(A) shows a single orifice nozzle, with wall thickness t_w, ejecting a water droplet with diameter d_d at an initial trajectory angle α_i to the horizontal at a height z above the ground. It is assumed that the droplet forms instantly at the orifice outlet, is spherical in shape, and retains its mass during flight.

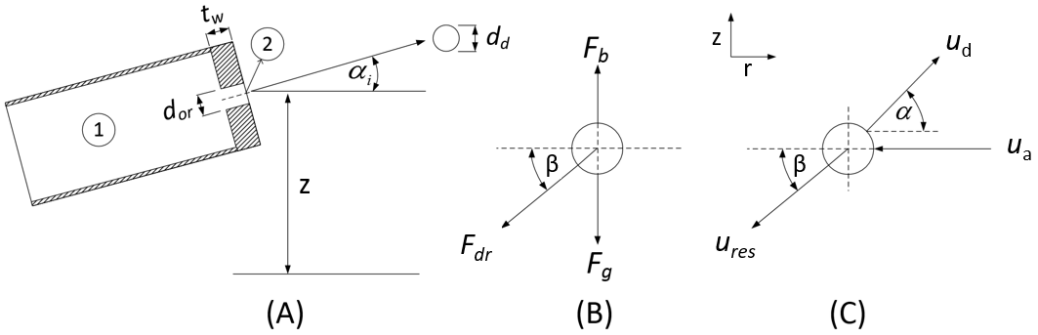

Figure 4-2: Droplet emitted from an orifice nozzle with associated kinetic and kinematic conditions

The initial velocity of the droplet at the exit of the orifice is evaluated by employing the principle of energy conservation across the orifice nozzle:

$$\frac{P_1}{\rho_w\, g} + \frac{{u_1}^2}{2g} + z_1 = \frac{P_2}{\rho_w\, g} + \frac{{u_{d_2}}^2}{2g} + z_2 + h_L \tag{4.1}$$

where h_L is the head loss incurred across the orifice defined in terms of the droplet's initial exit velocity (u_{d_2}) and an orifice loss coefficient k_o:

$$h_L = k_o \frac{{u_{d_2}}^2}{2g} \tag{4.2}$$

Combining equations (4.1) and (4.2), and ignoring any elevation differences across the orifice while assuming the exit velocity is significantly larger than the fluid velocity in the nozzle chamber (u_{d_2} >> u_1), the exit velocity of the droplet is found to be:

$$u_{d_2} = \sqrt{\frac{2g\Delta H}{1 + k_o}} \tag{4.3}$$

where ΔH is the gauge pressure head measured inside the nozzle chamber. The trajectory of the droplet after leaving the orifice is governed by the kinetic and kinematic conditions experienced during its flight; which are illustrated in Figure 4-2(B) and Figure 4-2(C).

The forces acting on the droplet include gravity (F_g), a buoyancy force (F_b), and an aerodynamic drag force (F_{dr}) induced by the resultant air velocity (u_{res}) over the droplet, which is the sum of a horizontal wind component (u_a) and the droplet velocity (u_d). The forces acting on the droplet are defined as follows:

$$F_g = \rho_w\, g\, V_d = \frac{\pi}{6}\, \rho_w\, g\, {d_d}^3 \tag{4.4}$$

$$F_b = \rho_a\, g\, V_d = \frac{\pi}{6}\, \rho_a\, g\, {d_d}^3 \tag{4.5}$$

$$F_{dr} = \frac{1}{2}\, \rho_a\, C_d\, A_d\, {u_{res}}^2 = \frac{\pi}{8}\, \rho_a\, C_d\, {d_d}^2\, {u_{res}}^2 \tag{4.6}$$

where the drag coefficient over the droplet (C_d) in equation (4.6) is approximated by the equation presented by Turton & Levenspiel (1986):

$$C_d = \frac{24(1 + 0.173\, Re^{0.657})}{Re} + \frac{0.413}{1 + 16300\, Re^{-1.09}} \tag{4.7}$$

With the Reynolds number given by,

$$Re = \frac{\rho_a u_{res} d_d}{\mu_a} \tag{4.8}$$

The motion of the droplet in the r-direction is subject to Newton's second law of motion prescribed as,

$$\sum F_r = \frac{d}{dt}(m_d\, u_{d_r}) = m_d \frac{d}{dt}(u_{d_r}) + u_{d_r} \frac{d}{dt}(m_d) \tag{4.9}$$

Since the mass of the droplet is assumed to remain constant during flight, equation (4.9) reduces to,

$$\sum F_r = -F_{dr_r} = m_d \frac{d}{dt}(u_{d_r}) \tag{4.10}$$

Using a second order truncated Taylor series, the rate of change of velocity of the droplet can be approximated as,

$$\frac{d}{dt}(u_{d_r}) = \frac{{u_{d_r}}^{t+1} - {u_{d_r}}^{t}}{\Delta t} \tag{4.11}$$

Combining equations (4.10) and (4.11), the kinematic equation governing the motion of the droplet in the r-direction can be expressed as,

$${u_{d_r}}^{t+1} = {u_{d_r}}^{t} - \frac{F_{dr_r}\, \Delta t}{m_d} \tag{4.12}$$

In a similar manner the kinematic equation governing the motion of the droplet in the z-direction is derived to be:

$${u_{d_z}}^{t+1} = {u_{d_z}}^{t} + \frac{(F_b - F_g - F_{dr_z})\, \Delta t}{m_d} \tag{4.13}$$

The speed of the droplet, and trajectory angle relative to the horizontal, at any stage during the flight is obtained from its r and z velocity components as follows:

$$u_d = \sqrt{{u_{d_r}}^2 + {u_{d_z}}^2} \tag{4.14}$$

$$\alpha = \tan^{-1}\left(\frac{u_{d_z}}{u_{d_r}}\right) \tag{4.15}$$

The resultant air velocity over the droplet and relative angle are defined as follows:

$$u_{res_r} = -(u_{d_r} + u_a) \tag{4.16}$$

$$u_{res_z} = -u_{d_z} \tag{4.17}$$

$$u_{res} = \sqrt{{u_{res_r}}^2 + {u_{res_z}}^2} \tag{4.18}$$

$$\beta = \tan^{-1}\left(\frac{u_{res_z}}{u_{res_r}}\right) \tag{4.19}$$

The displacement of the droplet in the radial direction (S_{d_r}) can be obtained by integrating the velocity of the droplet with respect to time:

$$u_{d_r} = \frac{d}{dt}\left(S_{d_r}\right) \tag{4.20}$$

$$\int_{t}^{t+\Delta t} u_{d_r}\, dt = \int_{r_1}^{r_2} dS_{d_r} \tag{4.21}$$

For a small time step, the velocity of the droplet can be approximated as the average velocity over the interval,

$$\int_{t}^{t+\Delta t} u_{d_r}\, dt \approx \left(\frac{{u_{d_r}}^{t} + {u_{d_r}}^{t+\Delta t}}{2}\right)\Delta t \tag{4.22}$$

Combining equations (4.21) and (4.22), the displacement of the droplet in the r-direction can be expressed as,

$$S_{d_{r2}} = S_{d_{r1}} + \left(\frac{{u_{d_r}}^{t} + {u_{d_r}}^{t+\Delta t}}{2}\right)\Delta t \tag{4.23}$$

Similarly, the displacement of the droplet in the z direction can be expressed as,

$$S_{d_{z2}} = S_{d_{z1}} + \left(\frac{{u_{d_z}}^{t} + {u_{d_z}}^{t+\Delta t}}{2}\right)\Delta t \tag{4.24}$$

The flow rate through the orifice is governed by the orifice diameter and droplet exit velocity as follows:

$$\dot{V}_{or} = A_{or}\, u_{d_2} = \frac{\pi}{4}\,(k_{vc}\, d_{or})^2 \sqrt{\frac{2g\Delta H}{1 + k_o}} \tag{4.25}$$

where k_{vc} is a contraction coefficient to account for vena contracta effects that may occur at the inlet of the orifice.

The kinetic and kinematic equations governing the motion of the droplet in flight are programmed in Microsoft Excel 2013 using a time step of $\Delta t = 0.002$ s. The input parameters include the orifice diameter, trajectory angle, nozzle chamber pressure head, nozzle elevation, orifice loss coefficient and contraction coefficient.

Figure 4-3 shows the trajectory of a droplet emitted from an orifice nozzle with a diameter of 1 mm at an initial trajectory angle of 30° and a chamber water pressure head of 0.5 m. The orifice loss coefficient was set to $k_o = 0$ and the contraction coefficient set to $k_{vc} = 1$.

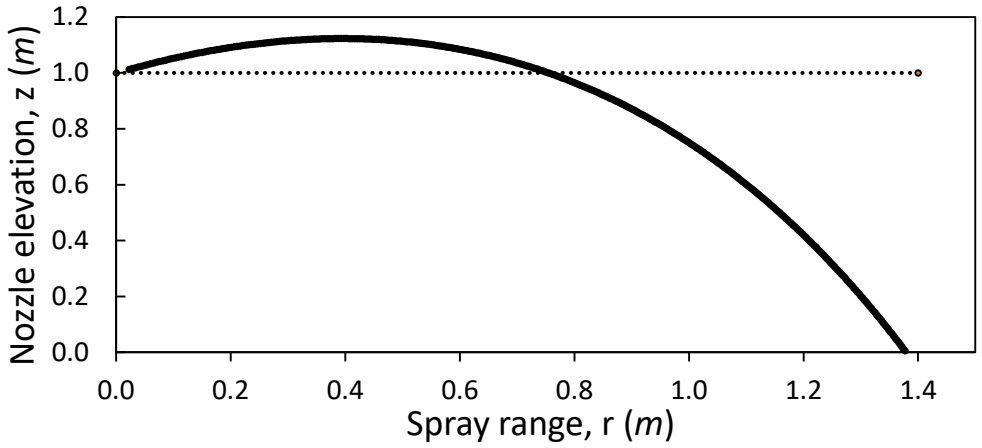

Figure 4-3: Single droplet trajectory modelled in Excel (d_{or} = 1 mm, ΔH = 0.5 m, α = 30°, k_o = 0)

4.1.2 Model validation

Roux (2012) conducted an experimental investigation in which the actual spray range of an orifice nozzle was measured and compared to the spray range predicted by a SDTM in which the losses across the orifice nozzle were ignored.

Roux (2012) presented the results in terms of a spray range deviation which shows the percentage deviation of the actual spray range from that predicted by the SDTM. The experiment was conducted for various orifice nozzle pressures, trajectory angles, nozzle elevations, and nozzle wall thicknesses. Roux (2012) observed that the nozzle pressure and wall thickness had the most significant impact on the spray range deviation. The influence of these two parameters on the spray range deviation is shown in Figure 4-4.

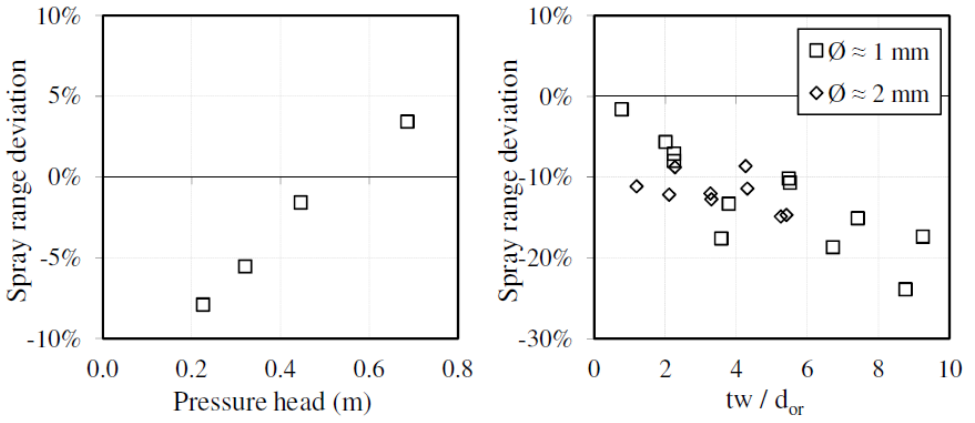

(a) Effect of pressure head on the spray range deviation

(b) Effect of orifice diameter and wall thickness on the spray range deviation

Figure 4-4: Spray range deviation (Roux, 2012)

The results show that for a pressure head below 0.8 m, and a wall thickness to orifice diameter ratio of $t_w/d_{or} \leq 2$, the spray range deviation of the orifice nozzle is within 10% of that modelled by the SDTM. To more accurately model the volume

flow rate and spray trajectories of an orifice nozzle, the losses incurred across the nozzle should be taken into account.

An attempt was made in this study to quantify the orifice loss coefficient (k_o) and contraction coefficient (k_{vc}) for an orifice nozzle with a ratio $t_w/d_{or} \leq 2$, operating at a pressure head under 0.8 m. This was achieved by measuring the spray range and volume flow rate through four orifice nozzles with varying diameters, and then adjusting the orifice loss coefficient and contraction coefficient in the SDTM to match the measured results.

The diameters of the four orifice nozzles were specified to be 1.3 mm, 1.5 mm, 1.6 mm, and 1.8 mm. The spray range and volume flow rates were measured for various pressure heads at a trajectory angle of α = 0°, and nozzle elevation of 3 m. The orifice nozzles were machined radially through the wall of a 150 mm long PVC pipe with a diameter of 40 mm and a wall thickness of 2 mm.

On measuring the machined orifice diameters under a 100 micron microscope, they were found to be larger than the specified drill bit size. The measured orifice diameters, and the wall thickness to orifice diameter ratio are presented in Table 4-1.

Table 4-1: Measured nozzle orifice diameters and wall thickness to orifice diameter ratio

Measured orifice diameter (d_{or}):	1.35	1.66	1.64	1.94
t_w/d_{or}	1.48	1.21	1.22	1.03

The measured spray range of the four orifice nozzles are shown in Figure 4-5. In each case, the measured spray range was found to be less than the spray range predicted by the SDTM when orifice losses are ignored ($k_o = 0$). When the orifice loss coefficient is adjusted to $k_o = 0.5$, the spray range of the SDTM better matches the measured spray range of the orifice nozzles.

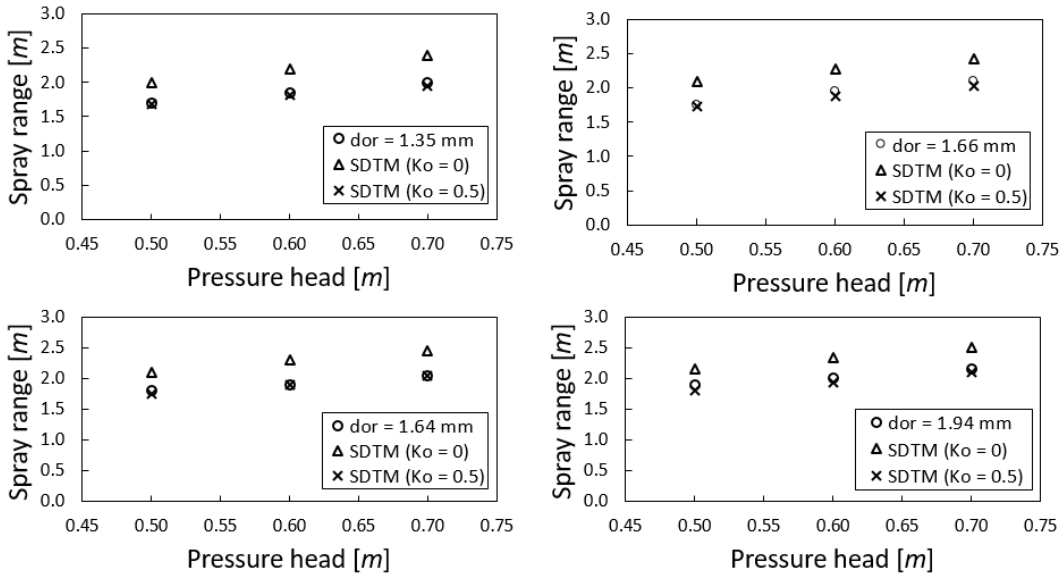

Figure 4-5: Spray range of a single orifice nozzle for various orifice diameters at a pressure head of 0.5 m, elevation of 3.0 m, and trajectory angle of 0°

Cengel & Cimbala (2010, 367) advocate the loss coefficient for a sharp-edged inlet from a larger chamber into a smaller conduit to be k_o = 0.5. The small orifice nozzles machined into the wall of the larger diameter sprinkler pipe constitute a similar sharp-edged reduction in water flow. An orifice loss coefficient of k_o = 0.5, therefore, appears to be consistent with known literature. This approximation of the orifice loss coefficient proved to match the measured data well, as shown in Figure 4-5.

The volume flow rates measured through each of the orifice nozzles are presented in Figure 4-6. Once again, the SDTM over predicted the actual flow rates when orifice losses were ignored. With the orifice loss coefficient adjusted to k_o = 0.5, the model better represented the measured results. Adjusting the contraction coefficient, however, did not improve the accuracy of the SDTM in modelling the orifice flow rates; hence vena contracta effects at the orifice inlet are ignored, and the contraction coefficient is set to k_{vc} = 1 in the SDTM.

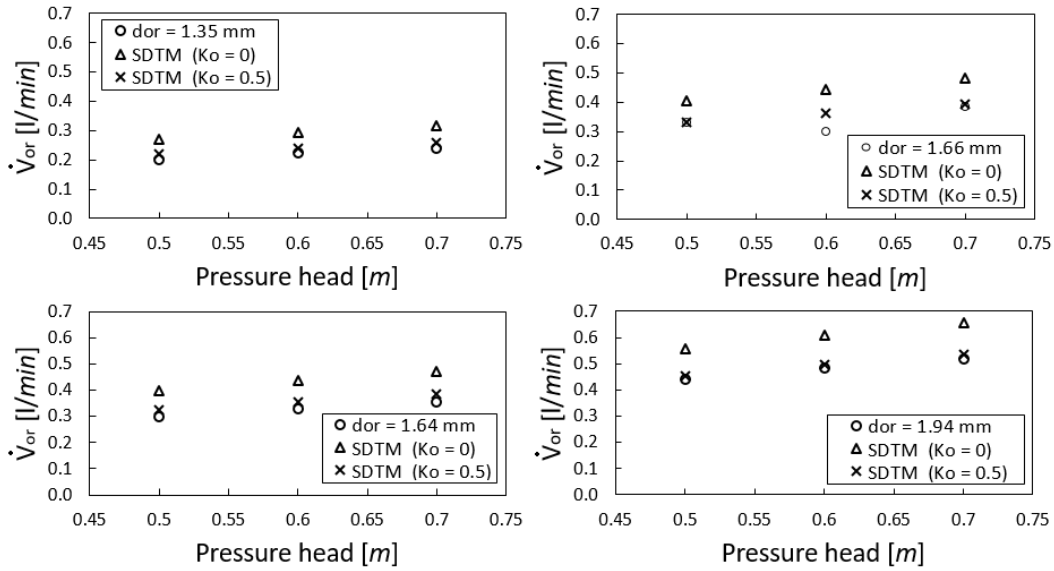

Figure 4-6: Comparison of the measured and modelled orifice nozzle flow rates for various orifice diameters and pressure heads

Table 4-2 presents the percentage deviation of the measured volume flow rates and spray ranges from that evaluated using the SDTM with a loss coefficient of k_o = 0.5.

Table 4-2: Percentage deviation of flow rate and spray range for the SDTM and measured data

Pressure head (*m*)	% Spray range deviation				% Flow rate deviation			
	Orifice diameter (mm)				Orifice diameter (mm)			
	1.35	*1.66*	*1.64*	*1.94*	1.35	1.66	1.64	1.94
0.5	1.2	1.1	2.8	5.3	-10.6	-1.2	-9.1	-2.7
0.6	1.6	3.6	0.0	3.0	-7.1	-22.6	-7.6	-2.7
0.7	2.5	3.8	0.0	2.3	-9.2	-2.6	-8.5	-3.7

The model predicts the spray range to within approximately 5% of that which was measured, and the flow rate to within approximately 10%. The 22.6% flow rate deviation encountered for the 1.66 mm diameter orifice at 0.6 m pressure head is ignored as an outlier, as the measured flow rate does not behave consistently with the trend shown in Figure 4-6.

By accounting for the losses incurred across the orifice nozzle in the SDTM, the accuracy of the model in simulating the flow rate and spray range has been improved. This holds true for an operating pressure head under 0.8 m and a wall thickness to orifice diameter ratio of $t_w/d_{or} \leq 2$.

4.2 Orifice set

An orifice set model (OSM) is developed in order to model the volume flow rate through an orifice set and the resulting spray distribution profile. The OSM relies on the SDTM to evaluate the volume flow rate and trajectory profile of each nozzle in the orifice set. The distribution profile of the orifice set is then the combination of the single orifice nozzle trajectories, and the volume flow rate of the orifice set ($\dot{V}_{os}$) is the sum of the flow rates through each of the orifice nozzles:

$$\dot{V}_{os} = \sum_{i=1}^{n} \dot{V}_{or_i} \tag{4.26}$$

where n is the number of orifice nozzles in the orifice set. The OSM input parameters include: the number of orifice nozzles comprising the orifice set; the orifice nozzle diameters and trajectory angles relative to the transverse axis of the sprinkler pipe; the operating pressure head in the sprinkler pipe, and the elevation of the sprinkler pipe above a target spray plane. A modelled spray distribution pattern of an orifice set is show in Figure 3-5.

To help visualise the water distribution beneath an orifice set, the OSM estimates the water application rate (AR) on a spray plane beneath each of the trajectory streams. During operation an orifice nozzle emits a jet-stream of water that consequently breaks into droplets during flight. These droplets fall to the soil surface having a certain degree of scatter. To more realistically model the application rates beneath a trajectory stream, the stream scatter on impact with a spray plane is taken into account.

Roux (2012) conducted an experimental investigation of the spray scatter of an orifice nozzle with a 2 mm diameter. The scatter of the trajectory stream was measured using a matrix array of 50 square collectors, each with a length and width of 0.02 m, placed beneath the impact point of the trajectory stream.

The spray scatter results are presented in Figure 4-7; expressed in terms of a water mass flux (G_w) at the spray range (r) of the trajectory stream. The spray scatter proved to be independent of the nozzle pressure head, with a change in pressure only increasing the spray range. The spray angle, however, did influence the spray scatter such that a larger trajectory angle resulted in an increased spray scatter. The maximum spray scatter was found to occur at a trajectory angle of α = 30°. Spray trajectories, not exceeding the horizontal, have a more concentrated spray scatter.

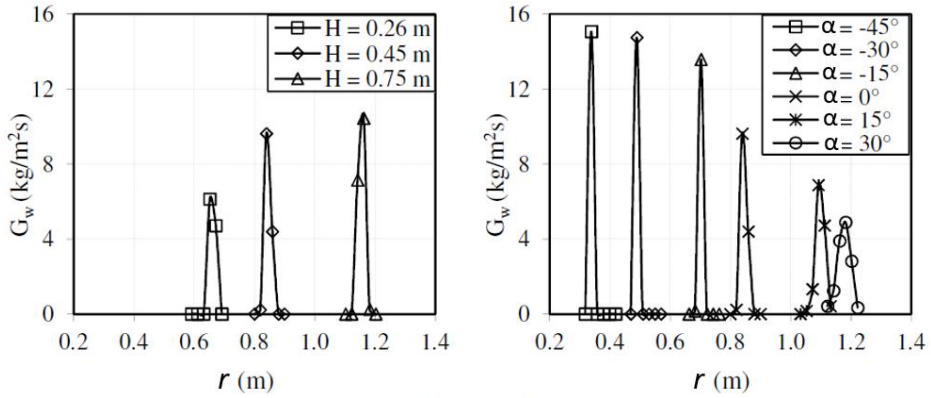

(a) Spray scatter with a spray angle of 0° and various pressure heads

(b) Spray scatter with a pressure head of 0.45 m and various spray angles

Figure 4-7: Orifice nozzle spray scatter at a height of 0.5 m for various pressure heads and spray angles (Roux, 2012)

From Figure 4-7 it appears the scatter of a trajectory stream is distributed over a radial distance approximately 10% in magnitude of that of the spray range of the trajectory stream. Based on the results presented by Roux (2012), two methods are employed to approximate the radial scatter of the trajectory streams: (1) a variable scatter approximation, and (2) a fixed scatter approximation.

The variable scatter approximation assumes the radial scatter of a trajectory stream (S_{sc_r}), on a given spray plane, spans a bandwidth with a distance that is 10% of that of the trajectory spray range (r_{sr}). The scatter bandwidth is equi-spaced about the trajectory stream's point of impact as modelled by the SDTM. The radial scatter of the i^{th} trajectory stream of an orifice set is given by:

$$S_{sc_{r_i}} = 0.1 \cdot r_{sr_i} \tag{4.27}$$

The fixed scatter approximation, on the other hand, assumes the radial scatter to be equitably distributed over a fixed bandwidth selected to be 10% of the spray range of the farthest spray trajectory on the spray plane:

$$S_{sc_r} = 0.1 \cdot r_{sr_{max}} \tag{4.28}$$

Figure 4-8 shows the two scatter bandwidth approximations at various spray planes for three trajectory streams of an orifice set. It can be seen that the scatter of a trajectory stream becomes more concentrated at smaller trajectory angles using the variable scatter approximation, but remains constant along a spray plane for the fixed scatter approximation.

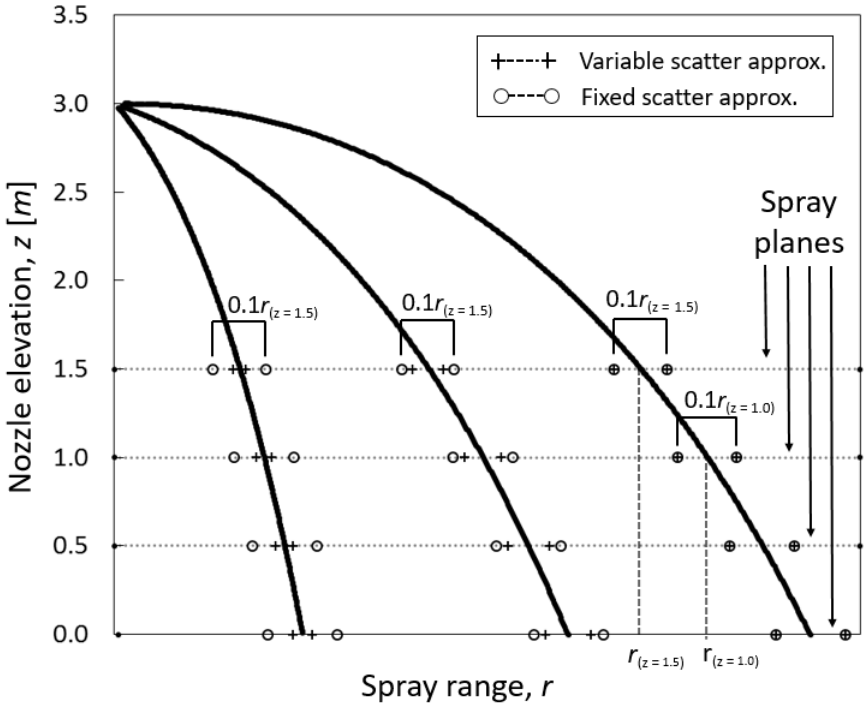

Figure 4-8: Illustration of scatter approximations

Using the spray scatter approximations, the application rates on a spray plane beneath an orifice set can be modelled. This is done by segmenting the spray plane into virtual compartments and summing the volume flow rate contributions each spray trajectory makes into a compartment. It is assumed the volume flow rate of a trajectory stream is equitably distributed over the radial scatter bandwidth.

The volume flow rate that a trajectory stream contributes to a compartment is the product of the stream volume flow rate ($\dot{V}_{or}$) and the fraction of the radial scatter bandwidth (S_{sc_r}) that the virtual compartment occupies, and is defined as the volume flow rate fraction (ε):

$$\varepsilon = \frac{r_{vc}}{S_{sc_r}} \cdot \dot{V}_{or} \tag{4.29}$$

where r_{vc} is the radial width of the virtual compartment. The application rate seen by the i^{th} virtual compartment (AR_{vc_i}) is then given by the total volume flow rate into the compartment over the compartment area:

$$AR_{vc_i} = \frac{1}{A_{vc}} \sum_{i=1}^{n} \epsilon_i = \frac{1}{A_{vc}} \sum_{i=1}^{n} \frac{r_{vc}}{S_{sc_r i}} \dot{V}_{or_i} \tag{4.30}$$

where ε_i is the volume flow rate fraction of the i^{th} trajectory stream falling into the i^{th} compartment, and A_{vc} is the virtual compartment area given by:

$$A_{vc} = r_{vc} \cdot \theta_{vc} = \frac{S_{sp}}{k} \cdot \theta_{vc} \tag{4.31}$$

where θ_{vc} is the circumferential length of the virtual compartment, S_{sp} is the length of the spray plane that has been compartmentalised, and k is the number of

compartments the spray range is subdivided into. By evaluating the application rate in each virtual compartment, the application rate over the entire spray plane can be modelled.

Figure 4-9 shows the application rates evaluated beneath the trajectory streams of four orifice nozzles using the two scatter approximations. The orifice nozzles have a diameter of 1.3 mm and trajectory angles of 0°, -25°, -40°, and -55°. The operating pressure head is 0.2 m and the nozzle elevation is 3 m. The spray plane is 1.2 m in length and is divided into 100 virtual compartments. The spray range of the trajectory streams, as evaluated by the SDTM, are 1.09 m, 0.92 m, 0.75 m, and 0.54 m. The scatter of each trajectory stream is approximated using equations (4.27) and (4.28), and the application rate in each compartment is evaluated using equation (4.30).

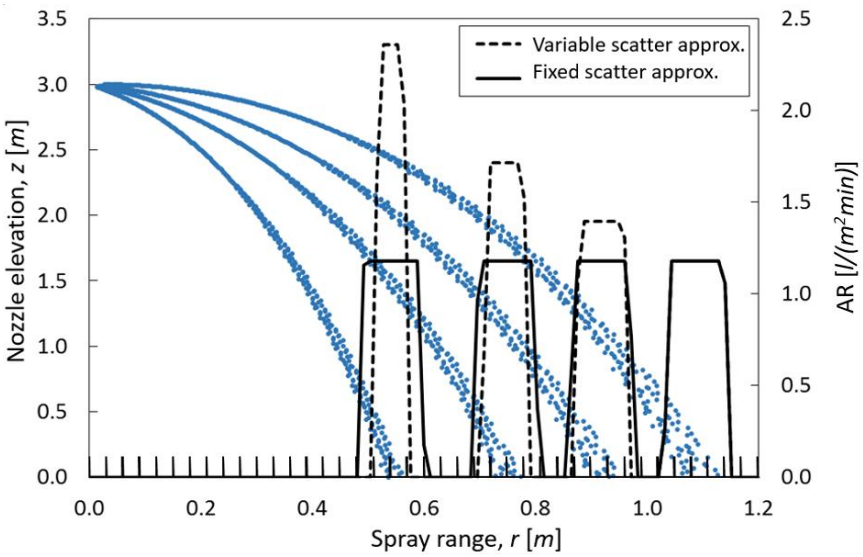

Figure 4-9: Mass flux under trajectory streams on compartmentalised spray plane

The effects of the two scatter approximations on the application rates modelled on a spray plane are illustrated in Figure 4-9. As the scatter of a trajectory stream becomes more concentrated at smaller trajectory angles, the application rate evaluated using the variable scatter approximation increases since the applied volume of water is distributed over a smaller scatter area. The fixed scatter approximation, on the other hand, reflects a more uniform application rate under each stream. Both scatter approximations provide useful insight into the performance of an orifice set, which are used in the orifice set design process.

The variable scatter approximation reflects the instantaneous watering conditions at a spray plane; that is, it provides a realistic indication of the instantaneous application rate on the soil at the moment of impact. A large instantaneous application rate is likely to exceed the soil infiltration capacity and result in localised runoff on the soil surface.

The fixed scatter approximation, on the other hand, provides a snap-shot in time of the application rate the soil surface experiences after some lateral water redistribution has occurred. A high application rate, on impact, will exceed soil

infiltration rates and localised lateral water redistribution will occur following a process illustrated in Figure 4-10.

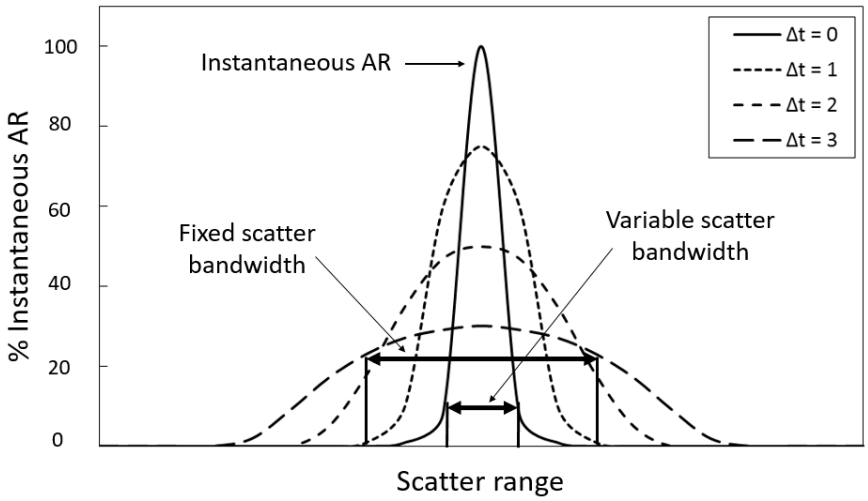

Figure 4-10: Dynamic application rate dispersion profile

The lateral redistribution of the water, over a differential time period Δt, effectively increases the soil surface area over which the irrigated water is distributed. Local redistribution of the water will occur until it is distributed over a sufficiently large soil surface area and is absorbed. The fixed scatter approximation shows the application rate experienced by the soil surface after a period of time in which lateral water redistribution has occurred.

The actual extent of the lateral redistribution that occurs around a trajectory stream is difficult to estimate, and depends on a number of factors, some of which are dynamic in nature: including the soil infiltration rate, soil moisture content, the slope of the soil surface, residue matter on the soil surface etc.

However, by using the fixed scatter approximation, the application rates beneath an orifice set are expressed with reference to that occurring under the trajectory stream with the largest scatter bandwidth. The resultant application rate profile under an orifice set is used to gauge the effectiveness of the orifice nozzle arrangement in creating a distribution pattern that provides a even application of water over a spray plane.

The drawback of having a sprinkler with discrete spray trajectories are the spaces between trajectories where there is no direct application of water. The mechanisms of water redistribution are relied on to make water available in the soil regions between trajectories. These mechanisms include the lateral redistribution of water on the soil surface due to high local water application rates, and the lateral movement of the water in the first few sublayers of the soil due to capillary effects.

Figure 4-11 illustrates the lateral redistribution of water between two trajectory streams of an orifice set, and the infiltration of the water into the root zone of the soil. If the spray trajectories are positioned sufficiently close to each other there will be adequate water redistribution for the plants between trajectories to access water. For a plant with a well-established root system, the distance between spray

trajectories may be increased. However, for a plant with a small, shallow root network the trajectories should be spaced closer together.

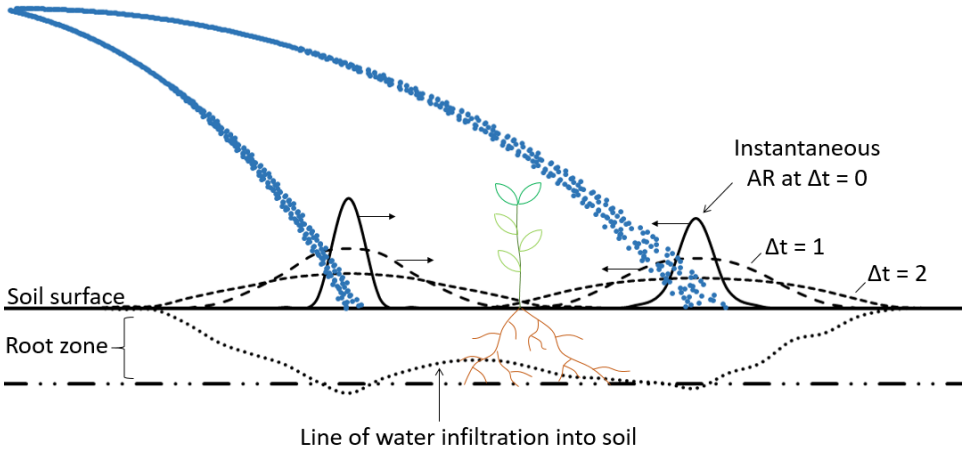

Figure 4-11: Lateral redistribution of water between stream trajectories after a differential time period Δt

When designing an orifice set, the application rates estimated by the fixed scatter approximation are used in determining the required spacing between trajectories to ensure an adequate cover of water over the spray plane. The variable scatter approximation, on the other hand, can be used to gauge whether the instantaneous application rates on the soil surface are too large, which may lead to excessive water runoff, gouging of the top soil, or the propagation of soil surface crusting.

4.3 Sprinkler pipe

4.3.1 Average application rate

The instantaneous application profile under a Powasave sprinkler in the circumferential direction is illustrated in Figure 4-12. Water is applied to the ground through each of the orifice set outlets distributed along the sprinkler pipe.

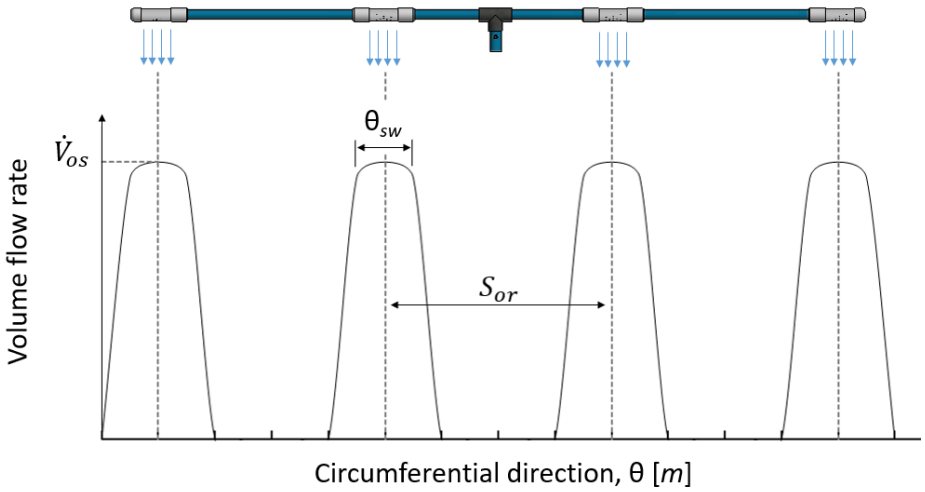

Figure 4-12: Instantaneous application profile in the circumferential direction under a sprinkler pipe fitted with 4 orifice set outlets

The spacing between consecutive orifice set outlets along the sprinkle pipe is given by S_{or}, and the circumferential spray width of a single orifice set outlet is given by θ_{sw}. The circumferential spray width is taken to be equivalent in length to the segment of pipe over which the orifice nozzles of an orifice set are distributed. The average application rate (AAR) beneath the Powasave sprinkler is given by the flow rate of the sprinkler over the sprinkler spray area:

$$A\dot{A}R = \frac{n_{os}\dot{V}_{os}}{A_{ps}} = \frac{n_{os}\dot{V}_{os}}{r_{sw}S_{ps_\theta}} \tag{4.32}$$

The spray area of the sprinkler is taken to be the product of the radial spray width (r_{sw}) and the circumferential length of the sprinkler pipe (S_{ps_θ}).

4.3.2 Average application depth applied over irrigated band

The average application depth (AAD) applied over the annular band irrigated by a Powasave sprinkler is governed by the timer setting of the centre pivot machine, the pivot travel velocity, and the volume flow rate of the sprinkler pipe.

The annular area irrigated by a single Powasave sprinkler installed at a distance R_o from the pivot tower is given by:

$$A_{irr} = 2\pi R_o r_{sw} \tag{4.33}$$

where r_{sw} is the radial spray width of the sprinkler pipe. The total travel time required for the sprinkler to complete a full revolution about the pivot tower is given by:

$$\Delta t_t = \frac{2\pi R_o}{t_s u_p} \tag{4.34}$$

where u_p is the travel velocity of the centre pivot system, and t_s is the timer setting of the tower on which the sprinkler is installed. The AAD applied over the annular band, under a sprinkler pipe fitted with n_{os} orifice sets, is given as follows:

$$AAD = \frac{n_{os}\,\dot{V}_{os}\,\Delta t_t}{A_{irr}} = \frac{n_{os}\,\dot{V}_{os}}{r_{sw}\,t_s\,u_p} \tag{4.35}$$

For a given centre pivot system, the sprinkler radial spray width (r_{sw}) and volume flow rate ($n_{os}\,\dot{V}_{os}$), and pivot travel velocity (u_p) remain constant. Therefore, the only variable influencing the AAD applied over the annular band is the timer setting (t_s). As the timer setting is reduced a larger volume of water is applied over the annular band, thereby increasing the AAD.

4.3.3 Circumferential application profile

The AAD applied over an annular band provides no indication as to the uniformity with which the irrigated water is applied. The application of water under a single orifice set over a 60 second operating cycle is discussed next.

The two distinct phases of a cycle include the travel period in which the orifice set is moving, and the stop period in which the orifice set is stationary. The timer setting dictates the length of the two periods. The travel time of a cycle is given by:

$$t_{tr} = 60 \cdot t_s \tag{4.36}$$

And the stop time of a cycle is given by:

$$t_{st} = 60(1 - t_s) \tag{4.37}$$

The total volume of water applied by a sprinkler during a cycle is a combination of the water volume applied while the sprinkler is in motion, and the volume of water applied while the sprinkler is stationary. The volume of water applied under a single orifice set during the travel and stop periods of a cycle is given as follows:

$$V_{os_{(tr)}} = \dot{V}_{os} \cdot t_{tr} \tag{4.38}$$

$$V_{os_{(st)}} = \dot{V}_{os} \cdot t_{st} \tag{4.39}$$

A ratio of the two volumes yields the following relation:

$$\frac{V_{os_{(st)}}}{V_{os_{(tr)}}} = \frac{1}{t_s} - 1 \tag{4.40}$$

From equation (4.40) it is evident that as the timer setting is decreased the volume of water applied during a stop period constitutes a larger portion of the total water volume applied during a cycle. The application depths applied during the travel and stop periods of a cycle are governed by the areas over which the respective water volume is distributed. The area over which water is applied during the travel period in a cycle is given by:

$$A_{cyc_{(tr)}} = r_{sw} S_{tr} \tag{4.41}$$

Where S_{tr} is the distance travelled by the sprinkler in a cycle:

$$S_{tr} = u_p \cdot 60 t_s \tag{4.42}$$

The application depth applied under a single orifice set outlet during the travel portion of the cycle is:

$$AD_{tr} = \frac{V_{os_{(tr)}}}{A_{cyc_{(tr)}}} = \frac{\dot{V}_{os}}{r_{sw}\, u_p} \tag{4.43}$$

Equation (4.43) is independent of the timer setting and remains constant for a given orifice set design and centre pivot system. It is referred to as the base application depth and is the minimum depth of water applied under an orifice set. The base application depth is always applied over the annular band since the orifice set moves at a constant velocity during travel periods.

During stop periods, additional water is applied over and above the base application depth. The additional water is applied over an area given by the product of the spray width of the orifice set in the radial and circumferential directions:

$$A_{cyc_{(st)}} = r_{sw}\, \theta_{sw} \tag{4.44}$$

The application depth under the orifice set during a stop is then given by:

$$AD_{st} = \frac{V_{os_{(st)}}}{A_{cyc_{(st)}}} = \frac{\dot{V}_{os}\, t_{st}}{r_{sw}\theta_{sw}} \tag{4.45}$$

The total application depth (AD_t) during a full 60 second cycle is given by the sum of the application depths during the travel and stop periods of the cycle:

$$AD_t = AD_{tr} + AD_{st} = \frac{\dot{V}_{os}}{r_{sw}\, u_p} + \frac{60 \cdot \dot{V}_{os}}{r_{sw}\theta_{sw}}(1 - t_s) \tag{4.46}$$

In equation (4.46) it is observed that when the timer setting is set to t_s = 1, then the application depth beneath the orifice set in a cycle is the base application depth. However, when the timer setting is decreased, the total application depth is increased. The additional water is applied at a fixed point during the stop. The ratio of the application depths applied during the travel and stop periods of a cycle is:

$$\frac{AD_{st}}{AD_{tr}} = \frac{u_p}{\theta_{sw}} t_{st} = \frac{u_p}{\theta_{sw}} \cdot 60(1 - t_s) = \zeta(1 - t_s) \tag{4.47}$$

Equation (4.47) expresses the proportion water depth applied during the stop in relation to the base application depth. This provides an interesting insight into the application depth profile to be expected in the circumferential direction beneath an orifice set for different timer settings and ζ values in equation (4.47). For a given centre pivot system, the travel speed will be constant, and therefore the magnitude of ζ in equation (4.47) is altered by changing the circumferential spray width of an orifice set (θ_{sw}).

Figure 4-13 illustrates the effects of changing the circumferential spray width of an orifice set on the magnitude of the peak AAD applied during the stop period of a 60 second cycle for a constant timer setting and travel speed.

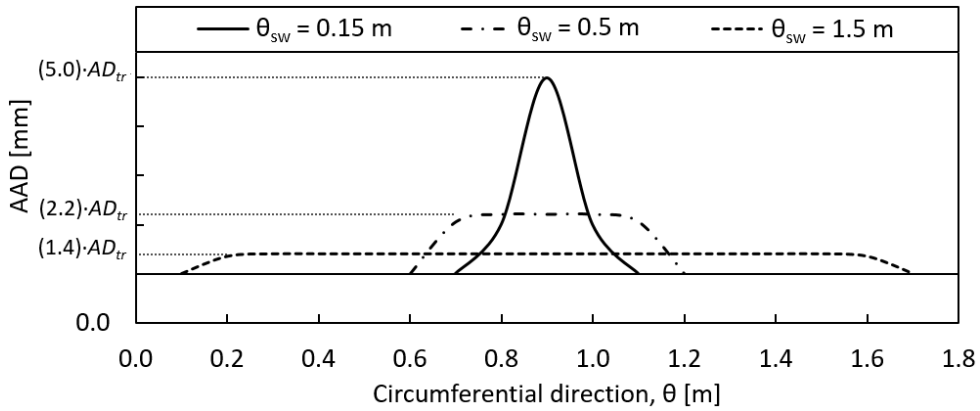

Figure 4-13: Effect of circumferential spray width (θ_{sw}) on the magnitude of the peak AAD for a constant timer setting of t_s = 0.6 and travel speed u_p = 1.5 m/min

It is evident, that as the circumferential spray width of the orifice set increases the magnitude of the peak AAD is reduced, since the applied water is distributed over a larger area. The smaller the spray width, the more exaggerated and pronounced the peak AAD becomes. Figure 4-14 illustrates the effect of various timer settings on the magnitude of the peak AAD applied during a cycle for a constant ζ value. As the timer setting decreases, the magnitude of the peak AAD is increased.

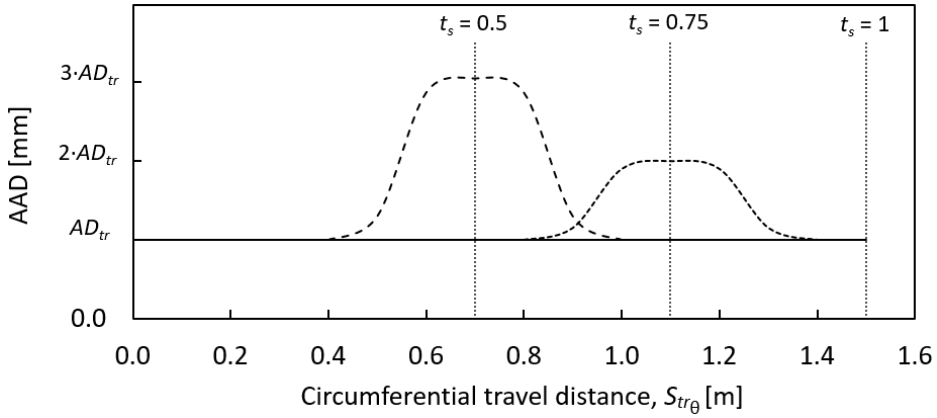

Figure 4-14: Effect of timer setting on magnitude and position of peak AAD in a 60 second cycle for a constant $\zeta = 4$ ($u_p = 1.5$ m/min, $\theta_{sw} = 0.375$ m)

Based on Figure 4-13 and Figure 4-14 it appears the larger the circumferential spray width of the orifice set the more uniform the AAD becomes over a 60 second cycle. The most uniform AAD can be achieved when the circumferential spray width is equivalent in magnitude to the travel speed of the pivot (m/min); in which case $\zeta = 1$. The effect of reducing the timer setting of the pivot is to increase the magnitude of the peak AAD and reduce the distance between peaks of consecutive cycles as the pivot travels smaller distances between stops.

4.4 Summary

In this chapter, a single droplet trajectory model (SDTM) was developed to simulate the volume flow rate and trajectory profiles of water droplets emitted from an orifice nozzle. A validation of the model showed the SDTM capable of approximating the spray range of a trajectory to within 5% accuracy, and the volume flow rate through the orifice to within 10% accuracy. The radial distribution profile and volume flow rate of an orifice set outlet is modelled using the SDTM.

Two scatter approximations were developed to model the instantaneous and time-averaged application rates beneath each of the trajectory streams of an orifice set. The application rate approximations are useful in determining the required spacing between trajectory streams on a plane to achieve an even distribution of water over the radial spray width, and determine the instantaneous application rates experienced at the soil surface.

The necessary theory to evaluate the average application rates (AAR) and average application depths (AAD) applied in the annular band beneath a Powasave sprinkler was then presented. Finally, a model of the AAD profile beneath an orifice set as it travels in the circumferential direction for a single operating cycle is developed. The models shows the shape and magnitude of the AAD profile to be dependent on the timer setting of the centre pivot and the circumferential spray width of the orifice set.

In conclusion, the sprinkler model developed in this chapter provide all the necessary relations to design a Powasave sprinkler package for specified operating conditions on a centre pivot system.

5 Experimental work

5.1 Overview

Water distribution tests were conducted in the field under a centre pivot system located on the Elsenburg agricultural farm in the Western Cape, South Africa. The objectives of the water distribution tests were two-fold:

1) Measure the coefficient of uniformity (CU) and distribution uniformity (DU) under three different sprinkler types, namely; the Nelson D3000 Sprayhead sprinkler, the Nelson S3000 Spinner sprinkler, and the Powasave sprinkler. The objective of the experiment is to evaluate the distribution efficiencies of the three types of sprinklers under normal operating conditions in the field, and compare their performances.

2) Determine the effects of round collectors and rectangular collectors on the measured DU and CU of the sprinklers; to determine how best to measure the performance of sprinklers with discrete trajectories.

The 22 Ha centre pivot irrigation system is fitted with a sprinkler package comprised of the Nelson D3000 Sprayhead sprinkler and the Nelson S3000 Spinner sprinkler. To facilitate the testing of all the Powasave sprinkler, under similar operating conditions in the field, the pivot was fitted with 7 Powasave sprinklers. Water distribution tests were conducted under each of the three sprinkler types in designated test zones using both round collectors and rectangular collectors arranged in different configurations.

Water distribution tests were also conducted under the unmodified centre pivot system, fitted with the D3000 Sprayhead and S3000 Spinner sprinkler package, in an ‘as-is’ analysis of the system’s DU and CU. The ‘as-is’ analysis provided a benchmark against which the various sprinkler performances could be compared.

The physical properties measured during the experimental investigation include the volume of water caught in the collectors positioned under the sprinklers during water distribution tests, the pressure distribution in the radial supply pipe of the centre pivot, and the field weather conditions during the distribution tests. The field layout, test apparatus, measurement equipment, water distribution test procedures, and data processing will be discussed in this chapter.

5.2 Field layout

A satellite view of the field irrigated by the Elsenburg centre pivot system is shown in Figure 5-1. The lines labelled 1 and 2 are the turning points of the centre pivot system. The system was set to rotate approximately 300° about the pivot tower, and would change direction when either of the turning points were reached.

Water distribution tests were conducted along three radial lines extending from the pivot tower, labelled A, B and C in Figure 5-1. These radial lines were selected because they include the highest and lowest points of the field, and the most level portion of the field.

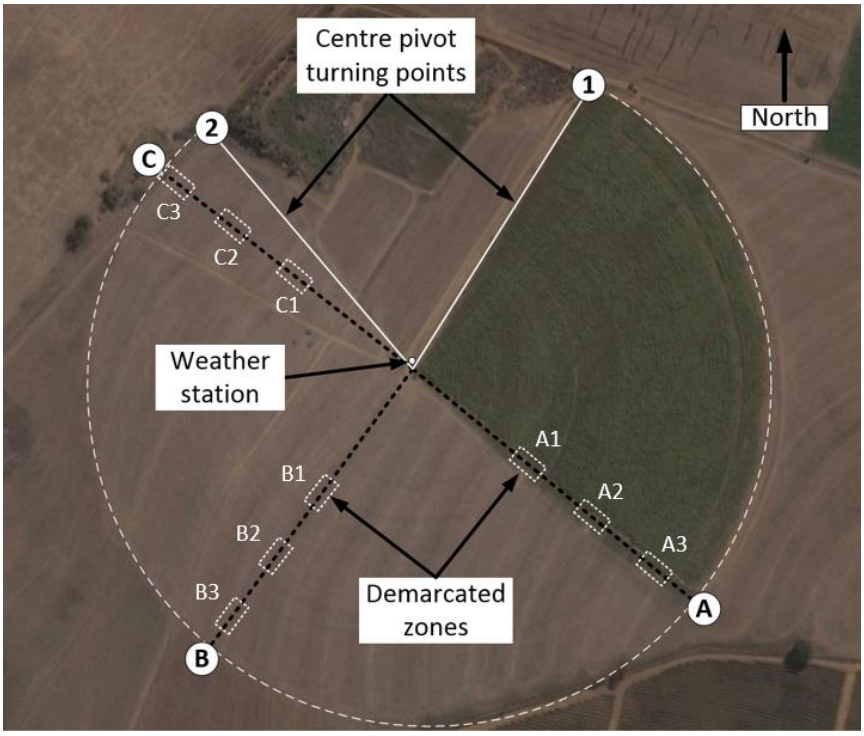

Figure 5-1: Satellite view of the field irrigated by the 22 Ha Elsenburg centre pivot system

An approximation of the elevation profiles along each of the radial test lines is shown in Figure 5-2. The elevation profiles were generated using Google Earth Pro.

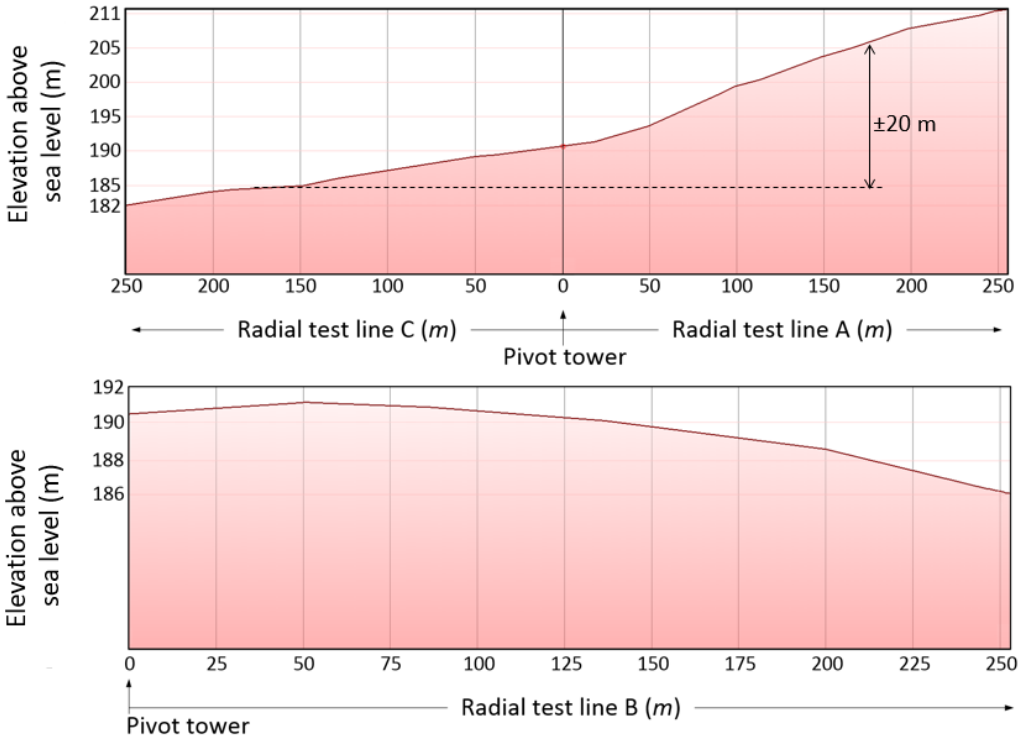

Figure 5-2: Field elevation profiles along radial lines A, B, and C

The highest point in the field occurred at the end of radial line A at approximately 211 m above sea level, and the lowest point in the field occurred at the end of radial line C, approximately 182 m above sea level. The maximum elevation difference in the field is 29 m occurring between the outermost regions of radial lines A and C.

Since variations in the field elevation influence the pressure distribution in the centre pivot radial supply pipe, distribution tests were conducted along each of the radial lines A, B, and C in Figure 5-1 to account for the fluctuations in the supply line pressure and measure a representative performance of the sprinklers over the field.

Three demarcated zones were selected along each of the radial test lines, as illustrated in Figure 5-1. Each zone along a radial line is situated under a different sprinkler type. The zones were located such that the outer ends of spans 2, 3, and 4 of the centre pivot system passed over them, as shown in Figure 5-3. The three zones were positioned at a radial distance of 106.30 m, 166.70 m, and 227.30 m from the pivot tower. The radial length of each test zone spans a distance of 7 m.

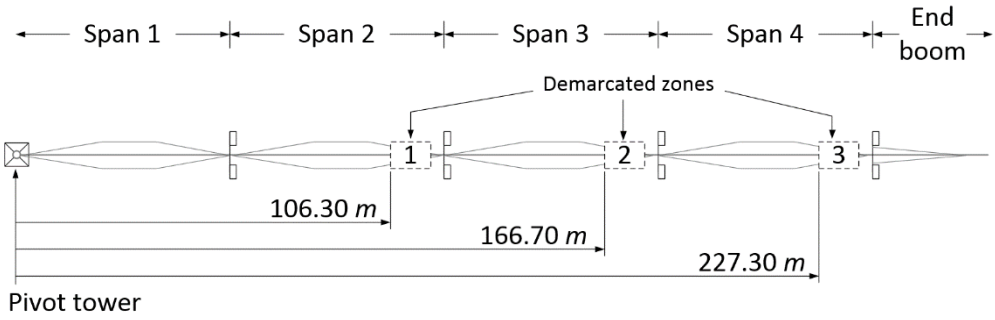

Figure 5-3: Position of zones 1, 2, and 3 relative to the pivot tower

5.3 Apparatus

The test apparatus includes the Elsenburg centre pivot irrigation system installed with the Nelson sprinkler package and fitted with seven Powasave sprinkler assemblies. The Powasave sprinklers were installed at the last seven outlets of the third span. The centre pivot system specifications, operating settings, and details of the installed sprinkler package are presented in this section.

5.3.1 Centre pivot system specifications

The 22 Ha Agrico centre pivot irrigation system is designed to deliver water at a rate of 84 m^3/hr, and applies 3.9 mm of water per pass at a timer setting of 100%.

The centre pivot system specifications are presented in Table 5-1. The system is comprised of four 60.5 m radial supply pipes, or spans, and a 20 m end-boom suspended from the last A-frame tower. The total radial length of the joined supply pipes is 262 m, with an effective irrigated radius of 268 m. The radial supply pipe diameter is telescoped from a 165 mm at the first two spans, to 127 mm in the outer two spans, and 101 mm at the end boom, as indicated in Table 5-1. The supply pipes have outlets spaced at 3.35 m intervals.

Table 5-1: Centre pivot system specifications

Span #	Pipe diameter (*mm*)	Span length (*m*)	Water delivered to crop (m^3/hr)	Number of sprinklers per span	Sprinkler type	Sprinkler series	Sprinkler plate colour
1	165	60.5	4.74	17	Sprayhead	D3000	Brown
2	165	60.5	12.83	18	Sprayhead	D3000	Brown
3	127	60.5	21.24	18	Spinner	S3000	Yellow
4	127	60.5	32.79	18	Spinner	S3000	Yellow
End boom	101	20	12.83	6	Spinner	S3000	Yellow
Total		**262**	**84.43**	**77**			

There are a total of 77 sprinklers installed on the pivot: 17 on the first span, 18 on each of the outer three spans, and 6 on the end-boom.

The operating pressure of the centre pivot system is specified to be 400 kPa at the pivot tower, and is measured by a pressure gauge mounted on the pivot tower. The pressure distribution in the radial supply line of the centre pivot, measured along radial line A in Figure 5-1, is shown in Figure 5-4. The static pressure at the last outlet of each radial supply pipe was measured using a pressure gauge assembly presented in Appendix B. The minimum Nelson sprinkler operating pressure is also shown in Figure 5-4.

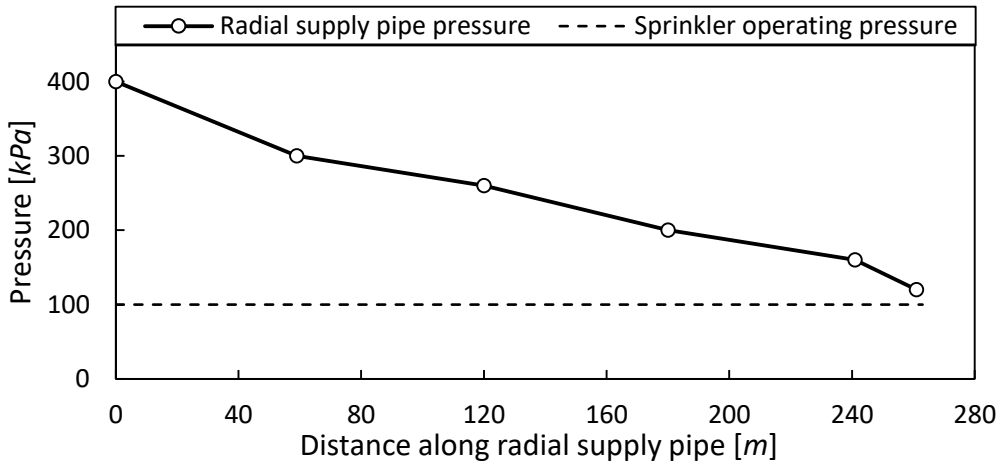

Figure 5-4: Pressure distribution in the radial supply pipe of the Elsenburg centre pivot system measured along radial line A

The timer setting of the centre pivot was set at 60% for the duration of the experimental work, at which the Nelson sprinkler package applies approximately 5 mm of water per pass. The time-averaged speed of the end tower was determined to be 2 m/min. Details of the centre pivot drive system, and end tower speed measurements are presented in Appendix C.1 and C.2.

5.3.2 Installed sprinkler package

The sprinkler package installed on the centre pivot system comprise a combination of the Nelson D3000 Sprayhead sprinkler, the Nelson S3000 Spinner sprinkler,

and the Powasave sprinkler. Figure 2-2 shows the Nelson Sprayhead and Spinner sprinklers that are installed on the centre pivot system.

The Nelson Sprayhead sprinkler is installed on the first two spans of the centre pivot system, and the Spinner sprinkler is installed on the remaining spans and end-boom, as indicated in Table 5-1. Detailed specifications of the nozzle sizes, specified flow rates, and sprinkler spray diameters of the sprinklers installed on the Elsenburg centre pivot system can be found in Table C5 in Appendix C.3. Each sprinkler is fitted with a 100 kPa Nelson Universal-flow pressure regulator, and suspended from the main supply pipe via a semi-rigid drop tube. The semi-rigid drop tube is part 20 mm flexible hose, and part 20 mm rigid PVC tube.

To accommodate the testing of the Powasave sprinklers on the centre pivot system, the last seven S3000 Spinner sprinklers installed on the third span of the centre pivot were replaced with seven Powasave sprinkler assemblies.

Water distribution tests under the D3000 Sprayhead sprinkler were conducted in zones A1, B1, and C1 shown in Figure 5-1*;* distributions tests under the Powasave sprinklers were conducted in zones A2, B2, and C2*;* and distribution tests under the S3000 spinner sprinkler were conducted in zones A3, B3, and C3. The test zones are positioned such that the last seven sprinklers of spans 2, 3, and 4 are influential in the water distribution tests.

The nozzles sizes, flow rates, and spray diameters of the last seven sprinklers installed on spans 2 and 4 are presented in Table 5-2. The spray diameters are those specified by the Nelson Irrigation Corporation for an operating pressure of 100 kPa and sprinkler elevation of 0.9 m above ground level. The spray diameters of the two Nelson sprinklers range between 11 m and 12 m*,* and have an overlap factor (defined as the ratio of the average sprinkler spray diameter to outlet spacing) of 3.5.

Table 5-2: Nelson sprinkler specifications at last seven outlets on span 2 and 4

	Span 2						
	Nelson D3000 Sprayhead (Brown Plate)						
Outlet Number	29	30	31	32	33	34	35
3TN Nozzle size	23	23	23	24	24	25	25
Flow rate (L/min)+	13.2	13.2	13.2	14.6	14.6	15.8	15.8
Spray diameter (m)++	11.4	11.4	11.4	11.7	11.7	12.0	12.0
	Span 4						
	Nelson S3000 Spinner (Yellow plate)						
Outlet Number	65	66	67	68	69	70	71
3TN Nozzle size	35	35	36	36	36	37	37
Flow rate (L/min)+	31.2	31.2	32.7	32.7	32.7	35.0	35.0
Spray diameter (m)++	11.0	11.0	11.0	11.0	11.0	11.0	11.0

+ The 3TN nozzle sizes and flow rates are attached in Figure C2 of Appendix C.3

++ The spray diameter correlations are attached in Figure C1 of Appendix C.3

Figure 5-5 shows a schematic layout of the last seven Nelson sprinklers installed on spans 2 and 4 of the centre pivot system. The positioning of the sprinklers relative to the test zone is clearly illustrated. The sprinklers are suspended at an elevation of 1.0 m to 1.5 m above the ground.

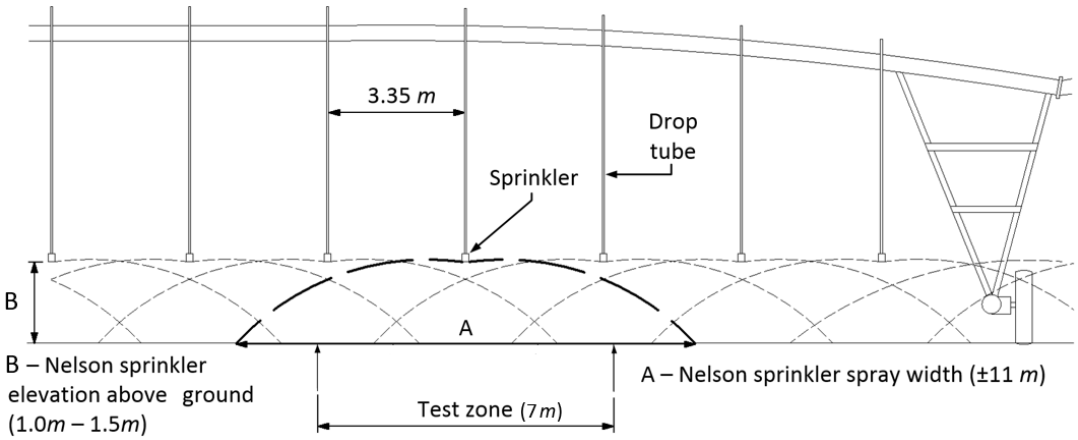

Figure 5-5: The last 7 Nelson Sprayhead and Spinner sprinklers installed on spans 2 and 4

Figure 5-6 shows the schematic layout of the Powasave sprinkler assemblies installed at the last seven outlets of the 3rd span of the centre pivot system. The sprinklers are spaced at intervals of 3.35 m and the sprinkler pipes are positioned at an average elevation of 4.0 m above the ground. The radial spray width of the sprinklers is 4.1 m, and the spray overlap between consecutive Powasave sprinklers is designed to be 0.75 m.

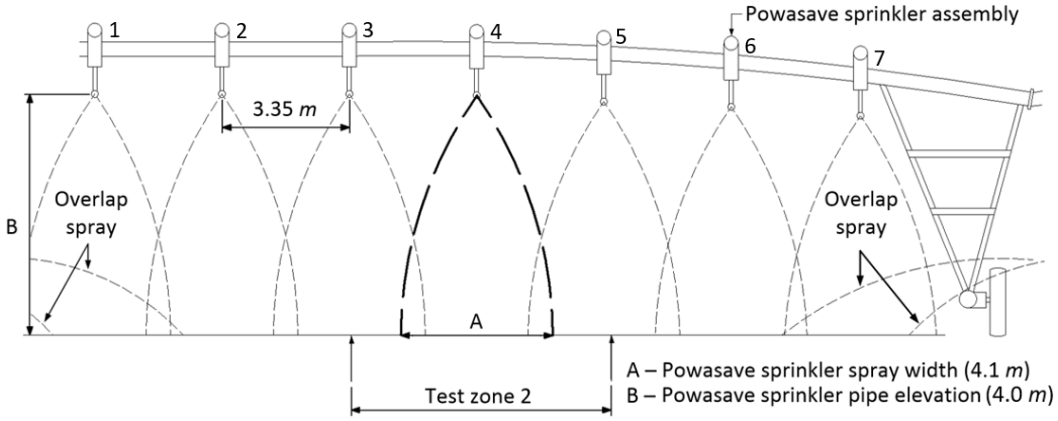

Figure 5-6: Powasave sprinklers installed at last seven outlets of span 3

The assemblies are numbered one to seven, with the assembly installed closest to the pivot tower labelled assembly number one, as indicated in Figure 5-6. Spray from neighbouring Nelson nozzles overlapped with the spray areas of the Powasave sprinklers numbered 1 and 7 in Figure 5-6. These two assemblies were therefore designed for a reduced flow rate to prevent over-watering in the overlap region. It was because of this overlap that it was considered necessary to replace seven Spinner sprinklers with Powasave sprinklers. The seven Powasave sprinklers would provide a sufficiently large spray region in which distribution tests could be conducted without overlap spray from neighbouring Nelson sprinklers interfering with the measurements, which took place under sprinkler assemblies 3,

4, and 5 in Figure 5-6. Powasave sprinkler assemblies 2 through to 6 were identical in design.

5.4 Powasave sprinkler assembly

The specifications of each Powasave sprinkler component are presented next. The Powasave sprinkler assemblies installed on the Elsenburg centre pivot system are shown in Figure 3-1.

The main components of the Powasave sprinkler assembly include: a pressure regulator assembly that receives a supply of water from the main centre pivot supply pipe via a flexible hose; a sprinkler pipe that distributes the water to the ground through four orifice sets spaced along the length of the pipe; a support structure consisting of an aluminium square tube supported at its centre by a bracket assembly, and at its end by cables; and a flexible pool pipe that connects the pressure regulator assembly and sprinkler pipe assembly.

5.4.1 Pressure regulator assembly

Figure 5-7 shows a partially sectioned view of the pressure regulator assembly used to govern the pressure head in the sprinkler pipe. The function of the assembly is to regulate the water level in the vertical riser pipe of the pressure regulator, which determines the static pressure head in the sprinkler pipe.

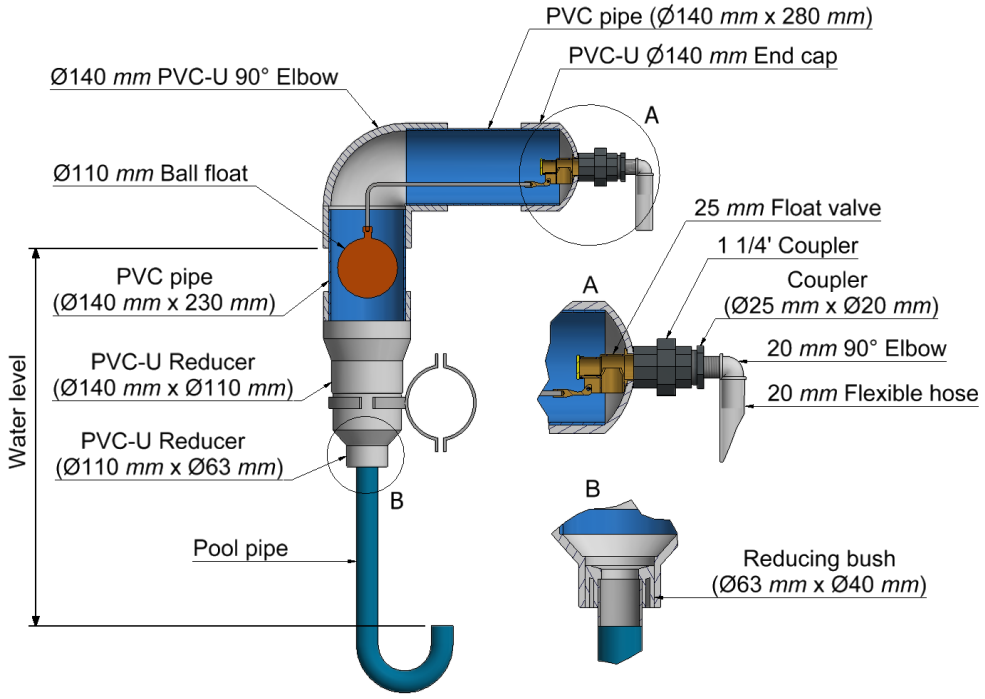

Figure 5-7: Pressure regulator assembly

The water level is regulated by means of a 25 mm float valve seated in an end cap fixed at the end of a horizontal PVC pipe, as illustrated in Figure 5-7(A). The float valve is connected to a 20 mm flexible hose fitted with an Emjay 20 micron in-line filter and attached to the radial water supply pipe, as shown in Figure 3-1. A lever arm, bent through 90°, connects the float valve to a ball float positioned in the

vertical riser pipe. The ball float actuates the lever arm on the float valve and throttles the water flowing in through the valve. The flexible 40 mm pool pipe is used to feed water from the pressure regulator assembly to the sprinkler pipe. The flexible pool pipe accommodates rotation of the sprinkler pipe in the vertical plane.

The water level in the pressure regulator is influenced by the static pressure upstream of the float valve. As the static pressure upstream of the valve increases, a larger actuation force is required to throttle the flow through the valve. Hence, a larger portion of the float needs to be submerged raising the water level in the riser pipe. The water level in the riser pipe will, therefore, fluctuate as the upstream valve pressure fluctuates. The water level measured in the pressure regulator is a direct measure of the static pressure head at the inlet to the sprinkler pipe.

The Powasave pressure regulator assemblies installed on the Elsenburg centre pivot system are required to govern the pressure head in the sprinkler pipe to 0.6 m for a radial supply pipe pressure ranging from 200 kPa to 400 kPa. The operating pressure range in the radial supply pipe is determined in Appendix D.1.

Figure 5-8 shows the pressure head measured in each of the seven pressure regulator assemblies for an upstream valve pressure varying from 200 kPa to 600 kPa. The pressure head is measured at the inlet of the sprinkler pipe by means of a manometer tube attached to a pressure tap. The upstream valve pressure is measured using a 1000 kPa pressure gauge fitted upstream of the ball valve in Figure 5-7(A).

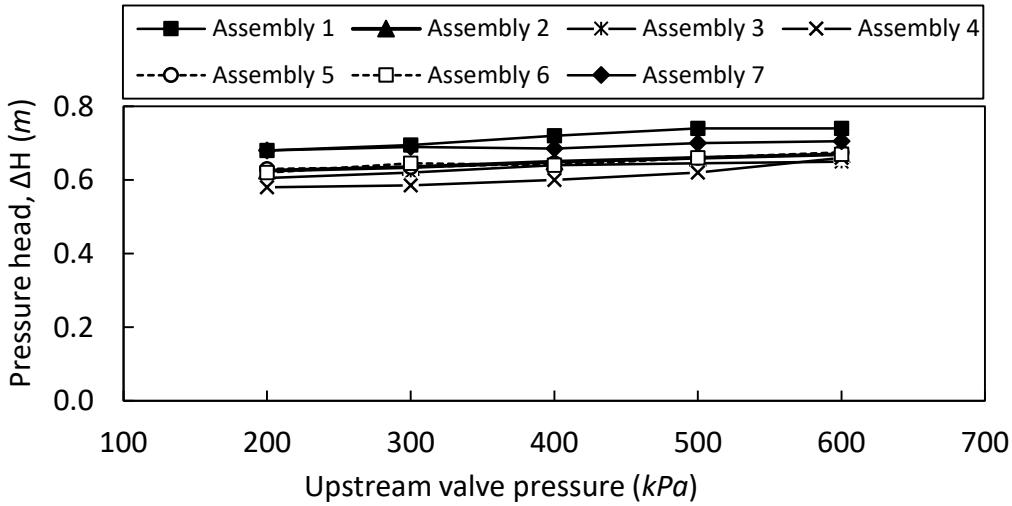

Figure 5-8: Pressure head in pressure regulator assemblies for various upstream valve pressures

The average pressure head measured in assemblies 2 through to 6 over the upstream valve pressure range is 0.637 m; which is sufficiently close to the design requirement of 0.6 m. The average pressure head fluctuation in the pressure regulator assemblies over the pressure range of 200 kPa to 400 kPa is measured to be 0.023 m, which is a variation of approximately 3.6% from the average pressure head of 0.637 m.

Using the SDTM, a pressure variation of 3.6% will result in a flow rate deviation of 2% through an orifice nozzle with a diameter of 1.5 mm designed to operate at a

pressure head of 0.637 m. The radial spray range deviation is 1.8% at an orifice nozzle elevation of 4 m.

The pressure head measured in assemblies 1 and 7 in Figure 5-8 are somewhat higher than the rest of the assemblies. Hence, for the same operating pressure, the float valves of assemblies 1 and 7 had to throttle the incoming flow of water more so than the other assemblies; requiring a higher water level to do so. These sprinklers, however, were not influential in the water distribution tests and served the sole purpose of providing a buffer from the overlap spray of the neighbouring Nelson Sprinklers.

More details of the pressure head measurements of the Powasave pressure regulator assemblies are attached in Table D1 of Appendix D.1.

5.4.2 Sprinkler pipe design

The Powasave sprinklers are required to apply a water depth of 5 mm per pass at a centre pivot timer setting of t_s = 60%. The spray width of the sprinkler is selected to be 4.1 m, to cover the distance between outlets of 3.35 m and provide approximately 0.75 m overlap spray between consecutive Powasave sprinklers. To achieve an application depth of 5 mm per pass at the selected radial spray width, the sprinklers are required to have a flow rate of 24.6 L/min. This was achieved using four orifice sets distributed along the sprinkler pipe each with a design flow rate of 6.29 L/min.

Each orifice set has 21 orifice nozzles with diameters of 1.3 mm and 1.6 mm, which produce a Sauter mean droplet diameter ranging between 2.5 mm and 3.0 mm. The 21 orifice nozzles are distributed over five cross-sectional planes spaced 12.5 mm apart, and are machined into a 150 mm length of polycarbonate pipe with a diameter of 40 mm using a 5-axis CNC machine. The orifice set is designed to operating from an average elevation of 4 m above the ground at a pressure head of 0.6 m. The orifice nozzle diameters and trajectory angles are attached in Table D3 in Appendix D.2.

Figure 5-9 shows the modelled distribution profile of two consecutive Powasave sprinklers installed 3.35 m apart at an elevation of 4 m above the ground, and operating at a pressure head of 0.6 m. The trajectory streams in the overlap region are designed for a reduced flow rate to prevent over watering. This is done by using a smaller orifice nozzle diameter for those trajectories in the overlap region.

The overlap spray of 0.75 m between sprinklers is sufficient to accommodate a 15° field incline angle. The steepest incline angle in the field beneath the Elsenburg centre pivot system occurs along radial line A in Figure 5-2, and is calculated to be approximately 5°. The centre pivot system, however, crosses the steepest incline at right angles. Therefore the actual field incline angle experienced by the Powasave sprinklers is expected to not exceed 5°.

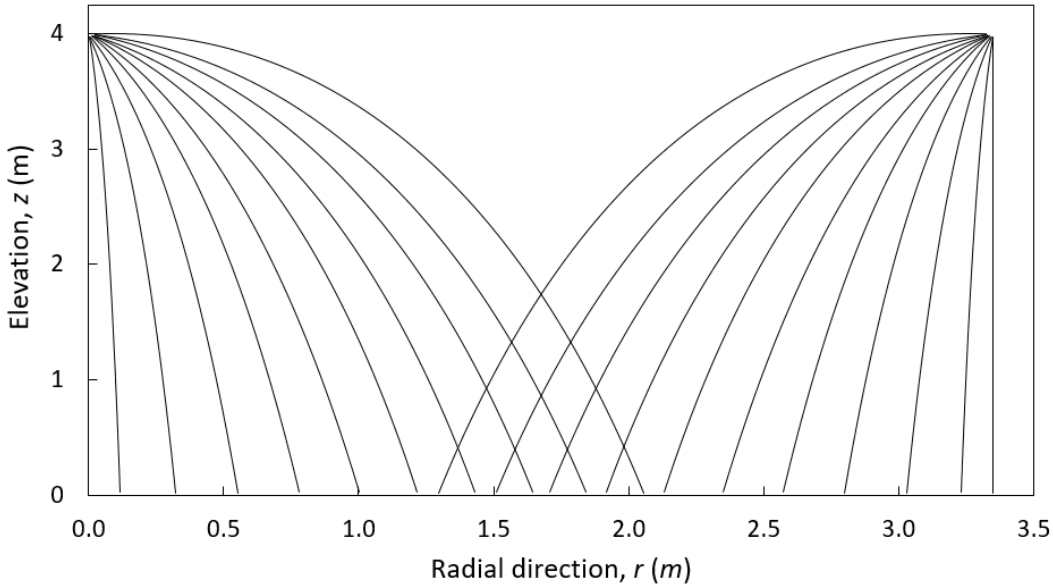

Figure 5-9: Modelled distribution profile of two consecutive Powasave sprinklers installed 3.35 m apart, at an elevation of 4 m, and operating at a pressure head of 0.6 m

To achieve an average application rate (AAR), similar to those under the Nelson sprinklers, the four orifice sets are distributed over a sprinkler pipe with a circumferential length of 6 m. The AAR under the Powasave sprinkler is determined to be 0.25 mm/min, which is similar to the AAR under the Spinner sprinklers that were replaced by the Powasave sprinklers; which were determined to be 0.24 mm/min. The Powasave sprinkler design procedure, using the sprinkler model presented in Chapter 4, is detailed in Appendix D.2.

The Powasave sprinkler pipe assembly is shown in Figure 5-10. The four orifice sets are connected by a PVC pipe with a diameter of 32 mm.

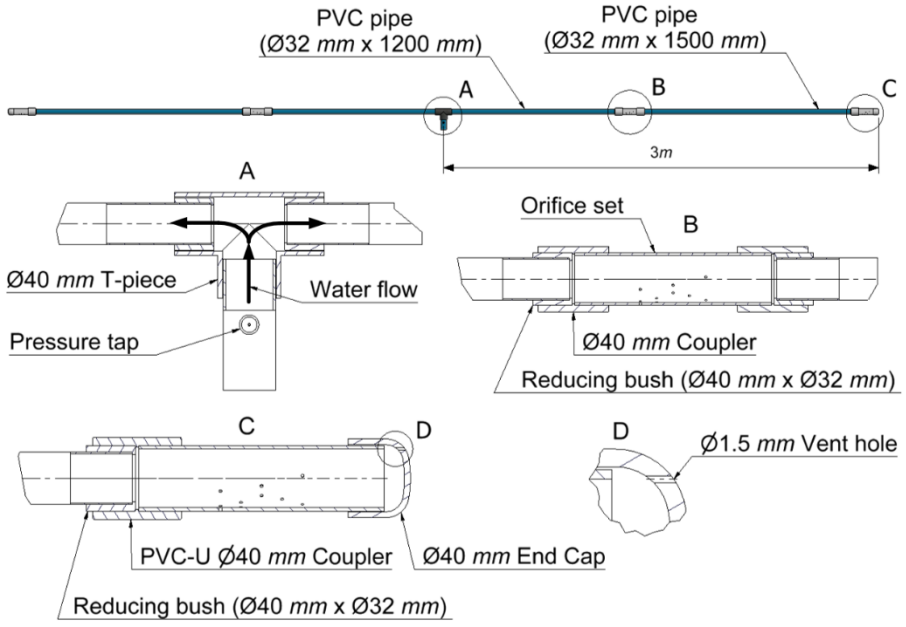

Figure 5-10: Sprinkler pipe assembly with partially sectioned exploded views

Two branches extend from a T-piece situated at the centre of the sprinkler pipe, labelled A in Figure 5-10. Each branch extends a length of 3 m. Water is fed from the pressure regulator into the sprinkler pipe at the T-piece. A pressure tap is mounted at the base of the T-piece in order to measure the static pressure at the inlet of the sprinkler pipe.

A 1.5 mm vent hole is machined into the end caps of the orifice sets mounted on either end of the sprinkler pipe as shown in Figure 5-10(D). The vent hole allows air to escape the sprinkler pipe when the pipe fills with water at the beginning of an irrigation event.

Figure 5-11 shows the measured flow rates through the seven Powasave sprinklers over a supply line pressure range of 200 kPa - 600 kPa. It can be seen that the flow rates vary only marginally over the pressure range. The average volume flow rate for Powasave sprinklers 2 through to 6 is measured to be 20.92 L/min. This flow rate is approximately 15% less than the design flow rate of 24.6 L/min. This reduced flow rate, however, should not significantly affect the radial spray distribution of the sprinklers, as is demonstrated in Appendix D.3.

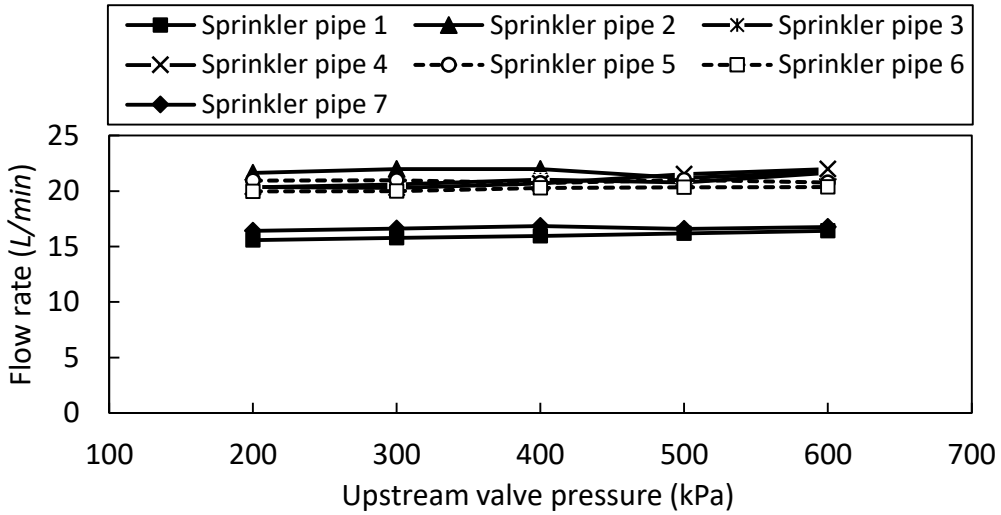

Figure 5-11: Volume flow rates measured through the seven Powasave sprinkler prototypes

Powasave sprinklers number 1 and 7 were fitted with only three orifice sets, and hence have a lower flow rate than the other sprinkler pipes. The average flow rates through sprinklers 1 and 7 is measured to be 16.31 L/min.

5.4.3 Support structure assembly

Figure 5-12 shows the support structure used to suspend the sprinkler pipes from the centre pivot radial supply pipe. The structure consists of a 6 m aluminium square tube beam bolted to the foot of a steel tube leg attached to a bracket. The ends of the aluminium beam are supported by 4 mm steel cables tensioned by turn buckles fixed to the top of the leg. The bracket clamps onto the radial supply pipe of the centre pivot and allows the leg and support beam to freely pivot about the pivot point indicated in Figure 5-12(A). It is necessary for the support structure to be able to pivot in order to ensure the sprinkler pipe remains horizontal during operation.

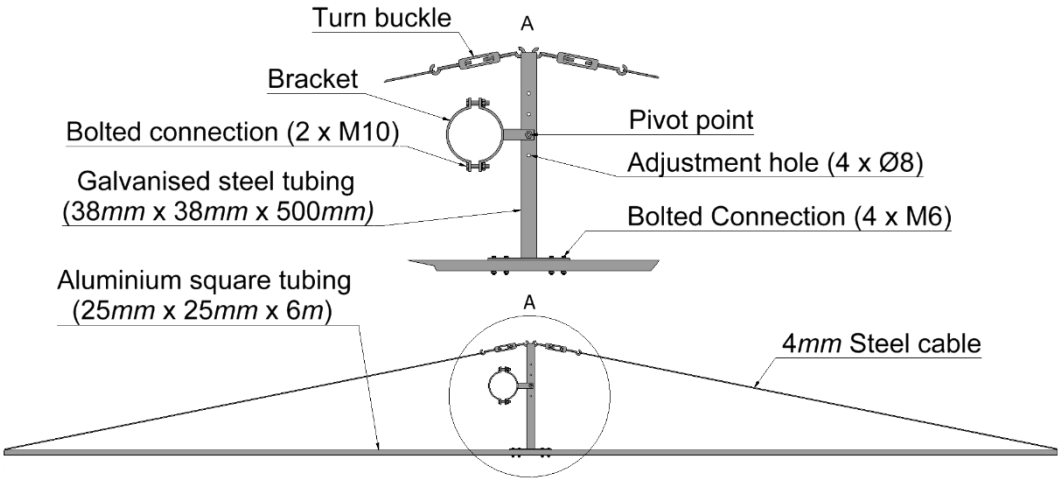

Figure 5-12: Sprinkler pipe support structure

5.5 Measurement equipment

5.5.1 Weather station

A WH2303 Wireless Weather Station was erected near the pivot tower, at the location indicated in Figure 5-1, to sample the field weather conditions during water distribution tests. The station was mount 2.5 m off the ground on a pole.

The weather station consists of a compact outdoor sensor array housed in a waterproof casing. The sensor array transmits the measured weather conditions wirelessly to a data logger console at a 433 MHz transmission frequency. The data is then downloaded off the data logger as a csv file using Weather Smart software, and processed in Excel. The weather station is ICASA approved with a certificate number TA-2016/1422.

The parameters measured during a water distribution test include the air temperature, relative humidity, wind speed, and wind direction. Table 5-3 summarizes the units, range, resolution, and accuracy of the weather station in measuring these parameters.

Table 5-3: WH2303 Weather station specifications

Parameter	Units	Range	Resolution	Accuracy
Air temperature	°C	-40 to 60	0.1	± 1
Wind speed	m/s	0 to 50	0.1	± 1 for < 5 m/s ± 10% for > 5 m/s
Wind direction	deg	0 to 360	1.0	-
Relative humidity	%	1 to 99	1.0	± 5%

The data logger console was set to log the data at 2 minute intervals. The pivot took approximately 20 minutes to cross a test zone. Sampling the weather conditions at 2 minute intervals was considered sufficient to capture the average conditions over the 20 minute duration of a distribution test.

5.5.2 Collectors

Two types of collectors were used during the water distribution tests: a white, plastic round bucket with a diameter of 158 mm and depth of 155 mm; and a white, plastic rectangular container with a width, length, and depth of 150 mm, 210 mm, and 70 mm respectively.

The American Society of Agricultural Engineers (ASAE) recommend using light coloured collectors to reflect solar radiation and hence reduce water evaporation during a distribution test. A 500 mL plastic measuring beaker with 5 mL increments is used to measure the volume of water caught in a collector during a water distribution test.

5.6 Collector layout

Different collector configurations were used for the system distribution tests and zone distribution tests. For the system distribution tests, round collectors are used as is typically done when measuring the uniformity beneath a centre pivot system.

For the zone distribution tests, both round collectors and rectangular collectors are used; each arranged in a different configuration in the test zones. It was decided that distribution tests would also be conducted in the zones using rectangular collectors because of the shortcomings of using round collectors to measure the application uniformity of sprinklers with discrete trajectory streams, like the Powasave sprinkler and Sprayhead sprinkler. The arrangement of the rectangular collectors in the test zones is considered a more reliable collector arrangement to better measure the application uniformity of sprinklers with discrete trajectory streams. The round collector shortcomings are discussed in Appendix E.

The collector configurations used for the system distribution tests and the zone distribution tests are presented next.

5.6.1 System distribution tests

The centre pivot system distribution tests were conducted along radial test line *A*, in Figure 5-1, using round collectors. The collectors were positioned in accordance with the specifications prescribed by the ASAE for measuring the uniformity of water distribution of a centre pivot system (American Society of Agricultural Engineers, 2003).

For a given system distribution test, 68 round collectors were positioned at 3 m intervals along the radial test line. The first collector was positioned at a distance of 63 m from the pivot tower, and the last collector was positioned 264 m from the pivot tower. Collectors were not positioned under the first span of the centre pivot system, as recommended by the ASAE. Figure 5-13 shows the round bucket collectors spaced at 3 m intervals along radial test line A in Figure 5-1.

Figure 5-13: Round bucket collectors positioned along radial test line A

5.6.2 Zone distribution tests: round collectors

Zone distribution tests were conducted using round collectors in the three zones along radial test lines A and B. For a single test event, 24 round collectors were evenly spaced along the radial direction of each of the three test zones of a test line. The collectors in a zone were spaced at 300 mm intervals. Figure 5-14 shows the configuration of the round bucket collectors in zone A2.

A collector spacing of 300 mm was considered a sufficient resolution to measure the distribution uniformities of the sprinkler, based on the premise that sufficient lateral water redistribution would take place on the surface of the soil, or in the first few layers of the topsoil, such that a non-uniform water distribution at a resolution less than 300 mm would have little impact on the ability of a plant, germinating in that 300 mm bandwidth, to access the irrigated water.

Figure 5-14: Round bucket collector configuration in zone A2

5.6.3 Zone distribution tests: Rectangular collectors

Zone distribution tests were also conducted using a matrix of rectangular collectors. For a given distribution test, 220 rectangular collectors were arranged in a matrix array consisting of 10 rows and 22 columns.

The matrix of collectors span an area of 3.3 m x 2.1 m, and are positioned at the centre of a test zone. The collectors are orientated with the rows extending in the radial direction of the field, and the columns extending in the circumferential direction of the field. Figure 5-15 shows the configuration of the rectangular collectors in zone A2.

Figure 5-15: Rectangular collector configuration in zone A2 beneath the Powasave sprinklers

5.7 Test procedure

The centre pivot system was turned on in the mornings and set to automatically turn off when the water pump was shut down in the late afternoons. The timer setting of the centre pivot was set at 60% for the duration of the experimental investigation. The collector setup took place while the pivot moved between the radial test lines, which took approximately 3 hours.

The water distribution test procedure is as follows:

1. The weather station is set up at the pivot tower, and programmed to record the weather conditions at 2 minute intervals.
2. The collectors are setup along the radial test line over which the centre pivot system is to pass next:
    2.1. For system distribution tests, the round collectors are setup along the length of the radial test line as prescribed in section 5.6.1.
    2.2. For zone distribution tests using round collectors, the collectors are setup in the three zones of the radial test line as prescribed in 5.6.2.

2.3. For zone distribution tests using the matrix of rectangular collectors, the collectors are setup in a single zone of a radial test line as prescribed in 5.6.3.

3. As soon as the spray of the sprinklers has fully passed over the collectors, the volume of water caught in each collector is measured using the 500 mL measuring beaker and recorded in a table.
4. Steps 2 and 3 are repeated for the next radial test line the pivot is set to cross.
5. The weather data recorded during the distribution tests is then downloaded off the weather system console.

5.8 Data processing

The processing of the data obtained from the system distribution test, zone distribution tests, and weather station is discussed next.

5.8.1 Water distribution tests

The equations used to evaluate the DU and CU beneath the spray sprinklers for the various water distribution tests, are presented in Table 5-4.

Table 5-4: Distribution efficiency equations

Parameter	Equation	Equation	Comments
AAD	2.7	$\text{AAD} = \left(\frac{\bar{V}}{A_c}\right)$	$A_{c(round)} = 0.0196\ \text{m}^2$ $A_{c(rect)} = 0.0315\ \text{m}^2$
	2.5	$\bar{V} = \frac{\sum_{i=1}^{n} V_i S_i}{\sum_{i=1}^{n} S_i}$	System distribution test (n = 68)
		$\bar{V} = \frac{\sum_{i=1}^{n} V_i}{n}$	Zone distribution test
LQD	2.8	$\text{LQD} = \frac{\bar{V}_{(LQ)}}{A_c}$	-
	2.9	$\bar{V}_{LQ} = \frac{\sum_{j=1}^{n_{LQ}} V_j S_j}{\sum_{j=1}^{n_{LQ}} S_j}$	System distribution test
		$\bar{V}_{LQ} = \frac{\sum_{j=1}^{n_{LQ}} V_j}{n_{LQ}}$	Zone distribution test
CU	2.4	$\text{CU}_\text{H} = 100\left[1 - \frac{\sum_{i=1}^{n} S_i \lvert V_i - \bar{V}_p \rvert}{\sum_{i=1}^{n} S_i V_i}\right]$	System distribution test
	2.3	$\text{CU} = 100\left[1 - \frac{\sum_{i=1}^{n} \lvert V_i - \bar{V} \rvert}{\sum_{i=1}^{n} V_i}\right]$	Zone distribution test
DU	2.6	$\text{DU} = 100\left(\frac{\text{LQD}}{\text{AAD}}\right)$	-

For a system distribution test, the DU and CU are calculated using the volume measurements of the 68 intermittently spaced round collectors. Since the collectors are spaced along the length of the centre pivot system, each consecutive collector represents an increasing proportion of the entire irrigated area. The CU and DU are, therefore, given by equations (2.4) and (2.6) in Table 5-4. A distribution profile is plotted for each of the system tests.

For the round collector zone distribution tests, the DU and CU are evaluated using the volume measurements of the 24 intermittently spaced round bucket collectors. Since the collectors are positioned close together in the spray zone of only a few sprinklers, each collector is considered to represent an equal proportion of the spray area. Hence, the CU and DU are given by equations (2.3) and (2.6) in Table 5-4. In evaluating the CU in equation (2.3), the number of collectors is n = 24. The DU and CU measured in the zones provide a measure of the uniformity of the sprinklers in the radial direction only.

For the rectangular collector zone distribution tests, the volume measurements of the 224 rectangular collectors are used to evaluate the CU and DU beneath a sprinkler. The CU and DU are evaluated using equations (2.3) and (2.6) in Table 5-4. The rectangular matrix of collectors provide distribution measurements in both the radial and circumferential directions. Figure 5-16 shows a schematic layout of the rectangular collectors in a test zone. The rows of the collector matrix extend in the r-direction, and the columns of the matrix extend in the θ-direction.

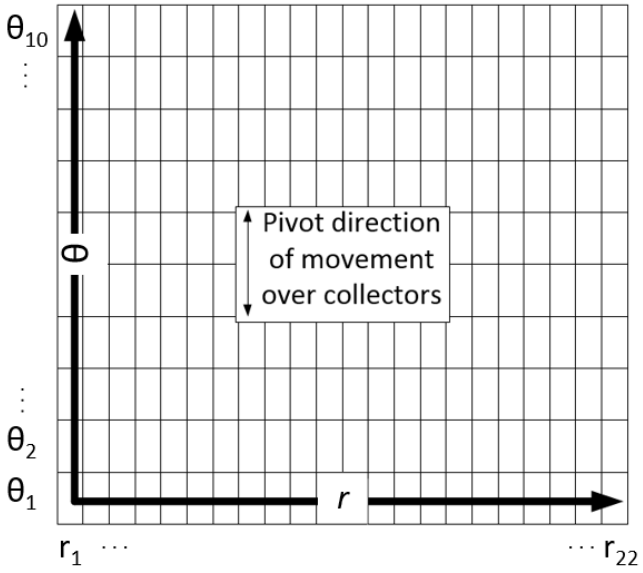

Figure 5-16: Rectangular collector matrix orientation and layout

The DU and CU are evaluated over the entire matrix of 220 collectors to provide a single measure of the uniformity of a sprinkler in both the radial and circumferential directions simultaneously. The average DU and CU along the radial and circumferential directions are also evaluated separately. The average CU in the radial direction, is taken to be the average of the 10 CU values calculated along each of the matrix rows extending in the radial direction. The average CU in the circumferential direction, is given by the average of the CU values calculated along

each matrix column extending in the circumferential direction. The DU is evaluated in a similar manner.

When the DU and CU are evaluated over the matrix of collectors, n = 220. When the DU and CU are evaluated along a matrix row or columns, then n = 10 or 22 respectively.

For each water distribution test conducted along a radial test line or in a test zone, a distribution profile is generated showing the applied depth of water in each of the collectors. In the case of the rectangular bucket distribution tests, two-dimensional water distribution profiles are generated along each row and column, and a three-dimensional profile is generated showing the distribution over the entire matrix.

5.8.2 Weather measurements

The data logged by the weather station is downloaded as a csv file and imported into excel. The wind speed and direction, air temperature, and relative humidity for the duration of time it took the sprinklers to fully cross the collectors in the tests zones is extracted. On average it took the centre pivot system approximately 15 to 20 minutes to fully cross the collectors in the zones. The minimum, maximum, and average wind speed, air temperature, and relative humidity over the time period are calculated.

5.9 Summary

The primary objectives of the experimental investigation, presented in this chapter, is the evaluation of the application uniformity of the three sprinkler types installed on a working centre pivot system. The installed sprinkles include the Powasave sprinkler assemblies, and the commercial Nelson D3000 Sprayhead and S3000 Spinner sprinklers.

The water distribution characteristics that were measured include the average application depth (AAD), the lowest-quarter application depth (LQD), the coefficient of uniformity (CU), and the distribution uniformity (DU).

Details of the experimental apparatus consisting of a 22 Ha centre pivot irrigation system fitted with seven Powasave sprinklers were provided, along with the field setup, measurement equipment, test procedures and the data processing procedures.

6 Results

In this chapter, the results of the centre pivot system evaluation are presented in which the accepted methods of evaluating the DU and CU beneath a sprinkler package on centre pivot system are used to obtain a benchmark performance of the Nelson sprinkler package installed on the centre pivot located at the Elsenburg agricultural research farm in the Western Cape, South Africa. The results of the zone distribution tests conducted beneath the three sprinkler types are also presented for the two collector configurations: (1) the round collector distribution test, and (2) the rectangular collector distribution test.

6.1 Centre pivot system evaluation

Three system distribution tests were conducted along radial test line A, shown in Figure 5-1, using round collectors positioned under the length of the centre pivot as specified in section 5.6.1. The sprinkler package installed on the centre pivot system is the Nelson sprinkler package described in Appendix C.3. The recorded volumes of water caught in each of the collectors is processed as outlined in section 5.8.1, and the results are summarized in Table 6-1.

Table 6-1: Centre pivot system distribution indicators

Test #	Date	Distribution indicators			
		AAD [mm]	LQD [mm]	DU [%]	CU [%]
1	15-03-2016	4.98	3.88	77.97	85.81
2	17-03-2016	5.39	4.37	81.01	88.55
3	23-05-2016	5.21	4.28	82.13	86.66
Average		5.19	4.18	80.37	87.01

The benchmark performance of the centre pivot is approximately 5.2 mm of water applied per pass with a DU and CU averaging 80.4% and 87.0% respectively.

A summary of the weather conditions during each distribution test is given in Table 6-2. A distribution test took approximately 20 minutes to complete, and the weather conditions were sampled at 2 minute intervals.

Table 6-2: Weather data for system distribution tests

Test #	Temperature [℃]			Wind Speed [m/s]				Humidity [%]		
	Max	*Min*	*Ave*	*Max*	*Min*	*Ave*	*Dir*	*Max*	*Min*	*Ave*
1	29.2	26.5	28.0	9.7	1.4	5.9	SE	46	40	42
2	24.5	22.9	23.8	7.0	3.9	5.6	SSW	63	58	61
3	17.2	15.5	16.3	5.6	2.2	3.6	NEE	72	65	70

The application depth profiles of each of the three distribution tests are displayed on a single plot in Figure 6-1. The overall trend shows an increasing application depth at the outer spans of the centre pivot, which is typical of centre pivot systems.

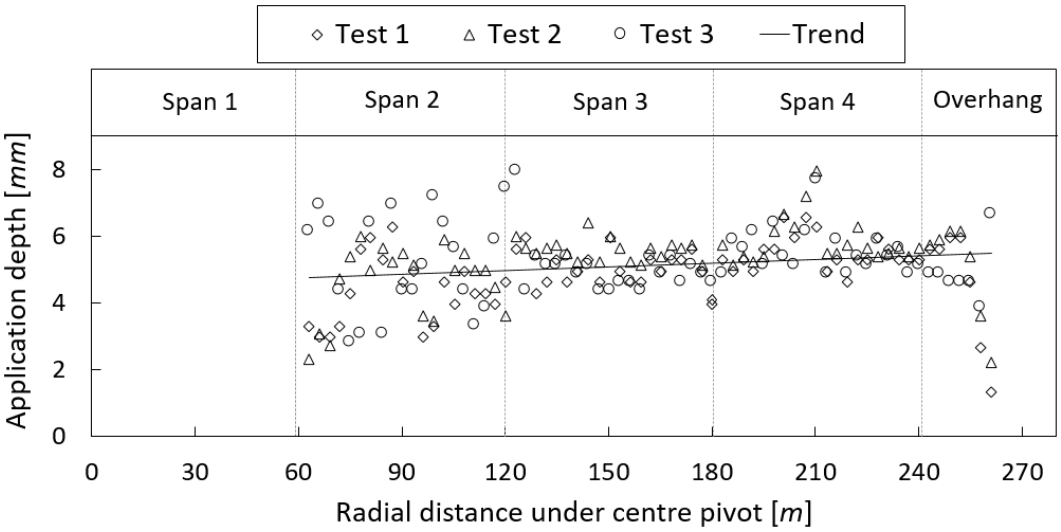

Figure 6-1: Application depth profile measured beneath the Nelson sprinkler package on the Elsenburg centre pivot system

It is noted that there is significantly more variation in the measured application depths under the Nelson Sprayhead sprinkler installed on the first two spans of the centre pivot than the Spinner sprinklers installed on the remaining spans. The larger variation in the measured application depths under the Nelson Sprayhead sprinklers may indicate the following: (1) a poorer application uniformity is to be expected under the Sprayhead sprinklers, (2) the method of using round collectors, placed at discrete intervals, to measure the application profile under a sprinkler with discrete spray trajectories may misrepresent the actual distribution profile under the sprinkler.

The application depths measured under the Nelson Spinner sprinklers, on the other hand, fall within a narrower bandwidth; which is indicative of a better application uniformity and should be reflected so by the CU and DU indicators in the zone distribution tests conducted under each of the sprinkler types.

A few of the application depths measured under span 4, in Figure 6-1, show a deviation from the trend line. This deviation may be attributed to the sprinklers in that region being positioned too close to the ground, as indicated in Figure 6-2. Being too close to the ground, the spray range of the sprinklers is reduced, and the application rate beneath the sprinkler increases. As a result the collectors positioned beneath those sprinklers record an increased volume of water.

In addition, the last two application depths measured under the end-boom vary considerably from the trend for each of the three distribution tests, as shown in Figure 6-1. The round collectors used to capture these application depths were situated in the very tail end of the effective spray range of the centre pivot system, and hence caught less water. These application depth readings were disregarded in evaluating the DU and CU of the centre pivot system.

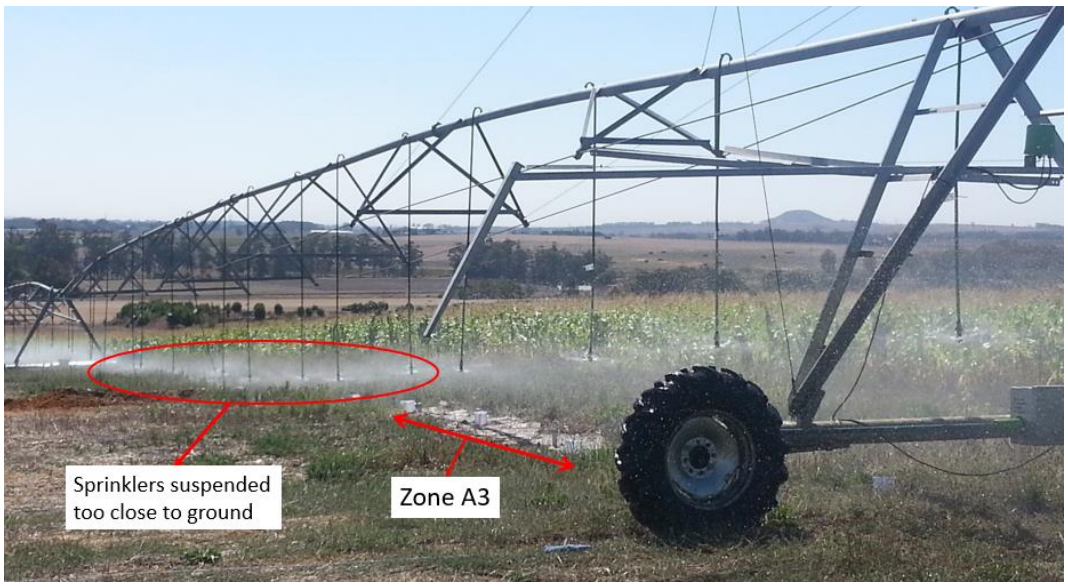

Figure 6-2: Spinner sprinklers under span 4, adjacent to zone A3, positioned too close to ground

6.2 Round collector zone distribution tests

Three round collector zone distribution tests were conducted along radial lines A and B, shown in Figure 5-1. Two zone distribution tests were conducted along radial line A, denoted A_I and A_{II}, and a third round collector zone distribution test was conducted along radial line B, denoted B_{III}.

The first of the zone distribution tests, A_I, took place under the unmodified centre pivot system fitted with the Nelson sprinkler package, while the other two zone distribution tests, A_{II} and B_{III}, took place under the modified centre pivot system fitted with the seven Powasave sprinklers. The round collectors were setup in each zone along a radial line as specified in section 5.6.2, and the volume measurements processed according to section 5.8.1.

The results are presented in Table 6-3, showing the relevant performance indicators of each sprinkler type at each zone. A comparison of the AAD in Table 6-3 shows a significant difference between the AAD measured beneath the Powasave sprinkler and the other two sprinkler types. Furthermore, there is a significant difference in the AAD's measured beneath the Powasave sprinkler for the two test instances A_{II} and B_{III}. This suggests that a single row of intermittently spaced round collectors is insufficient to correctly and consistently measure the AAD beneath the Powasave sprinkler. This also casts doubt as to the validity of the results measured beneath the Sprayhead sprinkler which has discrete spray trajectories, similar to that of the Powasave sprinkler.

Table 6-3: Round bucket zone distribution results

Zone distribution test		A_I			A_{II}			B_{III}		
Parameters	**Units**	*Zone 1* Sprayhead	*Zone 2* Spinner	*Zone 3* Spinner	*Zone 1* Sprayhead	*Zone 2* **Powasave**	*Zone 3* Spinner	*Zone 1* Sprayhead	*Zone 2* **Powasave**	*Zone 3* Spinner
AAD	mm	4.68	4.87	4.65	4.94	2.92	4.99	4.83	4.01	5.68
LQD	mm	2.77	4.46	3.96	2.92	1.87	4.55	2.65	2.93	5.35
DU	%	59.31	91.52	85.10	59.05	64.09	91.14	54.84	73.13	94.19
CU	%	66.52	94.31	90.09	65.38	70.98	92.69	59.74	79.99	96.03

Table 6-4: Round bucket zone distribution weather conditions

Test line & sprinkler package	**Temperature [℃]**			**Wind speed [m/s]**				**Humidity [%]**		
	Max	*Min*	*Ave*	*Max*	*Min*	*Ave*	*Dir*	*Max*	*Min*	*Ave*
Radial test A_I - Nelson sprinkler package	27.1	26.2	26.7	5.7	2.9	4.3	NE	38	35	37
Radial test A_{II} - modified with Powasave	17.2	16.8	17.0	4.1	2.7	3.5	NEE	48	42	45
Radial test B_{III} - modified with Powasave	15.6	15.4	15.5	5.9	4.1	4.9	NE	59	56	57

The corresponding sprinkler radial distribution profiles are presented in Figure 6-3. The distribution profiles under the Spinner sprinklers in zone 2 and 3 are more uniform than those measured under the Sprayhead and Powasave sprinklers in zones 1 and 2, as reflected by the scatter of the application depth measurements. Moreover, the radial distribution profile of the Powasave sprinkler appears to be more uniform than that of the Sprayhead sprinkler.

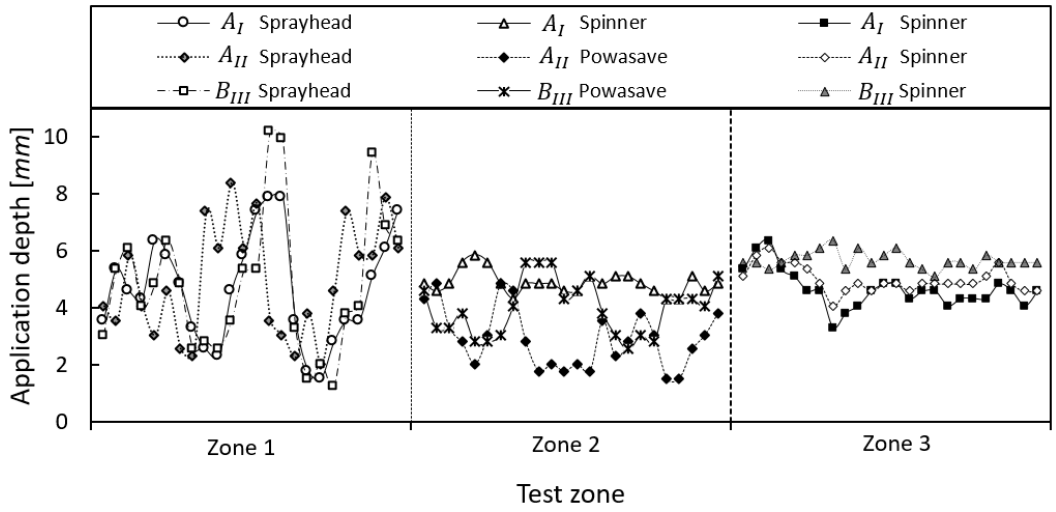

Figure 6-3: Distribution profiles of round bucket zone distribution tests along radial line A and B

This is confirmed by the CU values presented in Figure 6-4, drawn from the data in Table 6-3, showing the CU of each sprinkler type in each of the three zones. From Figure 6-4, it is evident that the Spinner sprinkler has the best CU, followed by the Powasave sprinkler, and finally the Sprayhead sprinkler.

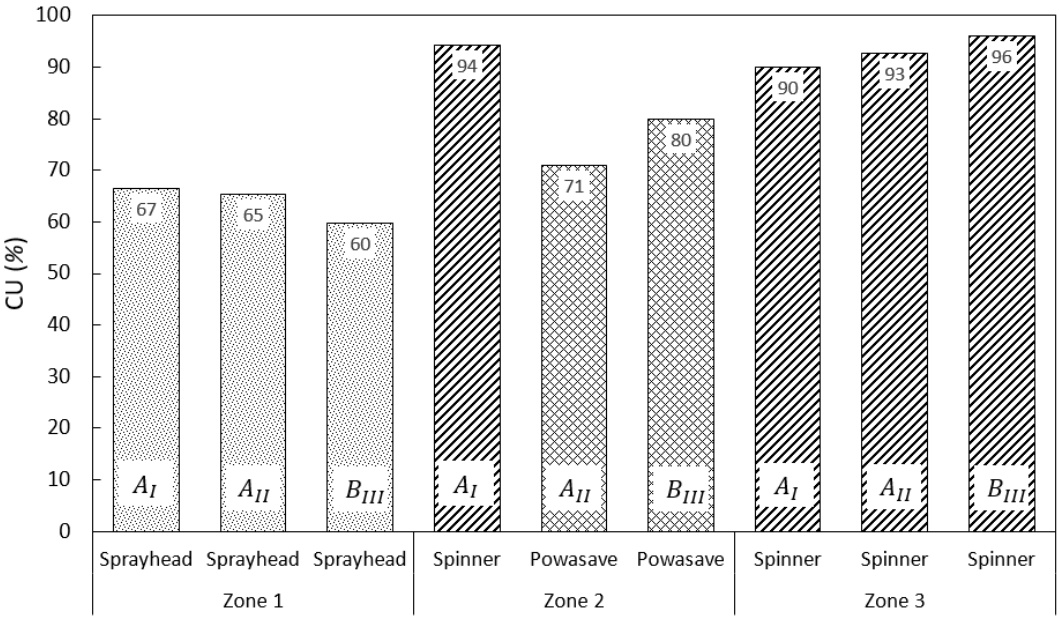

Figure 6-4: CU of sprinkler types measured in round bucket zone distribution tests

The application depth profiles measured beneath the Sprayhead and Spinner sprinklers in Figure 6-4 prove to be similar to that measured in the system evaluations shown in Figure 6-1; where there is significantly more variation in the application depths measured beneath the Sprayhead sprinkler than the Spinner sprinkler.

The accompanying weather conditions of the round collector zone evaluations are presented in Table 6-4.There is no significant difference between the wind speed and direction of the three zone tests. However, hotter and less humid conditions were experienced during test A_I and may account for the reduced AAD measured on that day. The weather conditions during test A_{II} and B_{III} proved to be very similar.

Based on all three zone evaluations, the results prove to be similar; the Spinner sprinkler has a better CU than both the Powasave and Sprayhead sprinklers, and the Powasave sprinkler appears to have a better CU than the Sprayhead sprinkler.

The results do suggest, however, that the method of using a single row of intermittently placed round collectors may not accurately depict the distribution profile of a sprinkler with discrete trajectories, as appears to be the case with the Powasave sprinkler.

6.3 Rectangular collector zone distribution tests

Zone distribution tests were conducted under the three sprinkler types using 220 rectangular collectors arranged in a matrix consisting of 10 rows and 22 columns, orientated as shown in Figure 5-16. The collectors are arranged as outlined in section 5.6.3, and the corresponding data processed as described in sections 5.8.1.

Results are presented for the Sprayhead sprinkler, Powasave sprinkler, and Spinner sprinkler accordingly.

6.3.1 Sprayhead sprinkler

The 3-dimensional water distribution profile measured over the matrix of rectangular collectors positioned in zone A1 under the Nelson Sprayhead sprinkler is shown in Figure 6-5. The distribution profile shows a significant variation in the applied water volume over the collector matrix with a minimum applied volume of 70 mL and a maximum of 250 mL.

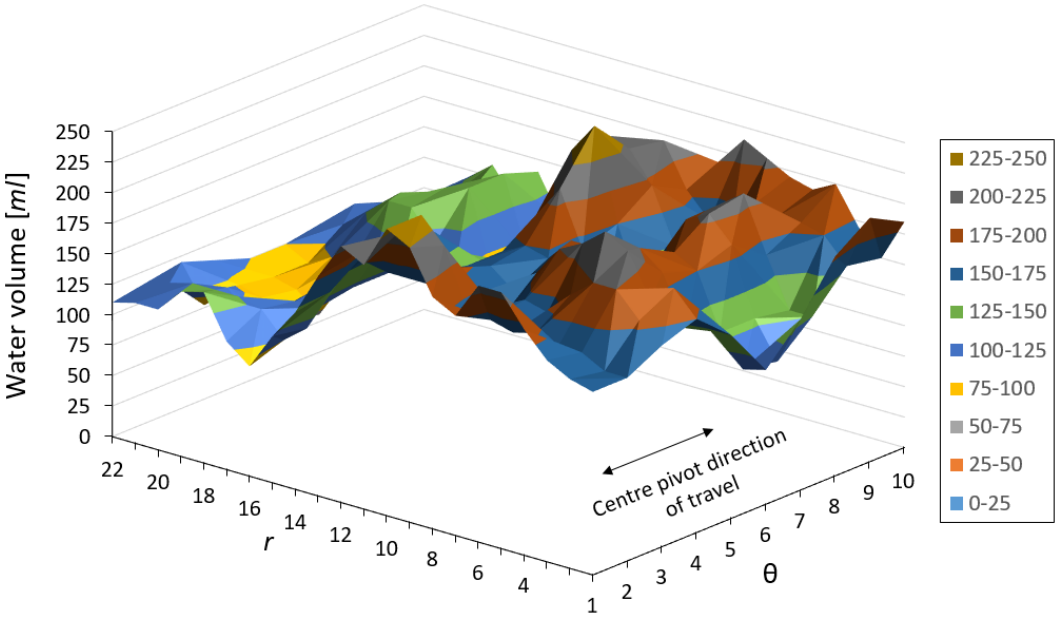

Figure 6-5: Zone A1 Sprayhead sprinkler distribution profile

The distribution parameters evaluated over the matrix of collectors are presented in Table 6-5. The AAD beneath the Sprayhead sprinkler is measured to be 4.94 mm, with a DU and CU of 69.7% and 77.3% respectively.

Table 6-5: Zone A1 Sprayhead sprinkler matrix performance parameters

Min AD [mm]	*Max AD* [mm]	*AAD* [mm]	*LQD* [mm]	*DU* [%]	*CU* [%]
2.33	8.33	4.94	3.44	69.74	77.28

Figure 6-6 shows the average application depth (AAD), the lowest-quarter application depth (LQD), and the maximum application depth (AD) in the radial direction beneath the sprinkler.

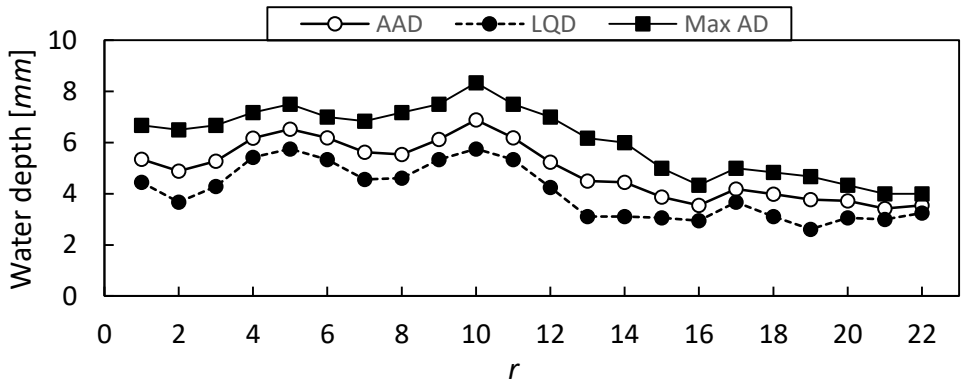

Figure 6-6: Zone A1 Sprayhead AAD, LQD and max AD in radial direction

From Figure 6-6 it is evident that there is a non-uniform application of water along the radial direction, with a variation of approximately 3.5 mm between the least-watered and most-watered sections. The severity of the non-uniform application in the radial direction is reflected by the DU and CU evaluated along each of the

matrix rows in Figure 5-16. Figure 6-7 show the DU and CU evaluated along each of the 10 matrix rows. The average DU and CU over the rows are 71.0% and 78.1% respectively.

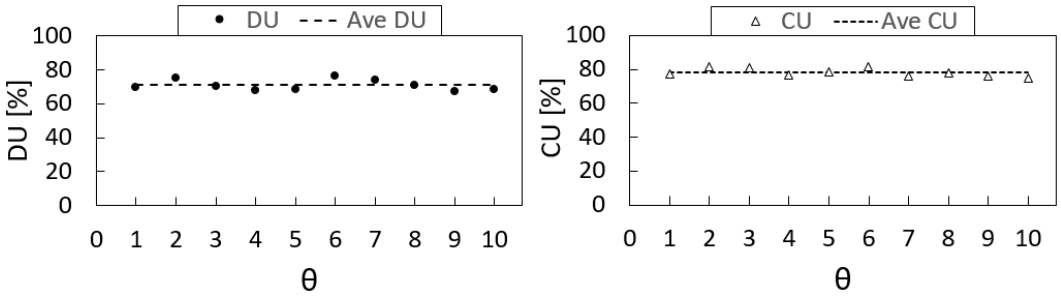

Figure 6-7: Zone A1 Sprayhead DU and CU evaluated along each matrix row

The AAD, LQD, and maximum AD in the circumferential direction are shown in Figure 6-8. The AAD is fairly uniform, averaging about 4.95 mm. However, the difference between the maximum AD and the AAD is more significant than in Figure 6-6.

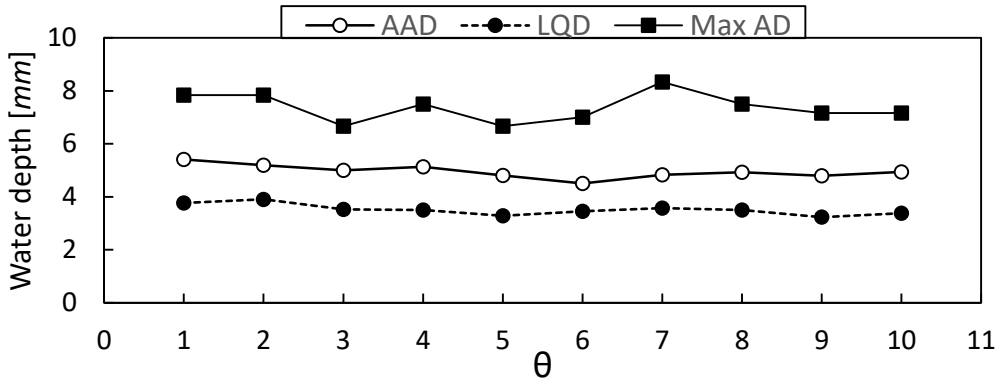

Figure 6-8: Zone A1 Sprayhead AAD and LQD in circumferential direction

The application uniformity measured in the circumferential direction is reflected by the DU and CU evaluated along each of the matrix columns in Figure 5-16. Figure 6-9 shows the DU and CU evaluated along each matrix column.

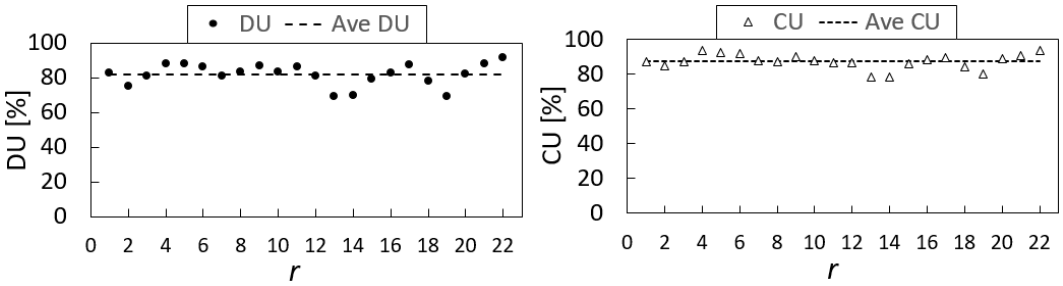

Figure 6-9: Zone A1 Sprayhead DU and CU evaluated along each matrix column

The average DU and CU over all 22 columns is 81.9% and 87.4% respectively. The higher DU and CU values in Figure 6-9 suggest the application of water in the circumferential direction is more uniform than that in the radial direction shown in Figure 6-7.

6.3.2 Spinner sprinkler

Two Spinner sprinkler zone distribution tests were conducted at zones A2 and A3. The results measured in each zone are presented next.

The water distribution profile over the matrix of collectors in zone A2 is presented in Figure 6-10. The maximum and minimum applied water volumes recorded over the matrix of collectors is 175 mL and 130 mL respectively.

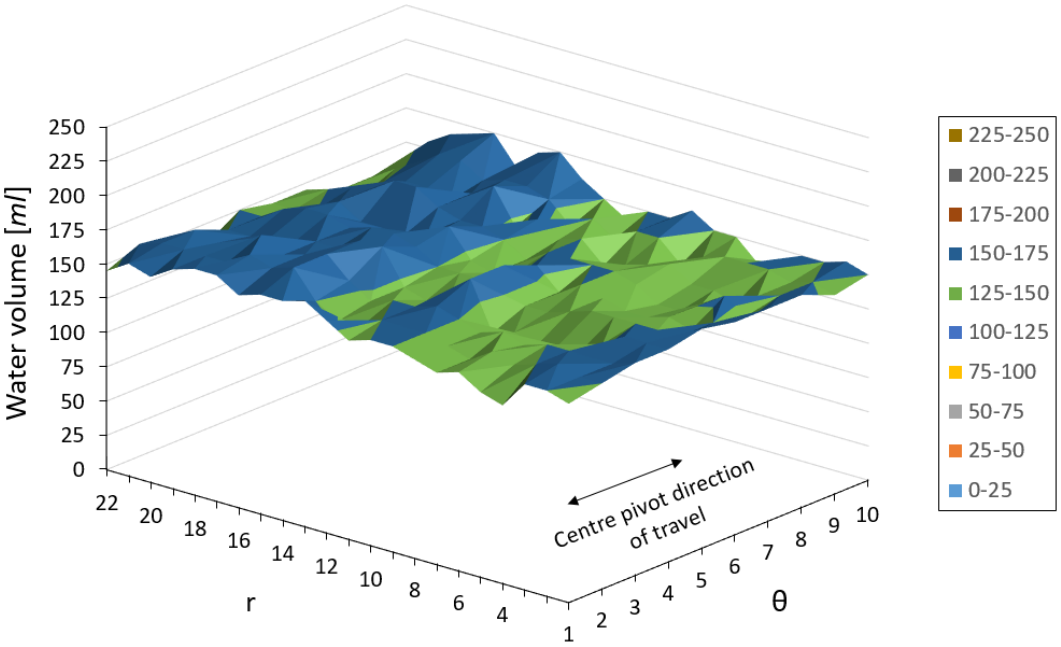

Figure 6-10: Zone A2 Spinner sprinkler distribution profile

The distribution parameters of the Spinner sprinkler, evaluated over the matrix of collectors, are presented in Table 6-6. The Spinner sprinkler proves to have an excellent DU and CU of 92.5% and 95.2% respectively, and applied an AAD of 5.04 mm of water over the matrix of collectors.

Table 6-6: Zone A2 Spinner sprinkler matrix distribution parameters

Min AD [mm]	*Max AD* [mm]	*AAD* [mm]	*LQD* [mm]	*DU* [%]	*CU* [%]
4.33	5.83	5.04	4.70	92.51	95.19

Figure 6-11 show the AAD, LQD and max AD in the radial direction. The AAD is uniform, with a variation of approximately 0.8 mm between the least-watered and most-watered sections. Furthermore, there is little variation between the AAD, LQD, and maximum AD.

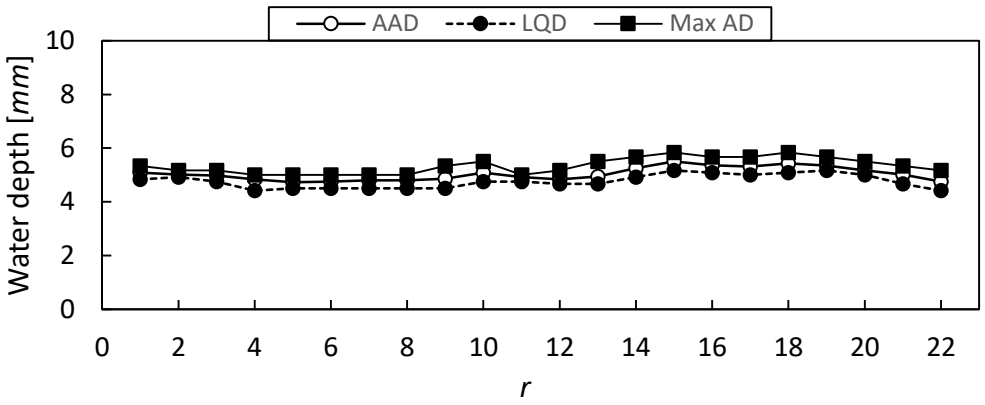

Figure 6-11: Zone A2 spinner sprinkler AAD, LQD and max AD in radial direction

Figure 6-12 shows the AAD, LQD and maximum AD evaluated in the circumferential direction. The resulting profile also proves to be very uniform.

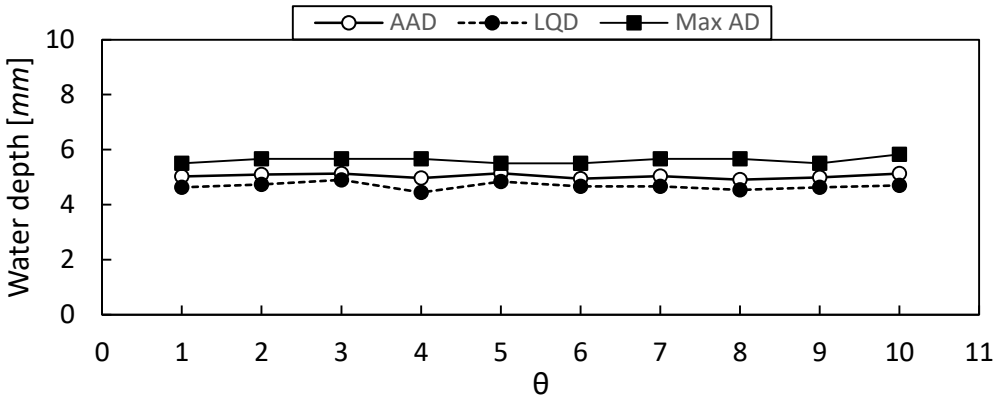

Figure 6-12: Zone A2 Spinner sprinkler AAD, LQD, max AD in circumferential direction

The distribution profiles measured beneath the Spinner sprinkler in zone A3 show a similar uniformity in the radial and circumferential directions, as shown in Figure 6-11 and Figure 6-12. The distribution profiles measured in zone A3 are attached in Appendix F.1. The distribution parameters of the Spinner sprinkler in zone A3, evaluated over the matrix of collectors, are presented in Table 6-7. The DU and CU is evaluated to be 89.1% and 92.3% respectively.

Table 6-7: Zone A3 Spinner sprinkler matrix distribution parameters

Min AD [mm]	*Max AD* [mm]	*AAD* [mm]	*LQD* [mm]	*DU* [%]	*CU* [%]
3.83	6.00	4.82	4.3	89.11	92.32

The application uniformity in the radial and circumferential directions beneath the Spinner sprinklers are reflected by the DU and CU evaluated along the rows and columns of the collector matrix. Figure 6-13 shows the DU and CU evaluated along the matrix rows extending in the radial direction for the distribution tests conducted in zones A2 and A3. The average DU and CU are evaluated to be 93.8% and 96.3% respectively.

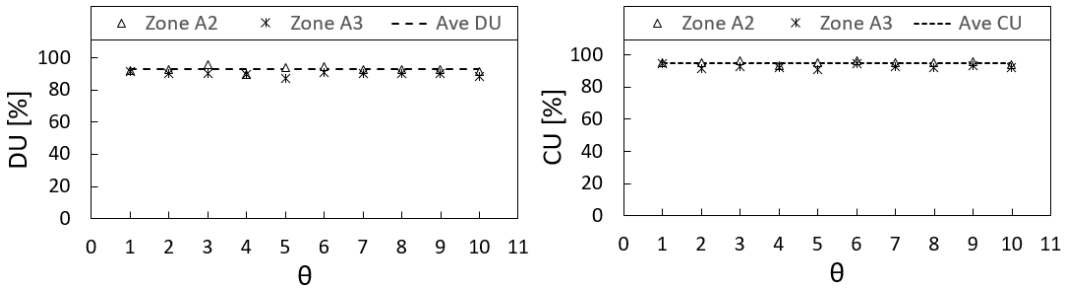

Figure 6-13: DU and CU of Spinner sprinkler evaluated along matrix rows

Figure 6-14 shows the DU and CU evaluated along each of the matrix columns. The average DU and CU over the columns is 93.8% and 96.3% respectively.

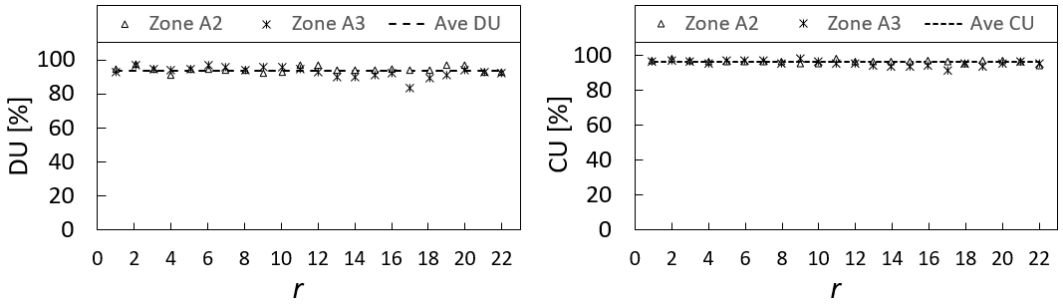

Figure 6-14: DU and CU of Spinner sprinkler evaluated along matrix columns

Both zone A2 and A3 distribution tests show the Spinner sprinkler to have an excellent distribution uniformity in the radial and circumferential directions. The water distribution is uniform and consistent in both directions. The average DU and CU measured over the matrix of collectors for the two zones are 90.8% and 93.8% respectively.

6.3.3 Powasave sprinkler

Three Powasave sprinkler zone distribution tests were conducted at zones A2, B2 and C2. The results of the three zone distribution tests are presented next.

The water distribution profile of the Powasave sprinklers in zone A2 is shown in Figure 6-15. There is a significant variation in the applied volume of water over the matrix of collectors with the maximum and minimum applied volumes being 300 mL and 35 mL respectively.

The Powasave sprinkler distribution parameters, evaluated over the matrix of collectors, are presented in Table 6-8. An AAD of 5.02 mm of water is applied, with a DU and CU of 63.5% and 72.0% respectively.

Table 6-8: Zone A2 Powasave sprinkler matrix distribution parameters

Min AD [mm]	*Max AD* [mm]	*AAD* [mm]	*LQD* [mm]	*DU* [%]	*CU* [%]
1.17	10.00	5.02	3.20	63.47	71.96

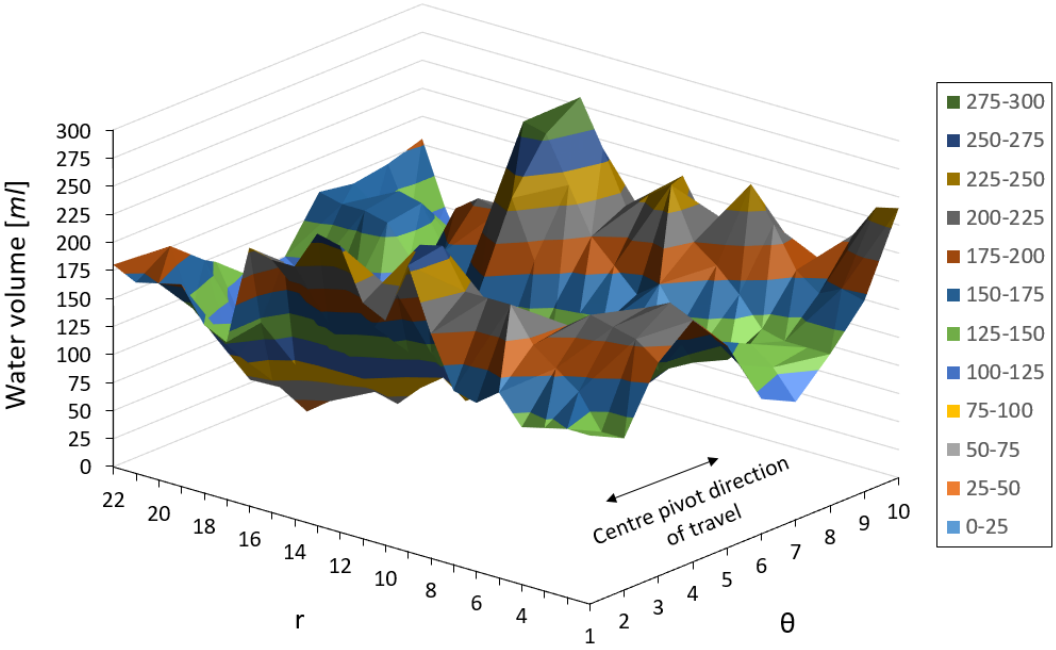

Figure 6-15: Zone A2 Powasave sprinkler distribution profile

There is a definite peak-trough-peak cycle that appears across the distribution profile in the circumferential direction in Figure 6-15, resulting in a significant difference in the maximum and minimum application depths measured over the collectors, as shown in Table 6-8. The water distribution is not uniform and there are obvious regions where over- and under-watering occur in the circumferential direction. The measured DU and CU are not impressive, as would be expected based on the profile in Figure 6-15.

Figure 6-16 shows the AAD, LQD and the maximum AD in the radial direction. The AAD profile in the radial direction is non-uniform with a variation of approximately 3.3 mm between the least-watered and most-watered sections.

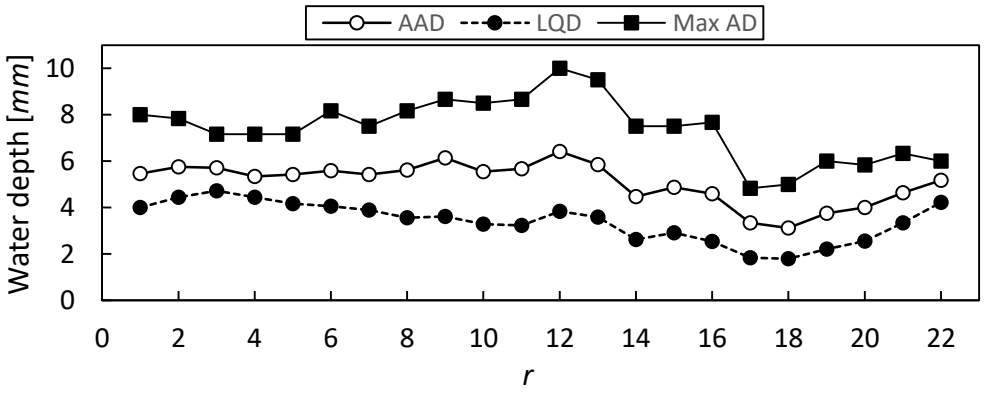

Figure 6-16: Zone A2 Powasave sprinkler AAD, LQD and max AD in radial direction

The Powasave sprinkler shows a similar degree of radial uniformity as the Sprayhead sprinkler in Figure 6-6. However, there is a more substantial variation between the maximum AD and the LQD which is caused by the peaks and troughs in the application profile of the sprinkler in the circumferential direction.

Figure 6-17 shows the AAD, LQD and the maximum AD of the Powasave sprinkler in the circumferential direction. The application profile is clearly not uniform with a definite peak-trough-peak cycle that occurs periodically in the circumferential direction.

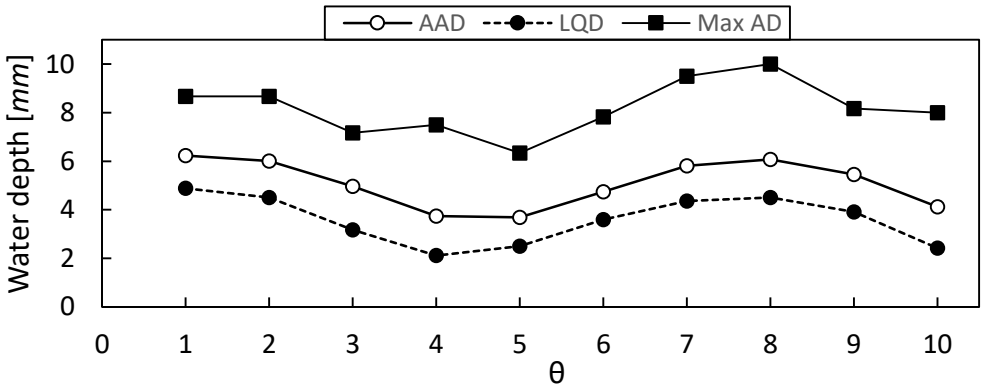

Figure 6-17: Zone A2 Powasave sprinkler AAD, LQD and max AD in circumferential direction

The distribution profiles of the Powasave sprinklers measured in zones B2 and C2 showed similar characteristics to that measured in zone A2, and can be found in Appendix F.2.

The Powasave sprinkler distribution parameters evaluated over the matrix of collectors, in zones B2 and C2 are presented in Table 6-9.

Table 6-9: Zone B2 & C2 Powasave sprinkler matrix distribution parameters

Zone	*Min AD* [mm]	*Max AD* [mm]	*AAD* [mm]	*LQD* [mm]	*DU* [%]	*CU* [%]
B2	1.17	13.33	4.69	2.70	57.79	64.33
C2	1.67	12.33	4.79	2.70	55.56	56.32

The distribution parameters in each of the two zones prove to be very similar. The DU and CU measured in zone B2 are evaluated to be 57.8% and 64.3% respectively, and the DU and CU measured in zone C2 are evaluated to be 55.6% and 56.3%. There is a substantial variation between the minimum and maximum application depths applied over the matrix of collectors in the two zones.

The severity of the non-uniform application profiles in the radial and circumferential directions beneath the Powasave sprinklers are reflected by the DU and CU evaluated along the rows and columns of matrix of collectors. Figure 6-18 shows the DU and CU evaluated along the matrix rows extending in the radial direction for the distribution tests conducted in zones A2, B2, and C2.

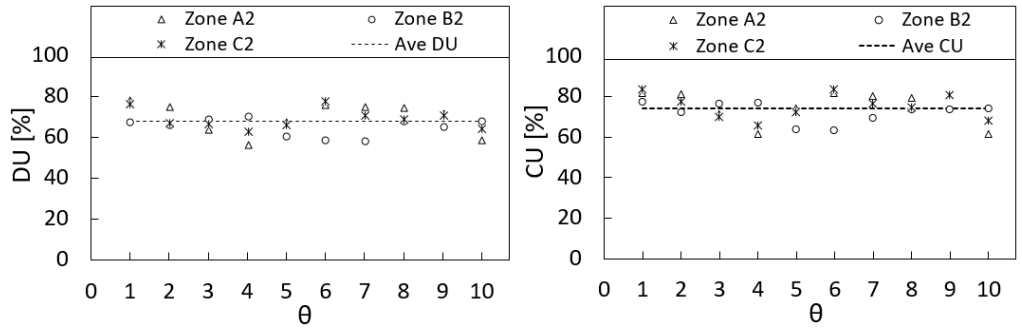

Figure 6-18: DU and CU of Powasave sprinkler evaluated along matrix rows

The average DU and CU along the matrix rows are 68.0% and 74.1% respectively. Figure 6-19 shows the DU and CU evaluated along the matrix columns extending in the circumferential direction. The average DU and CU along the matrix columns are 62.8% and 67.4% respectively.

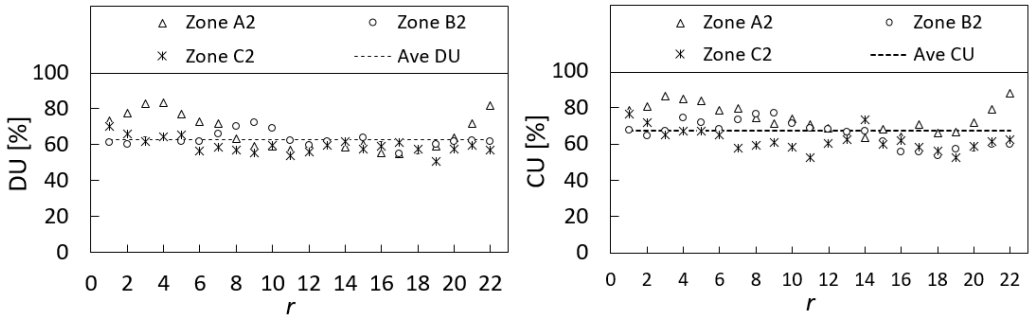

Figure 6-19: DU and CU of Powasave sprinkler evaluated along matrix columns

It is evident, based on all three zone tests, the Powasave sprinkler has a more uniform distribution profile in the radial direction than the circumferential direction. The resulting non-uniform application profile in the circumferential direction handicapped the sprinkler's performance. It is clear that having a series of distinct orifice set outlets with a circumferential spray width of 0.15 m distributed along the sprinkler pipe will not produce a uniform application profile, but instead produce a periodic peak-trough application profile in the circumferential direction. The average DU and CU of the Powasave sprinklers evaluated over the matrix of collectors in all three test zones A2, B2, and C2 is evaluated to be 58.9% and 64.2%.

6.3.4 Weather data

The weather data recorded during each of the rectangular bucket zone evaluations is presented in Table 6-10. The weather conditions during each of the zone evaluations do not vary significantly enough to be responsible for the significantly different results measured beneath the three sprinkler types. The effect of the weather conditions on the performance of the sprinklers is therefore considered negligible.

Table 6-10: Weather data for rectangular bucket zone evaluation

Date	Sprinkler type	Zone	Ave Temp (°C)	Average Wind Speed (m/s)	Average Wind Dir	Ave Humidity (%)
24-Nov-16	Sprayhead	A1	22.5	3.6	SW	58
24-Nov-16	Spinner	A2	22.5	6.1	SW	55
28-Nov-16	Spinner	A3	23.4	6.6	SSW	51
13-Jul-16	Powasave	A2	25.3	3.9	NNW	40
13-Jul-16	Powasave	B2	26.1	4.1	NW	68
14-Jul-16	Powasave	C2	19.2	4.2	NW	71

6.4 Summary

The results of the round collector and rectangular collector zone evaluations both show the Spinner sprinkler to outperform the Powasave sprinkler and Sprayhead sprinkler in terms of a uniform water distribution. Where the CU measured beneath the Sprayhead and Powasave sprinkler, using the rectangular collectors, was evaluated to be 77.3% and 64.2% respectively, the CU measured beneath the Spinner sprinkler was 93.8%. The Spinner sprinkler proved to have an excellent uniform water distribution in both the radial and circumferential directions.

The initial round collector zone evaluations seemed to show the Powasave sprinkler having a better CU in the radial direction than the Sprayhead sprinkler. However, the rectangular bucket evaluations showed otherwise. The Sprayhead sprinkler in fact measured a better uniformity in both the radial and circumferential directions in the rectangular collector zone evaluations.

The Powasave sprinkler on the other hand, proved to have an especially poor distribution uniformity in the circumferential direction with clear peak-trough cycles manifesting in the distribution profile.

Despite the poor uniformity in the circumferential direction, the Powasave sprinkler had a uniformity in the radial direction that competed with that of the Sprayhead sprinkler. Where the average CU measured along the matrix rows beneath the Sprayhead sprinkler was 78.1%, the average CU beneath the Powasave sprinkler was measured to be 74.1%. Unfortunately, the poor distribution profile of the Powasave sprinkler in the circumferential direction diminished the overall DU and CU beneath the sprinkler, evaluated over the matrix of collectors, to well below that of the Sprayhead sprinkler.

7 Discussion of results

7.1 Zone evaluation methods

Two evaluation methods where used to measure the application uniformity beneath the three sprinkler types: the round collector distribution test method and rectangular collector distribution test method.

The round collector evaluation method, detailed in section 5.6.2, by nature only captures a single distribution profile extending in the radial direction. The rectangular collector evaluation method on the other hand, captures the distribution profile of the sprinklers over a number of rows and columns extending in the radial and circumferential directions. To compare the results of the two evaluation methods, the DU and CU of the round collector evaluation method are compared against the average DU and CU measured along the rows of the collector matrix extending in the radial direction.

The insight each evaluation method gives regarding the performance of the sprinklers, and the difference in results produced by the two methods is discussed next with regards to each of the sprinkler types.

7.1.1 Spinner Sprinkler

The DU and CU measured beneath the Spinner sprinkler using the two zone evaluation methods are presented in Table 7-1.

Table 7-1: DU & CU of the two zone evaluation methods beneath the Spinner sprinkler

Evaluation method	Radial		Circumferential		Collector matrix	
	DU	*CU*	*DU*	*CU*	*DU*	*CU*
Round collector[ǂ]	90.5	93.3	-	-	-	-
Rectangular collector[ǂǂ]	93.8	96.3	93.8	96.3	90.8	93.8

ǂ Parameters are the average of the four round collector evaluation tests in Table 6-3 of section 6.2
ǂǂ Parameters are the average of the two rectangular collector zone evaluations in section 6.3.2

The results of the rectangular collector evaluation method are presented showing the average DU and CU evaluated along the matrix rows and columns extending in the radial and circumferential directions, and the DU and CU evaluated over the entire matrix of collectors.

The results of the two evaluation methods in the radial direction prove to be very similar. Moreover, the DU and CU measured by the round collector evaluation method hold true with the DU and CU measured over the collector matrix. Both evaluation methods show the Spinner sprinkler to have a CU over 90%, which is considered an excellent uniformity.

The spinning action of the impact plate on the Spinner sprinkler, shown in Figure 2-2, produces a random canopy of droplets over the sprinkler spray zone. On centre pivot systems, the spray zones of adjacent Spinner sprinklers overlap resulting in a very uniform water application in both the radial and circumferential directions, as shown by the results in Table 7-1.

Due to the rain-like canopy of water droplets, and the excellent distribution uniformity, the shape of the collectors, or their relative positioning in the test zones, has little effect on the DU and CU measured in the zone evaluations. Each collector placed in the Spinner sprinkler spray zone will catch a representative portion of the applied water volume over the test zone. For this reason the round bucket evaluation method and the rectangular bucket evaluation method produced such similar results.

7.1.2 Sprayhead sprinkler

In the case of the Sprayhead sprinkler, the DU and CU measured using the two evaluation methods produced very different results, as shown in Table 7-2.

Table 7-2: DU & CU of the two zone evaluation methods beneath the Sprayhead sprinkler

Evaluation method	Radial		Circumferential		Collector matrix	
	DU	CU	DU	CU	DU	CU
Round collector[ł]	57.7	63.9	-	-	-	-
Rectangular collector[ǂ]	71.0	78.1	81.9	87.4	69.7	77.3

ł Parameters are the average of the tree round collector evaluation tests in Table 6-3 of section 6.2
ǂ Parameters are those of the rectangular collector zone evaluation in section 6.3.1

The round collector evaluation method produced a DU and CU significantly less than that measured by the rectangular collector evaluation method in the radial direction.

The different results measured by the round collector evaluation method may be attributed to the inherent shortcomings of using intermittently spaced round collectors to measure the distribution profile of a sprinkler with a finite number of discrete trajectories, as discussed in Appendix E.

The D3000 Sprayhead sprinkler has 33 discrete jet-streams of water that are distributed over a circular spray area whose diameter may range anywhere from 6 m to 12 m. A single row of intermittently spaced round collectors will at any given time only intercept a few of the spray trajectories in the spray zone beneath the sprinkler. Some trajectories may not be captured at all by the round collectors, while some collectors may catch two or three trajectory streams as the sprinkler passes over. The positioning of the round collectors in the spray zone does affect the measured results. Consequently, a level of uncertainty and inconsistency is introduced when measuring the DU and CU beneath the Sprayhead sprinkler using intermittently spaced round collectors.

The matrix array of rectangular collectors, however, captures each spray trajectory that pass over the collector matrix. Furthermore, the two-dimensional nature of the matrix array tracks the movement of a spray trajectory in the circumferential and radial directions. The block of rectangular collectors arranged in the tests zones will therefore provide a better measure of the DU and CU beneath the Sprayhead sprinkler. The round collector evaluation method, on the other hand, is more likely to understate the actual performance of the Sprayhead sprinkler.

7.1.3 Powasave sprinkler

The average DU and CU of the two evaluation methods beneath the Powasave sprinkler are presented in Table 7-2.

Table 7-3: DU & CU of the two zone evaluation methods beneath the Powasave sprinkler

Evaluation method	Radial		Circumferential		Collector matrix	
	DU	CU	DU	CU	DU	CU
Round collector[ł]	68.6	75.5	-	-	-	-
Rectangular collector[ǂǂ]	68.0	74.1	62.8	67.4	58.9	64.2

ł Parameters are the average of the three round collector evaluation tests in Table 6-3 of section 6.2
ǂǂ Parameters are the average of the three rectangular collector zone evaluations in section 6.3.3

The DU and CU of the round collector evaluation method proved similar to that of the rectangular collector evaluation method in the radial direction.

The similar results of the two evaluation methods in the radial direction is because of the manner in which the designed orifice set outlets distribute water to the soil surface. An orifice set outlet has 21 orifice outlets producing jet-streams that lie within a circumferential spray width of 0.15 m and span a radial distance of 4.1 m. When an orifice set outlet passes over a row of collectors, all the jet streams cross at approximately the same instant and at the same rate. The intermittently spaced round collectors intercept enough trajectory streams to establish a reliable application profile that proves consistent with that measured by the matrix of rectangular collectors.

However, the round collector evaluation method does not capture the distribution profile in the circumferential direction. It is the poor application profile of the Powasave sprinkler in the circumferential direction that results in the poor DU and CU measured over the matrix of collectors. It is for this reason that the DU and CU results evaluated using the round collector evaluation method differ so substantially from that measured over the matrix of rectangular collectors, as shown in Table 7-3.

While the round collector evaluation method proves sufficient to capture the radial distribution profile of the Powasave sprinkler, it provides no indication of the poor distribution in the circumferential direction; which ultimately diminishes the overall performance of the Sprinkler.

7.2 System evaluation method

The method prescribed by the ASAE (American Society of Agricultural Engineers, 2003) to measure the uniformity of water distribution beneath a centre pivot system makes use of round collectors placed at intermittent intervals beneath the centre pivot sprinkler package. The zone evaluation results, however, show that while intermittently placed round collectors correctly measured the DU and CU beneath the Spinner sprinkler, the method proves insufficient to accurately measure the DU and CU beneath the Sprayhead sprinkler. Furthermore, in the round collector zone evaluation method the round collectors are spaced 300 mm apart, while in the system evaluation method the round collectors are spaced 3 m apart; which may

further exacerbate the problem of accurately measuring the uniformity beneath the Sprayhead sprinklers.

The system evaluation results measured beneath the Nelson sprinkler package show the CU to be 87.0%. While this doesn't accurately represent the actual performance of either the Spinner or Sprayhead sprinkler, it does appear to be a good average performance of the installed Nelson sprinkler package. However, since the performance beneath the spinner sprinkler is understated using intermittently spaced round collectors, the actual CU beneath the system may be better than the measured 87.0%.

The ASAE method of evaluating the uniformity beneath a sprinkler package provides a measure of the uniformity in the radial direction only, and provides no insight into the uniformity of the package in the circumferential direction. A comparison of the results measured beneath the Powasave sprinkler using the two zone evaluation methods show that while a sprinkler may show a satisfactory uniformity in the radial direction, it may have a poor uniformity in the circumferential direction. Therefore, one should not rely solely on the uniformity results measured in the radial direction to provide an indication of the uniformity applied over the whole irrigated field, unless the spray uniformity beneath the sprinklers in the circumferential directions are well understood.

While it is not practical to measure the distribution uniformity in the radial and circumferential directions beneath a sprinkler package on a centre pivot system using a matrix of collectors, it may be worth supplementing the single row of round collectors used in the ASAE method with a few dissecting rows of collectors extending in the circumferential direction to provide insight into the uniformity of the sprinkler package in both the radial and circumferential directions.

7.3 Improvements on the Powasave sprinkler

The rectangular collector evaluation results show that the Powasave sprinkler has a satisfactory uniformity in the radial direction, but a poor uniformity in the circumferential direction. The poor uniformity in the radial direction is attributed to the stop-start motion of the pivot as it moves about the field, and the manner in which the orifice set outlets apply water to the soil surface.

The orifice set design used on the Powasave sprinkler prototypes has a circumferential spray width (θ_{sw}) of 0.15 m. For a time-averaged travel speed of 1.5 m/min, ζ in equation (4.47) has a magnitude of 10 min^{-1}, and the resulting circumferential profile beneath the orifice set over a given 60 second operating cycle is like that shown in Figure 4-13. The small circumferential spray width results in sharp AAD peaks protruding from the base application depth of the orifice set. As the orifice set moves about the field, the resulting distribution profile will exhibit a cyclic profile consisting of peaks and troughs; which is indeed the profile measured beneath the Powasave sprinklers in the circumferential direction, as shown in Figure 6-15.

To improve the distribution profile, the orifice set circumferential spray width should be increased to a minimum length of 1.5 m, in which case ζ will have a magnitude of 1 min^{-1}. The resulting AAD peak is broad and flat like that shown in Figure 4-13

and will improve the circumferential application uniformity. The best AAD profile beneath a Powasave sprinkler may be achieved if all the orifice nozzles are equi-spaced over the length of the sprinkler pipe. However, this may be difficult to manufacture without compromising on the accuracy of the orifice nozzle placement on the pipe circumference.

To improve the application uniformity in the radial direction, a solution may be to increase the number of orifice nozzles comprising an orifice set, thereby reducing the spacing between trajectory streams at the soil surface; in so doing achieving a better uniformity. However, for a required sprinkler volume flow rate this would require reducing the orifice nozzle diameters, which in turn will produce a smaller droplet size making them more susceptible to wind drift and evaporation. Furthermore, the smaller the diameter of the orifice nozzle, the more likely it is to get clogged with particulate matter in the water. A thorough straining system would then be required to clean the water before it passes through the orifice set.

For the selected orifice nozzle diameters used on the Powasave prototypes, there was a visible difference in the spray droplet size beneath the Powasave sprinklers and Nelson sprinklers as shown in Figure 7-1. The Spinner sprinklers produce a mist like spray consisting of a range of droplet sizes that, while contributing to the excellent uniformities beneath the sprinkler, leave the sprinkler more susceptible to wind drift and evaporation losses.

Figure 7-1: Spray beneath the Nelson sprinkles and Powasave sprinklers installed on the Elsenburg centre pivot system

8 Conclusion

The purpose of this study was to evaluate the application uniformity of the novel, low pressure Powasave sprinkler. The sprinkler concept is shown to have the potential to reduce operating pressures on centre pivot systems by up to 35%, and is capable of a producing a uniform droplet size that will provide numerous advantages during irrigation. However, for the Powasave sprinkler to be a feasible overhead spray sprinkler solution, it is required to have a uniform application. In this study, a Powasave sprinkler prototype was designed, manufactured, and installed on a working centre pivot system in order to evaluate the application uniformity beneath the sprinkler concept under operating conditions in the field.

A theoretical model of the Powasave sprinkler was developed to simulate the volume flow rate through the sprinkler, the spray distribution profiles in the radial and circumferential directions, and the applied application rates beneath an orifice set outlet. The model was capable of simulating the flow rates through an orifice nozzle, the core component of the Powasave sprinkler, to within 10% accuracy, and the spray range to within 5% accuracy. The model was used to design seven Powasave sprinklers that were required to apply an average application depth of 5 mm of water per pass at a centre pivot timer setting of 60%.

The Powasave prototypes were successfully installed on the Elsenburg centre pivot system and several water distribution tests conducted beneath the Powasave sprinklers and two commercial Nelson spray sprinklers: the Nelson D3000 Sprayhead sprinkler and the S3000 Spinner sprinkler. Two methods of water distribution tests were used to evaluate the application uniformity beneath the three sprinkler types. The rectangular collector method, considered to be the more reliable method, showed the Powasave sprinkler to have a CU less than that of the Sprayhead and Spinner sprinklers. The CU measured beneath the Powasave sprinkler was 64.2%, evaluated over the matrix of rectangular collectors, while that of the Sprayhead and Spinner sprinkler were measured to be 77.3% and 93.8% respectively. The Spinner sprinkler proved to have an excellent distribution uniformity.

The application uniformity of the Powasave sprinkler was diminished by the poor distribution profile in the circumferential direction, consisting of recurring cycles of peaks and troughs in the measured average application depth (AAD). Distinct peaks in the AAD profile were caused by a combination of the stop-start motion of the centre pivot and the configuration of the orifice set outlets on the sprinkler pipes. The average CU measured in the circumferential direction beneath the Powasave sprinkler was evaluated to be 67.4%, while that of the Nelson Sprayhead and Spinner sprinklers were measured to be 87.4% and 96.3% respectively.

Despite the poor application uniformity in the circumferential direction, the Powasave sprinkler measured a CU in the radial direction similar to that of the Sprayhead sprinkler. The average CU in the radial direction beneath the Powasave sprinkler was measured to be 74.1%, and that of the Sprayhead measured to be 78.1%. The Spinner sprinkler, on the other hand, measured an excellent CU of 96.3%.

The Powasave sprinkler, as it was designed in this study, is shown incapable of the application uniformities attainable by the Nelson Sprayhead and Spinner sprinklers. While the Powasave sprinkler may have the potential to reduce operating pressures in centre pivot systems, the pressure reductions are not, at this stage, justified at the expense of a uniform water distribution.

The study does, however, show potential for the application uniformities beneath the Powasave sprinkler to be improved by changing the configuration of the orifice set outlets. Future work should include the testing of various orifice set outlet configurations to determine the limits of the application uniformities attainable under the Powasave sprinkler. If a more uniform application profile can be attained beneath the Powasave sprinkler, there is potential for the sprinkler to improve application efficiencies of centre pivot systems while simultaneously reducing the energy requirements of the irrigation system. Moreover, the simplistic components of the Powasave sprinkler can be easily manufactured in the local South African economy, illuminating the dependency on imported sprinkler products from overseas.

References

Agrico, 2016. *Centre pivot irrigation.* [Online]. Available at: http://www.agrico.co.za/agrico-pivots [Feb 2016]

American Society of Agricultural Engineers, 2003. *Test procedure for determining the uniformity of water distribution of center pivot and lateral move irrigation machines equipped with spray sprinkler nozzles*. ASAE Standards, pp. 932-938.

Atlantis Engineering, 2012. *Atlantis.* [Online]. Available at: http://www.atlantis muhendislik.com/en/urunlerimiz.php?pid=22 [Sep 2017].

Budler, M. J. I., 2014. *Evaluation and enhancement of centre pivot irrigation systems.* BEng Honours Project.. Stellenbosch: Stellenbosch University.

Cengel, Y. A. & Cimbala, J. M., 2010. *Fluid mechanics fundamentals and applications.* Second Edition ed. New York: McGraw-Hill.

Howell, T. A., 2003. *Irrigation efficiency*. Encyclopedia of Soil Science, pp. 467-471.

King, B. A., Stark, J. C. & Kincaid, D. C., 2000. *Irrigation uniformity*. University of Idaho College of Agriculture Bulletin No. 824, pp 11.

Nelson Irrigation Corporation, 2016. *Nelson pivot products.* [Online]. Available at: http://www.nelsonirrigation.com/products/family/pivot-sprinklers/s3030-spinner [July 2016]

New, L. & Fipps, G., 2000. *Centre pivot irrigation.* [Online]. Available at: http://hdl.handle.net/1969.1/86877 [April 2016]

Rayleigh, L., 1878. *On the instability of jets*. Proceedings of the London Mathematical Society, Vol 10, pp. 4-13.

Reinke Manufacturing Company Inc., 2016. *Basic pivot center operator's manual*. [Online]. Available at: https://www.robertsirrigation.com/wp-content/uploads/PDF/Reinke_Basic_Manual.pdf [Sep 2017]

Reuter, H. C. R., 2010. *Performance evaluation of natural draft cooling towers with anisotropic fills*. PhD Dissertation. Stellenbosch: Stellenbosch University

Rogers, D. H., 1997. *Efficiencies and water losses of irrigation systems*. Cooperative Extension Service, Kansas State University.

Roux, D., 2012. *Evaluation and performance enhancement of cooling tower spray patterns*. MScEng Thesis. Stellenbosch: Stellenbosch University.

Turton, R. & Levenspiel, O., 1986. *A short note on the drag correlation for spheres*. Powder Technologies, Vol 47, pp. 83-86.

Viljoen, D. J., 2006. *Evaluation and performance prediction of cooling tower spray zones*. MScEng Thesis. Stellenbosch: Stellenbosch University

Xiaoni, Q., Zhenyan, L., & Dandan, L., 2006. *Performance characteristics of a shower cooling tower*. Energy Conservation and Management, Vol 48, pp. 193-203

Appendices

Appendix A Selection of lowest quarter values

Table A1 illustrates how the lowest-quarter values are selected for an experiment in which 10 collectors are positioned radially under a centre pivot system. The weighted catch, on the left hand side of Table A1, is the product of the collector's position from the pivot tower (S_i) and the volume of water caught in the collector (V_i). The collectors are assigned a ranking in column 5 based on the magnitudes of the water volume measurements with the smallest volume measurement receiving a ranking of 1.

The right hand side of Table A1 shows the data arranged in ascending order of rank. The lowest-quarter values are those values whose cumulative weighted catch, in column 10, is equal to the lowest-quarter threshold. The lowest-quarter threshold is taken to be 1/4th of the total weighted catch, given at the bottom of column 4. If there is no cumulative weighted catch score that equals the lowest-quarter threshold, then those values whose cumulative weighted catch are closest to, but not greater than, the lowest-quarter threshold are taken to be the lowest-quarter values. For the data given in Table A1, the number of measurements making up the lowest-quarter is two (n_{LQ} = *2*). Using equation (2.9), the average volume of the lowest quarter is 26250 / 150 = 175 mL.

Table A1: Table illustrating how the lowest-quarter values are selected

Collector number (i)	Collector distance from pivot tower [m]	Volume caught in collector [ml]	Weighted catch	Rank	Rank in ascending order (j)	Volume caught in collector [ml]	Collector distance from pivot tower [m]	Weighted catch	Cumulative weighted catch
	S_i	V_i	V_iS_i				S_j	V_jS_j	
1	60	180	10800	3	1	175	63	11025	11025
2	63	175	11025	1	2	175	87	15225	26250
3	66	200	13200	8	3	180	60	10800	37050
4	69	195	13455	6	4	185	75	13875	-
5	72	205	14760	9	5	190	78	14820	140175 / 4 = 35 044
6	75	185	13875	4	6	195	69	13455	-
7	78	190	14820	5	7	195	81	15795	Lowest-quarter threshold
8	81	195	15795	7	8	200	66	13200	
9	84	205	17220	10	9	205	72	14760	-
10	87	175	15225	2	10	205	84	17220	-
$n = 10$	$\sum_{i=1}^{n} S_i$	$\sum_{i=1}^{n} V_i$	$\sum_{i=1}^{n} V_iS_i$		$n_{LQ} = 2$		$\sum_{j=1}^{n_{LQ}} S_j$	$\sum_{j=1}^{n_{LQ}} V_jS_j$	
	735	1905	140175				150	26250	

Appendix B Pressure gauge assembly

A pressure gauge assembly, shown in Figure B1, was used to measure the pressure at various outlets along the radial supply pipe of the centre pivot system.

The assembly consists a 20 mm plastic T-piece which screws onto the rigid PVC portion of the drop tubes. A pressure gauge is fitted to the T-piece by means of a coupler and reducer, and a PVC ball valve is fitted to the bottom end of the T-piece onto which the Nelson pressure regulator and sprinkler are attached.

The Ball valve is used to shut off the flow through the sprinkler when taking a pressure reading. This is to ensure that only the static pressure of the radial supply pipe is measured on the pressure gauge. The pressure gauge has a measurement range of 0 - 1000 kPa, at a resolution of 20 kPa.

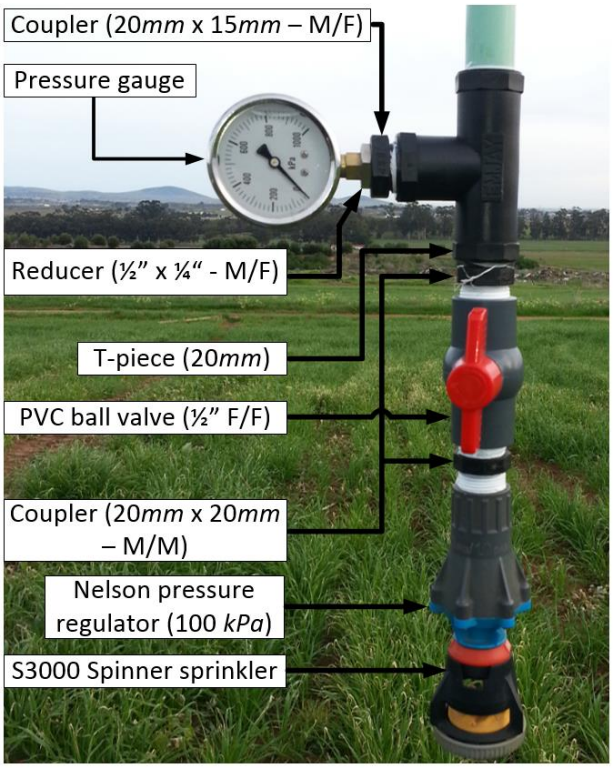

Figure B1: Pressure gauge assembly

Appendix C Elsenburg centre pivot specifications

C.1 Centre pivot drive system

The A-frame towers are each fitted with an electric 380 *VAC* two stage, spur gear centre drive with a gear ratio of 30:1. The centre drive powers two 50:1 gearboxes mounted at each wheel. Each tower is fitted with two 13.6 x 24 4-ply tractor tires with an overall diameter of 1207 mm.

C.2 End tower time-averaged travelling speed

The centre pivot percentage timer setting was set at 60% for the duration of the experimental work, and the time-averaged speed of the end tower was measured to be approximately 2 m/min, as shown in Table C1.

The centre pivot end tower speed (u_{p_4}) was determined by measuring the period of time taken for the end tower to travel the distance between two markers spaced 15 m apart. The markers were positioned alongside the wheel track of the end tower. The end tower speed was calculated according to equation (C.1):

$$u_{p_4} = \frac{Distance\ travelled}{total\ time\ in\ seconds} \cdot 60 \tag{C.1}$$

Table C1: Centre pivot end tower speed measurements

Experiment	Distance Travelled (m)	Measured time		Total time (Sec)	Tower Speed (m/s)	Tower Speed (m/min)
		(Mins)	(Sec)			
1	15	7	17	437	0.034	2.06
2	15	7	41	461	0.033	1.95
3	15	7	48	468	0.032	1.92
4	15	7	24	444	0.034	2.03
5	15	7	20	440	0.034	2.05
6	15	7	43	463	0.032	1.94
Average	15	7	32	452	0.033	1.99

C.3 Elsenburg centre pivot sprinkler package

The two types of sprinklers installed on the centre pivot include the D3000 Sprayhead sprinkler and the S3000 Spinner sprinkler. Each sprinkler is fitted with a 100 kPa Nelson Universal-flow pressure regulator, and is suspended from the pivot radial supply pipe using 20 mm flexible drop tubes. The sprinklers are suspended at a height ranging between 1.0 m and 1.5 m above ground level. Each sprinkler assembly consists of a sprinkler body, impact plate, cap, 3TN nozzle, and pressure regulator, as shown in Figure 2-2.

The D3000 Sprayhead impact plate and S3000 Spinner impact plate specifications are presented in Table C2.

Table C2: Sprayhead and Spinner sprinkler impact plate specifications

Sprinkler Type	Trajectory	Groove		3TN nozzle range	Sprinkler plate
		Description	No.		
D3000 Sprayhead	Triple-trajectory: +9°,+4°,-3°	Medium	33	9-44	
S3000 Spinner	Multiple trajectory	Course	8	14-50	

The D3000 Sprayhead has 33 medium depth grooves machined into the plate with trajectory angles of +9°, +4°, and −3°. The multiple trajectories help reduce stream collision and improve overlap between consecutive sprinklers. The recommended operating 3TN nozzle size range is 9 - 44. (See Figure C2 for the 3TN nozzle flow rates for various operating pressures)

The S3000 Spinner has 8 main grooves each with multiple trajectory lip angles for an even water distribution and good wind fighting ability. The recommended operating 3TN nozzle size range is 14 - 50.

The spray diameters of the D3000 Sprayhead sprinkler and the S3000 spinner sprinkler for various 3TN nozzle diameters and operating pressures are provided by the Nelson Irrigation Corporation, and are shown in Table C3 and Table C4.

Table C3: Nelson D3000 Sprayhead plate characteristics

	3TN nozzle size									
	9	14	18	24	28	32	36	42	50	
Water pressure (*Bar*) 0.4	3	4	5	7	7	7	7	8	8	Throw diameter (m)
0.7	4	7	8	9	10	10	11	11	12	
1	5	9	10	12	13	13	14	14	15	
1.4	7	10	12	14	15	15	15	16	16	

Table C4: Nelson S3000 Spinner plate characteristics

	3TN nozzle size									
	14	16	20	24	28	32	36	42	50	
Water pressure (*Bar*) 0.7		9	10	10	11	12	12	11	10	Throw diameter (m)
1	9	10	11	12	12	13	13	12	12	
1.4	10	10	12	13	13	14	14	14	13	

Since the throw diameter of the Sprayhead and Spinner sprinklers are not provided for the full range of 3TN nozzle sizes given in Figure C2, a curve fit is used to interpolate for the throw diameters at intermediate nozzles sizes, not included in

Table C3 and Table C4. Figure C1 shows the throw diameters of the sprinklers for an operating pressure of 100 kPa, and the curve fit equations used in the interpolations.

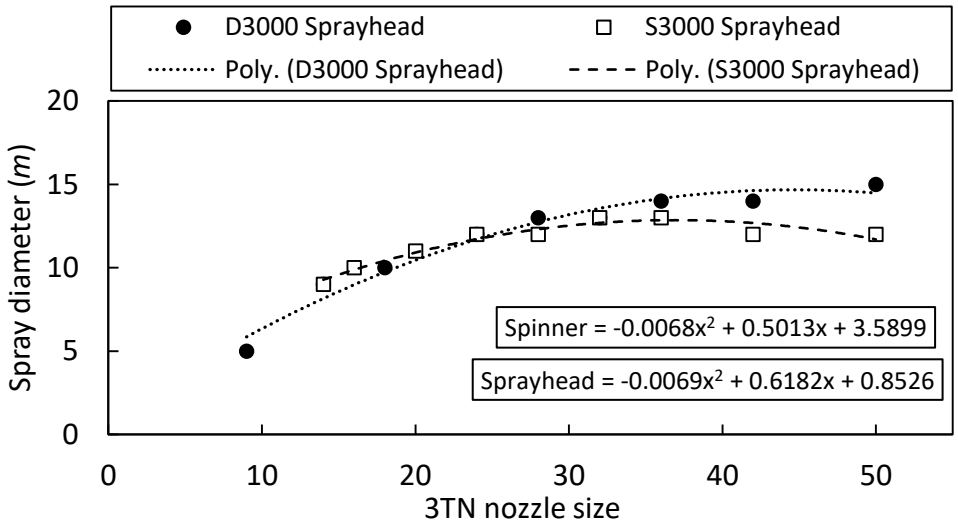

Figure C1: Sprayhead and Spinner sprinkler throw diameter correlations at 100 kPa

Figure C2 shows the flow rates of the Nelson 3TN nozzle series for various nozzle sizes and operating pressures. The 3TN nozzles form part of a nozzle range whose diameters vary in increments of 1/128 inch.

> 3000 Series 3TN Nozzle System > Metric Units (LPM)

- Quick-Change
- Color-Coded
- Precision Accuracy
- High Wear Resistance

The nozzle sizing system is based on 128th inch increments, i.e. 3TN Nozzle #22 has an orifice diameter of 22/128th inches while 3TN Nozzle #23 has an orifice diameter of 23/128th inches. Odd numbered nozzles have a color box around the number marking. This color box denotes the color of next larger nozzle size.

# Color Stripe	#9 Light Blue Beige	#10 Beige	#11 Beige Gold	#12 Gold	#13 Gold Lime	#14 Lime	#15 Lime Lavender	#16 Lavender	#17 Lavender Gray	#18 Gray	#19 Gray Turquoise
BAR	LPM	LPM	LPM	LPM	LPM	LPM	LPM	LPM	LPM	LPM	LPM
0,4	1,28	1,59	1,89	2,30	2,68	3,10	3,59	4,08	4,61	5,14	5,79
0,7	1,66	2,04	2,46	2,99	3,48	4,01	4,65	5,29	5,98	6,62	7,45
1.0	2.00	2.50	2.99	3.63	4.27	4.88	5.71	6.47	7.30	8.09	9.12
1.4	2.34	2.87	3.48	4.20	4.92	5.63	6.58	7.49	8.44	9.38	10.56
1.7	2.61	3.22	3.86	4.69	5.52	6.32	7.38	8.36	9.46	10.48	11.81
2.1	2.87	3.52	4.23	5.14	6.01	6.92	8.09	9.15	10.37	11.46	12.90
2.8	3.29	4.05	4.88	5.94	6.96	7.98	9.34	10.59	11.96	13.24	14.91
3.4	3.67	4.54	5.48	6.66	7.79	8.93	10.44	11.84	13.32	14.79	16.69

# Color Stripe	#20 Turquoise	#21 Turquoise Yellow	#22 Yellow	#23 Yellow Red	#24 Red	#25 Red White	#26 White	#27 White Blue	#28 Blue	#29 Blue Dark Brown	#30 Dark Brown
BAR	LPM	LPM	LPM	LPM	LPM	LPM	LPM	LPM	LPM	LPM	LPM
0,4	6,43	6,96	7,72	8,40	9,23	9,99	10,86	11,61	12,68	13,55	14,49
0,7	8,28	9,00	9,99	10,82	11,96	12,90	14,00	15,00	16,35	17,48	18,69
1,0	10,18	11,01	12,22	13,24	14,61	15,78	17,14	18,39	20,02	21,42	22,93
1,4	11,73	12,71	14,11	15,32	16,88	18,24	19,79	21,23	23,12	24,71	26,45
1,7	13.13	14.23	15.78	17.10	18.88	20.36	22.14	23.73	25.85	27.63	29.59
2.1	14.38	15.59	17.25	18.77	20.70	22.33	24.26	26.00	28.31	30.28	32.39
2.8	16.61	18.01	19.94	21.65	23.88	25.77	28.00	30.65	32.70	34.97	37.43
3.4	18.54	20.13	22.29	24.22	26.72	28.80	31.33	33.57	36.56	39.13	41.86

# Color Stripe	#31 Dark Brown Orange	#32 Orange	#33 Orange Dark Green	#34 Dark Green	#35 Dark Green Purple	#36 Purple	#37 Purple Black	#38 Black	#39 Black Dk. Turquoise	#40 Dark Turquoise	#41 Dk. Turquoise Mustard
BAR	LPM	LPM	LPM	LPM	LPM	LPM	LPM	LPM	LPM	LPM	LPM
0,4	15,36	16,50	17,60	18,69	19,68	20,07	22,10	23,39	24,68	25,92	27,48
0,7	19,83	21,50	22,71	24,11	25,43	26,72	28,54	30,16	31,87	33,49	35,47
1,0	24,26	26,07	29,71	29,56	31,15	32,74	34,97	36,98	39,02	41,02	43,45
1,4	28,00	30,12	32,13	34,10	35,95	37,77	40,38	42,69	45,08	47,35	50,19
1,7	31,34	33,68	35,91	38,15	40,19	42,24	45,11	47,72	50,38	52,95	56,09
2,1	34,32	36,90	39,32	41,78	44,05	46,29	49,43	52,27	55,19	58,02	61,43
2,8	36,62	42,62	45,42	48,25	50,87	53,44	57,07	60,37	63,74	66,99	70,97
3.4	44.32	47.65	50.79	53.93	56.85	59.76	63.81	67.48	71.20	74.90	79.33

# Color Stripe	#42 Mustard	#43 Mustard Maroon	#44 Maroon	#45 Maroon Cream	#46 Cream	#47 Cream Dark Blue	#48 Dark Blue	#49 Dark Blue Copper	#50 Copper
BAR	LPM	LPM	LPM	LPM	LPM	LPM	LPM	LPM	LPM
0,4	28,76	30,13	31,52	33,04	34,51	36,26	37,69	39,02	40,76
0,7	37,13	38,91	40,68	42,66	44,54	46,78	48,67	50,38	52,64
1,0	45,45	47,65	49,84	52,23	54,54	57,30	59,61	61,70	64,45
1,4	52,49	55,03	57,53	60,30	62,98	66,20	68,84	71,23	74,45
1,7	58,70	61,51	64,34	67,41	70,43	74,00	79,94	79,67	83,23
2,1	64,30	67,37	70,47	73,85	77,13	81,07	84,32	87,24	91,18
2,8	74,22	77,82	81,37	85,28	89,09	93,60	97,35	100,76	105,29
3,4	83,00	86,98	90,99	95,34	99,58	104,66	108,85	112,64	117,71

This flow data was obtained under ideal test conditions and may be adversely affected by poor hydraulic entrance conditions, turbulence or other factors. Nelson Irrigation makes no representation regarding sprinkler flow rate accuracy under various plumbing and drop pipe conditions.

WARRANTY AND DISCLAIMER: Nelson 3000 Series Pivot Products and accessories are warranted for one year from date of original sale to be free of defective materials and workmanship when used within the working specifications for which the products were designed and under normal use and service. The manufacturer assumes no responsibility for installation, removal or unauthorized repair of defective parts. The manufacturer's liability under this warranty is limited solely to replacement or repair of defective parts and the manufacturer will not be liable for any crop or other consequential damages resulting from defects or breach of warranty. THIS WARRANTY IS EXPRESSLY IN LIEU OF ALL OTHER WARRANTIES, EXPRESS OR IMPLIED, INCLUDING THE WARRANTIES OF MERCHANTABILITY AND FITNESS FOR PARTICULAR PURPOSES AND OF ALL OTHER OBLIGATIONS OR LIABILITIES OF MANUFACTURER. No agent, employee or representative of the manufacturer has authority to waive, alter or add to the provisions of this warranty, nor to make any representations or warranty not contained herein.

This product may be covered by one or more of the following U.S. Patent Nos. 4796811, RE33823, DES312865, 5415348, 5409168 and other U.S. Patents pending or corresponding issued or pending foreign patents.

NELSON
Nelson Irrigation Corporation
848 Airport Rd., Walla Walla, WA 99362 USA
Tel: 509.525.7660 — Fax: 509.525.7907
info@nelsonirrigation.com
WWW.NELSONIRRIGATION.COM

Figure C2: Nelson 3TN nozzle series

Table C5 presents the details of each spray sprinkler installed on the Elsenburg centre pivot system. There are a total of 77 installed sprinklers, operating at a governed pressure of 100 kPa. There are 35 Sprayhead sprinklers installed on the first two spans of the centre pivot system, and 42 Spinner sprinklers installed on the outer spans of the centre pivot system.

The flow rates through the sprinklers are given in Figure C2 for a specified 3TN nozzle size and operating pressure. The spray diameters of the sprinklers are determined using the polynomial equations in Figure C1.

Table C5: Centre pivot sprinkler package specifications

Span #	Outlet #	Distance from centre (m)	Regulator pressure (kPa)	Pressure regulator flow type	Sprinkler Type	3TN nozzle size (1/128")	Flow rate (*Lpm*)	Spray diameter (m)
1	1	5.65	100	Uni-flow	Sprayhead	9	2.00	5.86
1	2	9.00	100	Uni-flow	Sprayhead	9	2.00	5.86
1	3	12.35	100	Uni-flow	Sprayhead	9	2.00	5.86
1	4	15.70	100	Uni-flow	Sprayhead	10	2.50	6.34
1	5	19.05	100	Uni-flow	Sprayhead	11	2.99	6.82
1	6	22.40	100	Uni-flow	Sprayhead	12	3.63	7.28
1	7	25.75	100	Uni-flow	Sprayhead	13	4.27	7.72
1	8	29.10	100	Uni-flow	Sprayhead	13	4.27	7.72
1	9	32.45	100	Uni-flow	Sprayhead	13	4.27	7.72
1	10	35.80	100	Uni-flow	Sprayhead	14	4.88	8.16
1	11	39.15	100	Uni-flow	Sprayhead	15	5.71	8.57
1	12	42.50	100	Uni-flow	Sprayhead	15	5.71	8.57
1	13	45.85	100	Uni-flow	Sprayhead	16	6.47	8.98
1	14	49.20	100	Uni-flow	Sprayhead	16	6.47	8.98
1	15	52.55	100	Uni-flow	Sprayhead	17	7.30	9.37
1	16	55.90	100	Uni-flow	Sprayhead	17	7.30	9.37
1	17	59.25	100	Uni-flow	Sprayhead	17	7.30	9.37
2	18	62.80	100	Uni-flow	Sprayhead	18	8.09	9.74
2	19	66.15	100	Uni-flow	Sprayhead	19	9.12	10.11
2	20	69.50	100	Uni-flow	Sprayhead	19	9.12	10.11
2	21	72.85	100	Uni-flow	Sprayhead	19	9.12	10.11
2	22	76.20	100	Uni-flow	Sprayhead	20	10.18	10.46
2	23	79.55	100	Uni-flow	Sprayhead	20	10.18	10.46
2	24	82.90	100	Uni-flow	Sprayhead	21	11.01	10.79
2	25	86.25	100	Uni-flow	Sprayhead	21	11.01	10.79
2	26	89.60	100	Uni-flow	Sprayhead	21	11.01	10.79
2	27	92.95	100	Uni-flow	Sprayhead	22	12.22	11.11
2	28	96.30	100	Uni-flow	Sprayhead	22	12.22	11.11
2	29	99.65	100	Uni-flow	Sprayhead	23	13.24	11.42
2	30	103.00	100	Uni-flow	Sprayhead	23	13.24	11.42
2	31	106.35	100	Uni-flow	Sprayhead	23	13.24	11.42
2	32	109.70	100	Uni-flow	Sprayhead	24	14.61	11.72

2	33	113.05	100	Uni-flow	Sprayhead	24	14.61	11.72
2	34	116.40	100	Uni-flow	Sprayhead	25	15.78	12.00
2	35	119.75	100	Uni-flow	Sprayhead	25	15.78	12.00
3	36	123.30	100	Uni-flow	Spinner	25	15.78	11.00
3	37	126.65	100	Uni-flow	Spinner	26	17.14	11.00
3	38	130.00	100	Uni-flow	Spinner	26	17.14	11.00
3	39	133.35	100	Uni-flow	Spinner	26	17.14	11.00
3	40	136.70	100	Uni-flow	Spinner	26	17.14	11.00
3	41	140.05	100	Uni-flow	Spinner	27	18.39	11.00
3	42	143.40	100	Uni-flow	Spinner	27	18.39	11.00
3	43	146.75	100	Uni-flow	Spinner	27	18.39	11.00
3	44	150.10	100	Uni-flow	Spinner	28	20.02	11.00
3	45	153.45	100	Uni-flow	Spinner	28	20.02	11.00
3	46	156.80	100	Uni-flow	Spinner	28	20.02	11.00
3	47	160.15	100	Uni-flow	Spinner	29	21.42	11.00
3	48	163.50	100	Uni-flow	Spinner	29	21.42	11.00
3	49	166.85	100	Uni-flow	Spinner	29	21.42	11.00
3	50	170.20	100	Uni-flow	Spinner	29	21.42	11.00
3	51	173.55	100	Uni-flow	Spinner	30	22.93	11.00
3	52	176.90	100	Uni-flow	Spinner	30	22.93	11.00
3	53	180.25	100	Uni-flow	Spinner	30	22.93	11.00
4	54	183.80	100	Uni-flow	Spinner	32	26.07	11.00
4	55	187.15	100	Uni-flow	Spinner	32	26.07	11.00
4	56	190.50	100	Uni-flow	Spinner	32	26.07	11.00
4	57	193.85	100	Uni-flow	Spinner	32	26.07	11.00
4	58	197.20	100	Uni-flow	Spinner	34	29.56	11.00
4	59	200.55	100	Uni-flow	Spinner	34	29.56	11.00
4	60	203.90	100	Uni-flow	Spinner	34	29.56	11.00
4	61	207.25	100	Uni-flow	Spinner	34	29.56	11.00
4	62	210.60	100	Uni-flow	Spinner	35	31.15	11.00
4	63	213.95	100	Uni-flow	Spinner	35	31.15	11.00
4	64	217.30	100	Uni-flow	Spinner	35	31.15	11.00
4	65	220.65	100	Uni-flow	Spinner	35	31.15	11.00
4	66	224.00	100	Uni-flow	Spinner	35	31.15	11.00
4	67	227.35	100	Uni-flow	Spinner	36	32.74	11.00
4	68	230.70	100	Uni-flow	Spinner	36	32.74	11.00
4	69	234.05	100	Uni-flow	Spinner	36	32.74	11.00
4	70	237.40	100	Uni-flow	Spinner	37	34.97	11.00
4	71	240.75	100	Uni-flow	Spinner	37	34.97	11.00
5	72	244.30	100	Uni-flow	Spinner	37	34.97	11.00
5	73	247.65	100	Uni-flow	Spinner	37	34.97	11.00
5	74	251.00	100	Uni-flow	Spinner	37	34.97	11.00
5	75	254.35	100	Uni-flow	Spinner	37	34.97	11.00
5	76	257.70	100	Uni-flow	Spinner	38	36.98	11.00
5	77	261.05	100	Uni-flow	Spinner	38	36.98	11.00

Appendix D Powasave sprinkler assembly

D.1 Pressure regulator assembly

Figure 5-4 shows the pressure distribution inside the radial supply pipe of the Elsenburg centre pivot system measured along radial line A in Figure 5-1. The pressure measured in the last outlet of the 3rd span is 200 kPa. This is the minimum pressure that the Powasave pressure regulator assemblies will be required to regulate, since the maximum elevation of the centre pivot system occurs along radial line A.

However, as the pivot moves to lower elevations across the field, the pressure in the supply line will increase. The maximum pressure seen by the last outlet on the 3rd span will occur when the centre pivot system is positioned along the lowest part of the field, which occurs along radial line B in Figure 5-1. The pressure in the radial supply line at the last outlet on the 3rd span is increased by an elevation difference of approximately 20 m between radial line A and B, as shown in Figure 5-2. This elevation difference is equivalent to a pressure increase of approximately 200 kPa. Therefore, the maximum pressure that the Powasave pressure regulator assemblies will be required to regulate occurs at the last outlet along the 3rd span along radial line B, and is approximately 400 kPa.

The seven Powasave pressure regulator assemblies installed on the centre pivot system were tested over an operating pressure range of 200 kPa to 600 kPa. This was achieved by fitting a pressure gauge upstream of the float valve in Figure 5-7(A), and measuring the water level, or pressure head, in the Powasave pressure regulator for various upstream valve pressures. The results for the seven Powasave pressure regulator assemblies are presented in Table D1.

Table D1: Pressure head in pressure regulator assemblies for various upstream valve pressures

		Pressure Head (m)						
Sprinkler assembly		*#1*	*#2*	*#3*	*#4*	*#5*	*#6*	*#7*
Upstream valve pressure (kPa)	200	0.680	0.625	0.605	0.580	0.630	0.620	0.680
	300	0.695	0.635	0.620	0.585	0.635	0.645	0.690
	400	0.720	0.650	0.640	0.600	0.645	0.640	0.685
	500	0.740	0.660	0.645	0.620	0.660	0.660	0.700
	600	0.740	0.670	0.650	0.660	0.675	0.670	0.705
	Ave	**0.715**	**0.648**	**0.632**	**0.609**	**0.649**	**0.647**	**0.692**

The average pressure head measured in assemblies 2 through to 6 is calculated to be 0.637 m over the upstream valve pressure range of 200 kPa to 400 kPa. The marginal difference in the pressure heads measured in assemblies 2 to 6 is attributed to the variation of the flow characteristics through each of the 'off the shelf' float valves used in the pressure regulator assemblies, as shown in Figure 5-7(A).

The average pressure head measured in assemblies 1 and 7 is 0.704 m which is larger than the pressures in the other assemblies. These two Powasave sprinklers were designed for a reduced flow rate, for the reasons outlined at the end of section 5.4.2, and where therefore required to throttle the incoming flow of water through the float valve more so than the other assemblies; requiring a higher water level to do so.

D.2 Sprinkler design procedure

Seven Powasave sprinklers were installed on the last seven outlets of the third span of the Elsenburg centre pivot irrigation system. The procedure followed in designing the orifice sets and sprinkler pipes of the Powasave sprinklers is outlined in this section.

Specifications:

The sprinklers are required to apply an average water depth of 5 mm per pass at a centre pivot timer setting of t_s = 60%. The radial distance between outlets on the centre pivot main supply pipe is 3.35 m. The average elevation of the sprinklers is expected to be 4 m. The time averaged travel speed of the end-tower of the centre pivot system is measured to be 2 m/min.

For a desired Sauter mean droplet diameter ranging between 2.5 mm and 3 mm, an orifice nozzle diameter of between 1.3 mm and 1.6 mm is required. A radial sprinkler spray width of 4.1 m is selected to cover the 3.35 m distance between outlets and accommodate a 0.75 m spray overlap between consecutive Powasave sprinklers.

Using the single droplet trajectory model (SDTM), it is found that the radial spray range of 4.1 m can be achieved for an orifice nozzle with a diameter of 1.5 mm at a trajectory angle of 5°, an elevation of 4 m, and a pressure head of 0.6 m. The Powasave sprinkler design parameters and specifications are summarised in Table D2.

Table D2: Powasave sprinkler design parameters

Parameter	**Symbol**	***Units***	**Value**
Average application depth per pass	AAD	mm	5
Radial outlet spacing	r_{os}	m	3.35
Radial distance to 4th span A-frame tower	r_4	m	242
Radial distance to 3rd span A-frame tower	r_3	m	182
Radial spray width	r_{sw}	m	4.1
Average sprinkler elevation	z	m	4
Operating pressure head	ΔH	m	0.6
Orifice loss coefficient	k_o	-	0.5
Contraction coefficient	k_{cv}	-	1
Time averaged travel speed of 4th tower	u_{p_4}	m/min	2

Calculations:

(1) The time averaged velocity of the 3rd A-frame tower, on which the Powasave sprinklers are installed, is approximated as follows:

$$u_{p_3} = \frac{r_3}{r_4} u_{p_4} = \frac{182}{242}(2) = 1.5 \ \frac{\text{m}}{\text{min}} \tag{D.1}$$

(2) The total volume flow rate through a single Powasave sprinkler, required to apply an average application depth of 5 m over an annular band with a radial spray width of 4.1 m, is evaluated from equation (4.35):

$$n_{os}\dot{V}_{os} = AAD \cdot r_{sw} \cdot u_{p_3} = (5)(4.1)(1.5) = 24.6 \frac{\text{L}}{\text{min}} \tag{D.2}$$

(3) It was decided that four orifice sets would be used on a sprinkler pipe. The required volume flow rate through a single orifice set is then given by:

$$\dot{V}_{os} = \frac{24.6}{n_{os}} = \frac{24.6}{4} = 6.15 \frac{\text{L}}{\text{min}} \tag{D.3}$$

(4) A decision is now made as to the number of orifice nozzles comprising an orifice set. For a Sauter mean droplet diameter ranging between 2.5 mm and 3 mm, an orifice nozzle diameter between 1.3 mm and 1.6 mm should be used. An orifice nozzle diameter of 1.5 mm is selected, for which the Sauter mean droplet diameter is d_{32} = 2.85 mm. The flow rate through an orifice diameter is given by equation (4.25):

$$\dot{V}_{or} = \frac{\pi}{4} (k_{vc}\, d_{or})^2 \sqrt{\frac{2g\Delta H}{1 + k_o}} \tag{D.4}$$

The flow rate through an orifice set is given by the sum of the flow rates through each orifice nozzle, equation (4.26). For a constant orifice nozzle diameter:

$$\dot{V}_{os} = n_{or}\dot{V}_{or} \tag{D.5}$$

Therefore, the number of orifice nozzles in an orifice set is calculated by:

$$n_{or} = \frac{\dot{V}_{os}}{\dot{V}_{or}} = \left(\frac{6.15 \cdot (60)}{1000}\right)\left(\frac{\pi}{4}\left(\frac{1.5}{1000}\right)^2 \sqrt{\frac{2(9.81) \cdot (0.6)}{1.5}}\right)^{-1} = 20.7 \tag{D.6}$$

Therefore, from equation (D.6), 20.7 orifice nozzles are required in the orifice set; this is rounded up to 21. The volume flow rate for an orifice set with 21 orifice nozzles each with a diameter of 1.5 mm, operating at a pressure head of 0.6 m is given by:

$$\dot{V}_{os} = 21 \cdot \dot{V}_{or} = 21(60 \cdot 1000)\left(\frac{\pi}{4}\right)\left(\frac{1.5}{1000}\right)^2 \sqrt{\frac{2(9.81)(0.6)}{1.5}} \tag{D.7}$$

$$= 6.24 \frac{\text{L}}{\text{min}}$$

The orifice nozzle diameters of the spray trajectories falling in the overlap zone of consecutive sprinklers was later changed to d_{or} = 1.3 mm to reduce the application rates in that region and prevent over-watering. The diameters of the trajectories outside the overlap zone were adjusted to 1.6 mm. The final orifice set design consists of 10 orifice nozzles with diameters of 1.3 mm, and 11

orifice nozzles with diameters of 1.6 mm. The volume flow rate of the orifice set is calculated to be 6.29 L/min.

(5) The trajectory angles of the 21 orifice nozzles are selected such that the applied water is evenly distributed across the radial spray width of the orifice set. This is done using the SDTM and fixed scatter approximation to model the application rates at the soil surface. The trajectory angles are adjusted until an even distribution of trajectory streams, and hence application rate, is achieved across the radial spray width. The selected orifice diameters and trajectory angles are given in Table D3.

Table D3: Orifice nozzle diameters and trajectory angles

Orifice #	d_{or} (mm)	α (*Deg*)	Orifice #	d_{or} (mm)	α (*Deg*)	Orifice #	d_{or} (mm)	α (*Deg*)
1	1.3	5	8	1.6	289	15	1.6	243
2	1.3	345	9	1.6	281	16	1.6	235
3	1.3	334	10	1.6	274	17	1.3	225
4	1.3	324	11	1.6	270	18	1.3	216
5	1.3	315	12	1.6	266	19	1.3	206
6	1.6	305	13	1.6	259	20	1.3	195
7	1.6	297	14	1.6	289	21	1.3	175

The 21 orifice nozzles are distributed over 5 cross-sectional planes spaced 12.5 mm apart. The orifice sets are machined into a polycarbonate pipe with a diameter of 40 mm and length of 150 mm. Figure D2 shows the spacing of the orifice nozzles over the 5 cross-sectional planes and the trajectory angles relative to the transverse axis of the pipe.

The modelled application rates beneath overlapping orifice sets of consecutive Powasave sprinklers using the variable scatter approximation and fixed scatter approximation is shown in Figure D1. The spray plane is specified to be 3.36 m in length and is divided into 100 virtual compartments. The length of each compartment in the circumferential direction is taken to be 1 m. Therefore, the application rate profiles shown in Figure D1 are the application rates per meter in the circumferential direction. The application rate modelled using the fixed scatter approximation is relatively uniform across the spray width of the sprinkler.

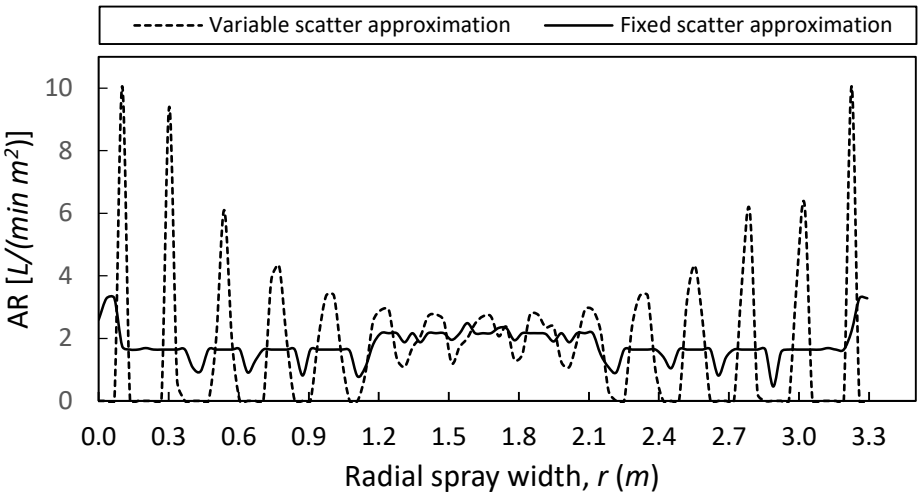

Figure D1: Modelled application rates beneath the trajectory streams of the orifice set

(6) The average application rate beneath the Powasave sprinkler is given by equation (4.32), as follows:

$$A\dot{A}R = \frac{n_{os}\dot{V}_{os}}{A_{ps}} \tag{D.8}$$

Where A_{ps} is the total spray area of the Powasave sprinkler given by the product of the radial spray width (r_{sw}) and the circumferential length of the sprinkler pipe (S_{sp_θ}):

$$A_{ps} = r_{sw} \cdot S_{sp_\theta} \tag{D.9}$$

The average application rates beneath the last few Nelson Spinner sprinklers on the third span of the centre pivot system, which were replaced with the Powasave sprinklers, are calculated as follows:

$$A\dot{A}R_{nel} = \frac{\dot{V}_{nel}}{A_{nel}} = \frac{22.93}{\frac{\pi}{4}(11^2)} = 0.24\frac{\text{mm}}{\text{min}} \tag{D.10}$$

The Nelson Spinner sprinkler volume flow rate ($\dot{V}_{nel}$) and throw diameters are shown in Table C5. To achieve a similar average application rate beneath the Powasave sprinkler, the length of the sprinkler pipe is calculated from equation (D.8) to be:

$$S_{sp_\theta} = \frac{n_{os}\dot{V}_{os}}{A\dot{A}R_{nel}r_{sw}} = \frac{6.24}{(0.24)(4.1)} = 6.3\text{ m} \tag{D.11}$$

A sprinkler pipe length of 6 m was selected for convenience as PVC pipes are typically supplied my manufacturers in 6 m lengths. The average application depth beneath a Powasave sprinkler with a 6 m long sprinkler pipe is given by equation (D.8) to be $A\dot{A}R = 0.25\frac{\text{mm}}{\text{min}}$.

D.3 Sprinkler flow rate measurements

The volume flow rates through each of the seven Powasave sprinkler assemblies were measured over a pressure range of 200 kPa to 600 kPa. The results are presented in Table D4. The average flow rate of sprinkler assemblies 2 to 6 is calculated to be 20.92 L/min. The average flow rate through sprinkler assemblies 1 and 7, which were fitted with only 3 orifice sets, is 16.32 L/min.

Table D4: Powasve sprinkler flow rate measurements

		Flow rate (L/min)						
Sprinkler assembly		*#1*	*#2*	*#3*	*#4*	*#5*	*#6*	*#7*
Valve upstream pressure (kPa)	200	15.59	21.63	20.33	20.35	20.93	19.97	16.41
	300	15.77	21.98	20.59	20.27	20.96	20.00	16.62
	400	15.96	21.99	21.02	20.67	20.71	20.27	16.84
	500	16.19	21.17	20.77	21.51	21.00	20.34	16.58
	600	16.42	21.74	21.63	21.99	20.76	20.36	16.76
	Ave	**15.99**	**21.70**	**20.87**	**20.96**	**20.87**	**20.19**	**16.64**

The average measured flow rate through spray sprinklers 2 to 6 deviate from the design flow rate by 15%. The difference between the design flow rate of 24.6 L/min and the average measured flow rate of 20.92 L/min is 3.68 L/min. For a sprinkler, fitted with 4 orifice sets, each having 21 orifice nozzles, the deviation in the flow rate through each orifice nozzle is 3.68/(84) = 0.0438 L/min. For an average orifice nozzle diameter of 1.5 mm, the change in pressure head required to produce a 0.0438 L/min change in flow rate can be obtained from equation (D.4):

$$\Delta H = \left(\frac{4 \cdot \Delta \dot{V}_{or}}{\pi (k_{vc} d_{or})^2}\right)^2 \left(\frac{1 + k_o}{2g}\right) \tag{D.12}$$

$$= \left(\frac{4 \cdot 0.0438}{\pi (0.0015)^2} \cdot \frac{1}{60(1000)}\right)^2 \left(\frac{1.5}{2 \cdot 9.81}\right) = 0.013 \text{ m}$$

Therefore, an average pressure head reduction of 0.013 m is experienced by each orifice nozzle. Using the single droplet trajectory model the change in the spray range of an orifice nozzle with a diameter of 1.5 mm, at an elevation of 4 m, for a change in pressure head of 0.013 m from 0.6 m to 0.587 m is small; approximately 20 mm.

The Powasave sprinklers are designed for an overlap of 0.75 m, and therefore the marginal variation in pressure head experienced by the orifice set outlets along the sprinkler pipe will not affect the overlap significantly. A uniform spray distribution should be maintained beneath the sprinkler. However, the application rates and average application depth applied beneath the sprinkler will change somewhat. But since the objective of the investigation is to measure the application uniformity beneath the Powasave sprinkler, a variation in the volume flow rates will not obscure the results; provided the spray distribution profile does not change drastically, which in this case it does not.

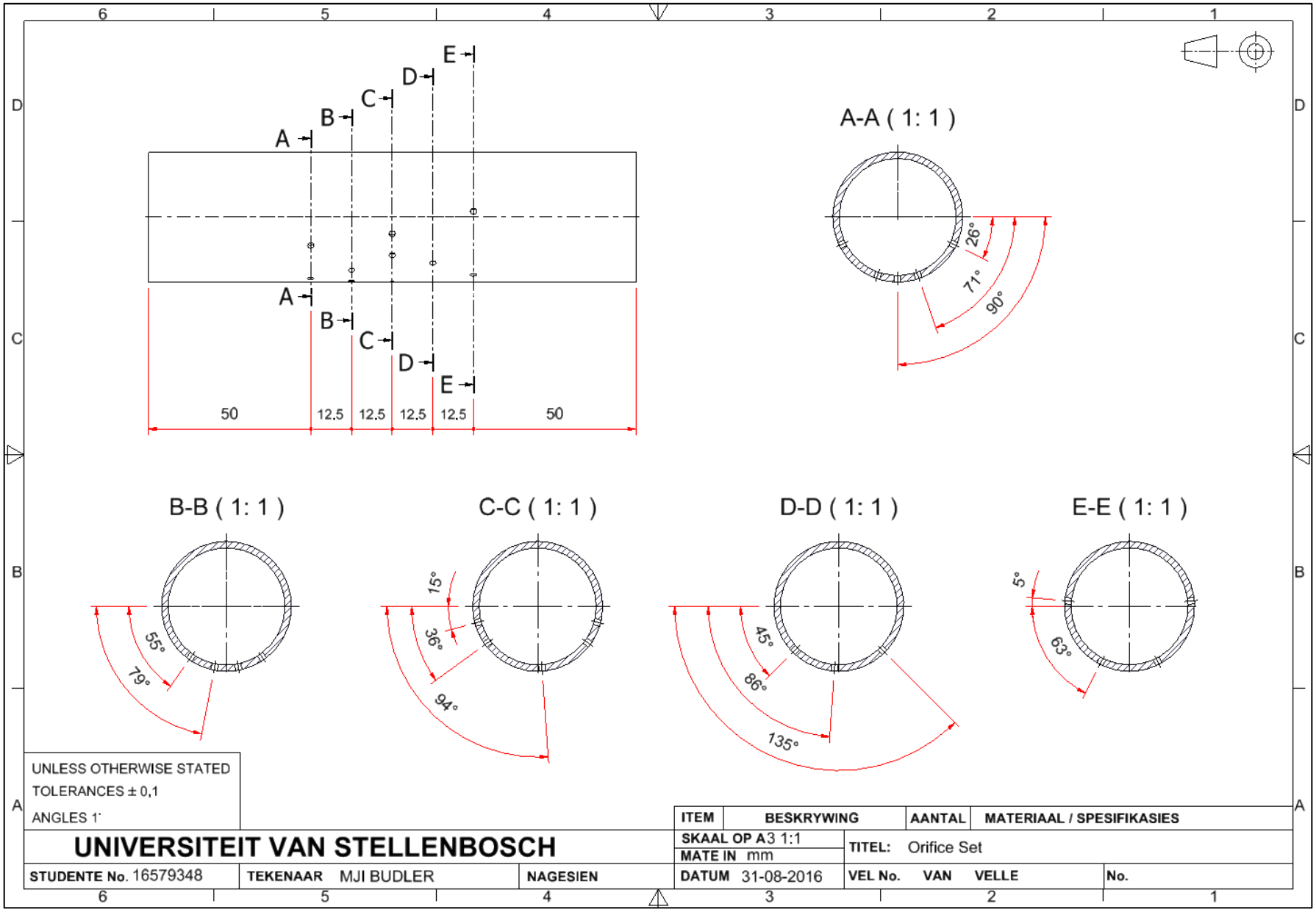

Figure D2: Orifice set manufacturing drawing

Appendix E Round collector vs rectangular collector

There are challenges in measuring the water distribution of a sprinkler with discrete trajectory streams. Consider the two buckets placed in the spray regions of a sprinkler with a random spray scatter, and a sprinkler with discrete spray streams, as shown in Figure E1.

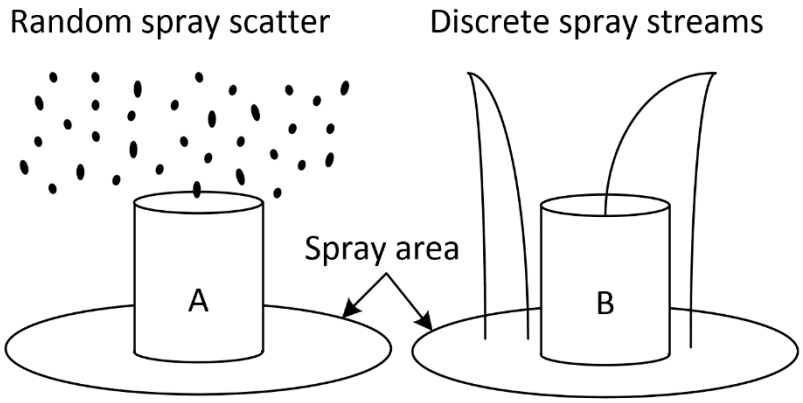

Figure E1: Random sprinkler spray versus discrete sprinkler trajectories

No matter where bucket A is positioned in the spray area, the random nature of the spray scatter will ensure that the bucket will catch a representative portion of the volume of water applied in the spray area. The application depth applied over the spray area can be estimated based on the application depth measured in the bucket.

However, the positioning of bucket B in the spray area under a sprinkler with discrete spray trajectories will influence the volume proportion caught by the bucket, and hence estimating the application depth over the entire spray region based on the measurements in bucket B may produce misleading results. Depending on the buckets position, as illustrated in Figure E1, it may catch one, two, or even three streamlets.

Moreover, the shape of the bucket also influences the volume of water caught, as illustrated in Figure E2-(A). As the discrete spray streams of a sprinkler pass over a round collector, the exposure time of the bucket to the stream is dependent on where the stream crosses the bucket. Maximum exposure will occur if the stream crosses over the centre of the bucket, but will be diminished if the stream crosses towards the edges of the bucket. A rectangular collector on the other hand has a constant exposure time to the sprinkler stream regardless of where the stream crosses the collector; provided the collector is placed perpendicular to the direction of travel of the stream.

The size of the collector also influences the distribution profile of a sprinkler with discrete streams. Consider the four water streams being collected in four rectangular collectors spaced directly alongside each other in Figure E2-(B). If the sprinkler streams are evenly distributed, and each fall into a collector, then the distribution profile is flat, and would be considered uniform with a CU and DU of 100%. In this case, increasing the size of the collector does not influence the distribution profile, as illustrated by the top graph in Figure E2-(B).

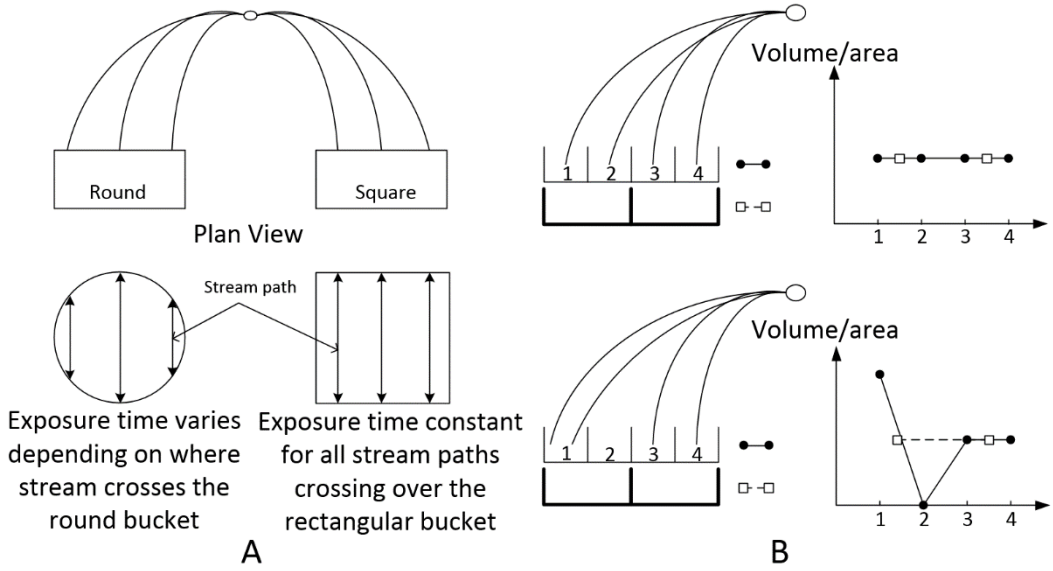

Figure E2: Difficulties in measuring discrete trajectories

However, if the sprinkler streams are not evenly spaced and the second stream hits the first collector, then the distribution profile becomes saw-toothed, as illustrated by the lower graph in Figure E2-(B). The distribution is no longer uniform, and the CU and DU would be less than 100%. However, if the collector size is increased, the distribution profile is once again flat with a CU and DU of 100%.

Ultimately, if one increased the collector size sufficiently, the distribution profile under any sprinkler can be made to appear uniform. However, individual plants in this spray area may in fact be experiencing over- or under-watering. The question is what collector size is acceptable to reflect a distribution profile that is not misleading?

The answer depends on what is considered a sufficient resolution for which a plant will not experience water stress taking into account the lateral water redistribution that takes place in the first few layers of the topsoil, and the reach of the plant root system. For instance, suppose sufficient lateral water redistribution occurs on clay-loam soils such that a plant can access irrigated water in a 300 mm radius around it. In such a case, a collector width of 300 mm is a sufficient resolution at which the distribution profile can be presented without overlooking the possibility of plant water stress.

Conventionally, the application uniformity beneath a sprinkler package on a centre pivot is measured using intermittently spaced round collectors. However, for this study a single row of intermittently spaced collectors is felt to be insufficient to provide an accurate measure of the application uniformities beneath the Powasave sprinkler and Sprayhead sprinkler; both of which have discrete trajectory streams. Therefore, a matrix of continuously packed rectangular collectors are used to measure the application uniformity beneath the sprinklers, the details of which are discussed in sections 5.6 of this document.

Appendix F Distribution test results

F.1 Spinner sprinkler zone distribution results

The 3-dimensional distribution profile of the Spinner sprinkler in zone A3 is shown in Figure F1. The Spinner sprinkler exhibits a relatively flat uniform distribution profile. The maximum and minimum water volumes recorded over the matrix of collectors is 180 mL and 115 mL respectively.

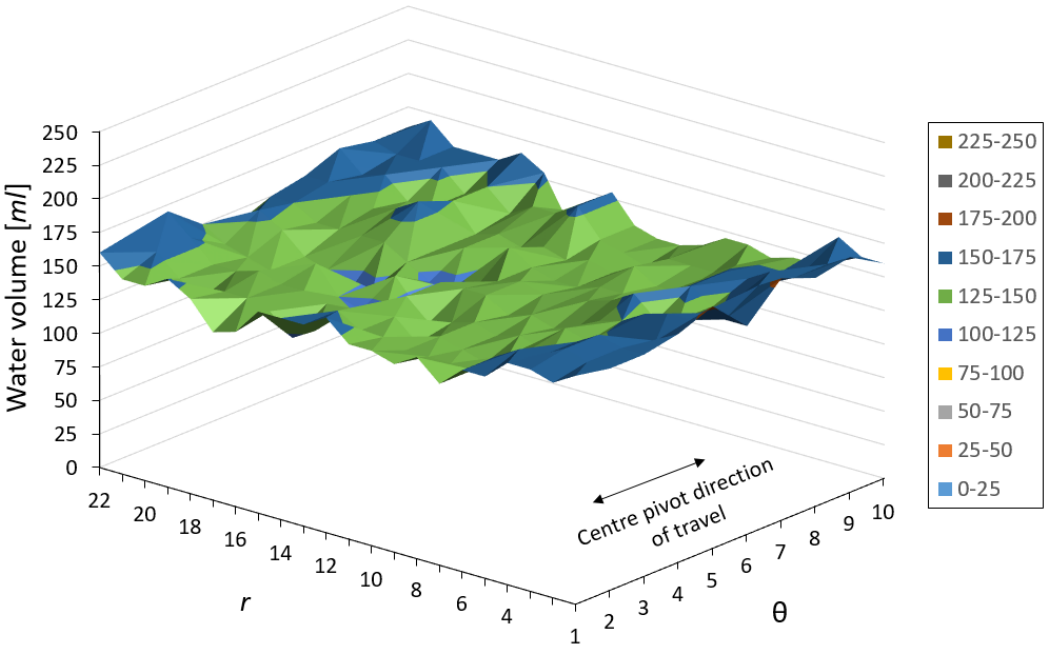

Figure F1: Zone A3 Spinner sprinkler distribution profile

The distribution parameters of the Spinner sprinkler evaluated over the matrix of collectors is presented in Table F1. The spinner sprinkler proves to have an excellent DU and CU of 89.1% and 92.3% respectively. The AAD applied over the matrix of collectors is 4.82 mm of water.

Table F1: Zone A3 Spinner sprinkler matrix distribution parameters

Min AD [mm]	*Max AD* [mm]	*AAD* [mm]	*LQD* [mm]	*DU* [%]	*CU* [%]
3.83	6.00	4.82	4.3	89.11	92.32

Figure F2 shows the AAD, LQD, and max AD in the radial direction beneath the spinner sprinkler. The profile appears to take on a concave shape. The concave profile may be attributed to Spinner sprinklers adjacent to zone 3 that were suspended too close to the ground, as shown in Figure 6-2, which reduced the effective spray range of those sprinklers; in turn affecting the application rates over the centre of zone 3.

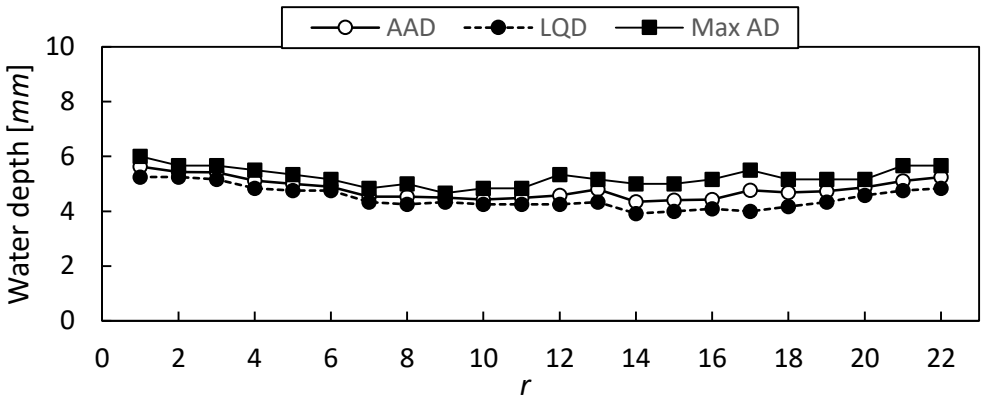

Figure F2: Zone A3 Spinner sprinkler AAD, LQD and max AD in radial direction

Despite the concave trend in the distribution profile there is little variation in the AAD, LQD, and maximum AD in the radial direction. The Spinner sprinkler exhibits excellent application consistency in the radial direction.

Figure F3 show the AAD, LQD and max AD in the circumferential direction. The AAD proves to be uniform, further illustrating the consistency of water application in the circumferential direction. The marginal variation between the maximum AD and the AAD is due to the concave profile in the radial direction.

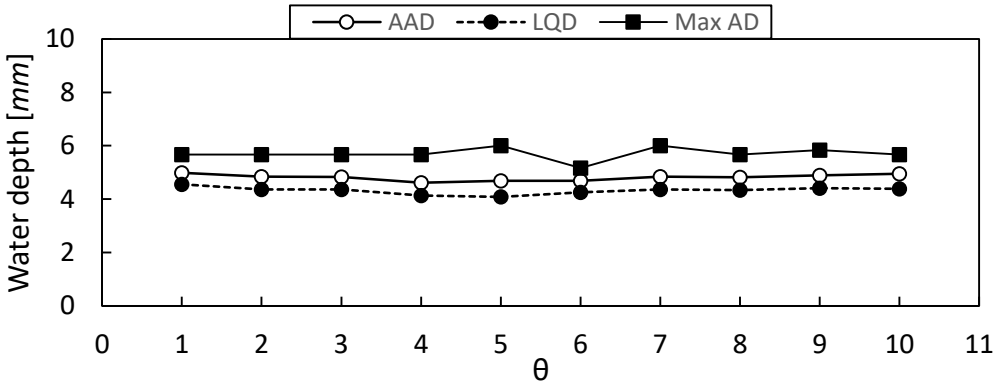

Figure F3: Zone A3 Spinner sprinkler AAD, LQD and max AD in circumferential direction

F.2 Powasave sprinkler zone distribution results

The rectangular collector zone distribution results measured beneath the Powasave sprinklers in zones B2 and C2 are presented.

Zone B2

The water distribution profile of the Powasave sprinklers in zone B2 is shown in Figure F4. The maximum and minimum volumes measured across the matrix of collectors is 400 mm and 35 mm respectively.

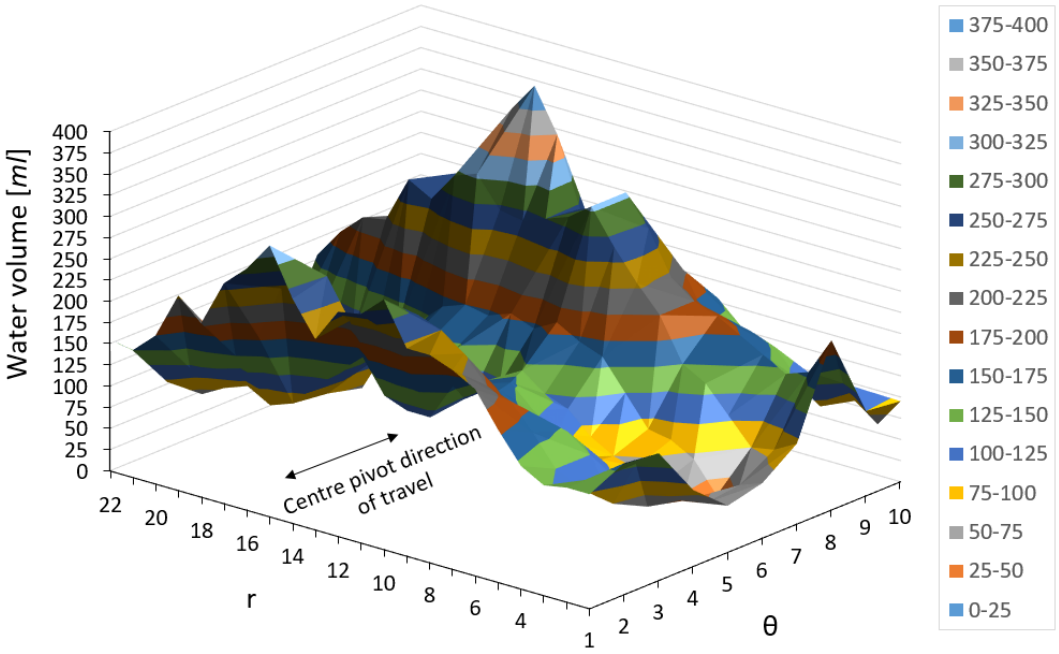

Figure F4: Zone B2 Powasave sprinkler distribution profile

The distribution parameters evaluated over the matrix of collectors is presented in Table F2. The DU and CU prove to be poor at 57.8% and 64.3% respectively. There is a substantial variation between the maximum and minimum AD measured over the matrix, and would result in over- and under-watering in regions beneath the sprinkler.

Table F2: Zone B2 Powasave sprinkler matrix distribution parameters

Min AD [mm]	*Max AD* [mm]	*AAD* [mm]	*LQD* [mm]	*DU* [%]	*CU* [%]
1.17	13.33	4.69	2.7	57.79	64.33

The AAD, LQD and max AD in the radial direction is shown in Figure F5. It is evident the AAD profile is non-uniform in the radial direction, with a variation of approximately 4.3 mm between the least-watered and most-watered sections

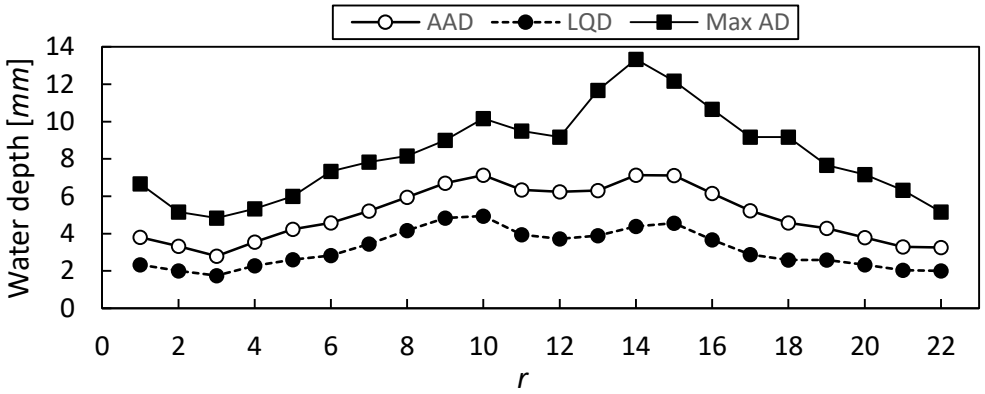

Figure F5: Zone B2 Powasave sprinkler AAD, LQD and max AD in radial direction

The AAD, LQD and the max AD in the circumferential direction is shown in Figure F6, and exhibits a similar non-uniform peak-trough cycle observed in zone A2.

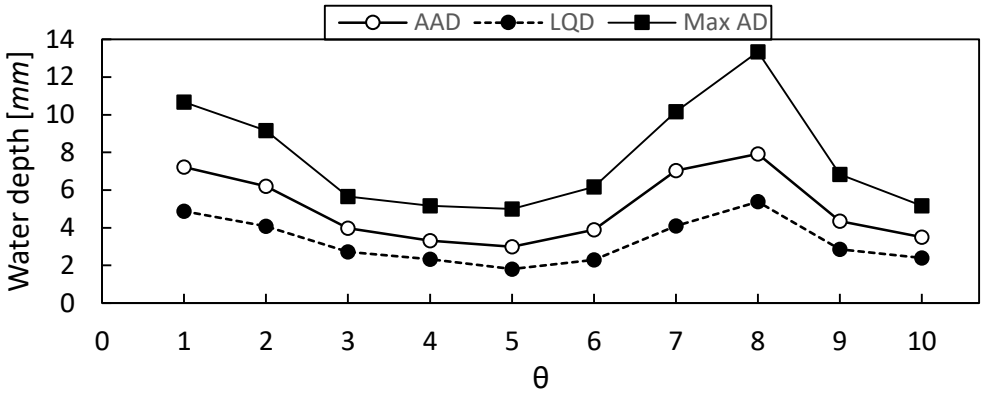

Figure F6: Zone B2 Powasave sprinkler AAD, LQD and max AD in circumferential direction

Zone C2

The water distribution profile measured beneath the Powasave sprinklers in Zone C2 is shown in Figure F7. The maximum and minimum volumes recorded over the matrix of collectors is 370 mL and 50 mL respectively.

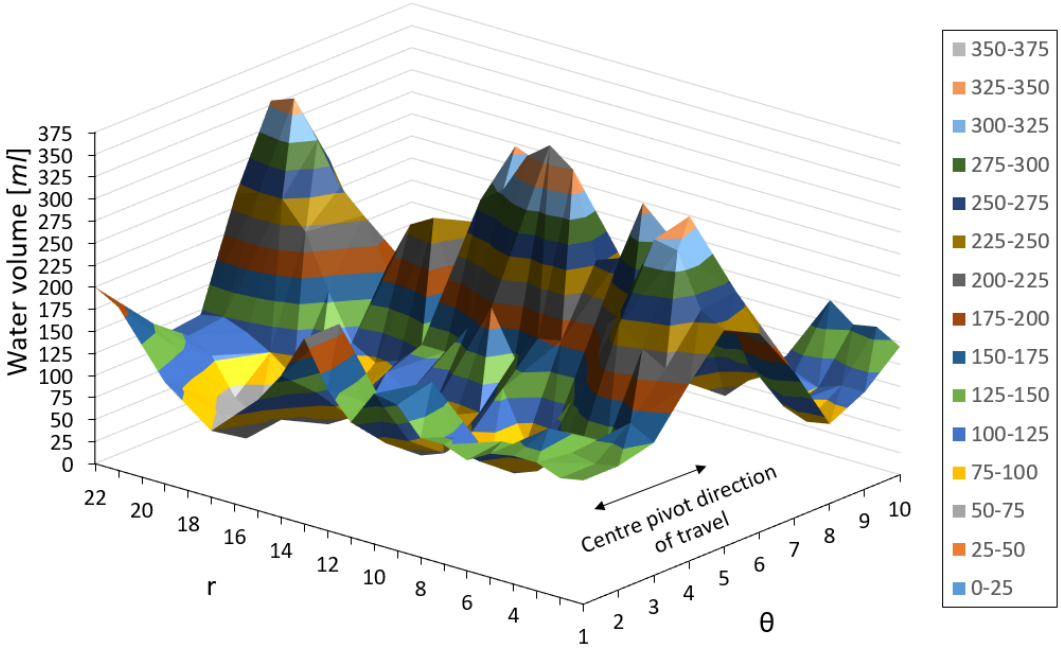

Figure F7: Zone C2 Powasave sprinkler distibution profile

The distribution indicators, evaluated over the matrix of collectors, are given in Table F3. The DU and CU are poor at 55.6% and 56.3%. There is also a significant variation in the minimum and maximum AD measured over the matrix of collectors.

Table F3: Zone C2 Powasave Sprinkler matrix distribution indicators

Min AD [mm]	*Max AD* [mm]	*AAD* [mm]	*LQD* [mm]	*DU* [%]	*CU* [%]
1.67	12.33	4.79	2.70	55.56	56.32

The AAD, LQD, and maximum AD in the radial direction are shown in Figure F8. The AAD is non-uniform, with a variation of approximately 3.8 mm between the least-watered and most-watered sections. There is also a significant variation between the AAD and the maximum AD.

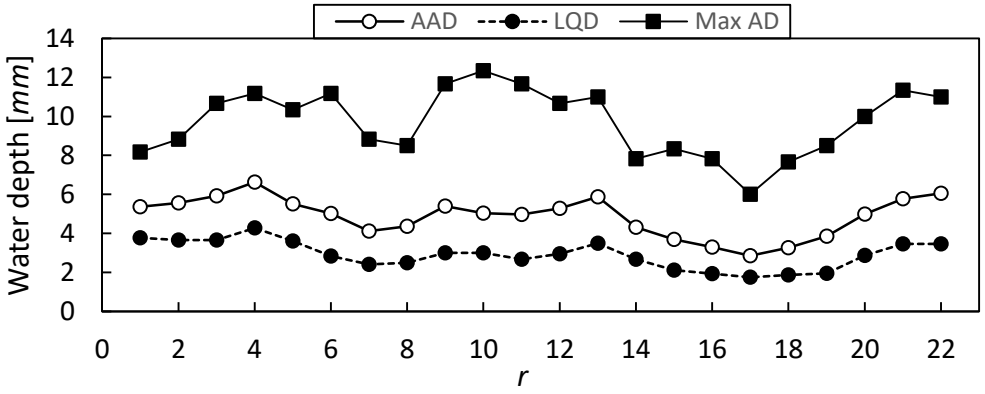

Figure F8: Zone C2 Powasave sprinkler AAD, LQD and max AD in radial direction

The AAD, LQD and max AD in the circumferential direction are shown in Figure F9. A peak is clearly evident in the distribution profile. The peak in the AAD profile is more than double the amplitude of the troughs.

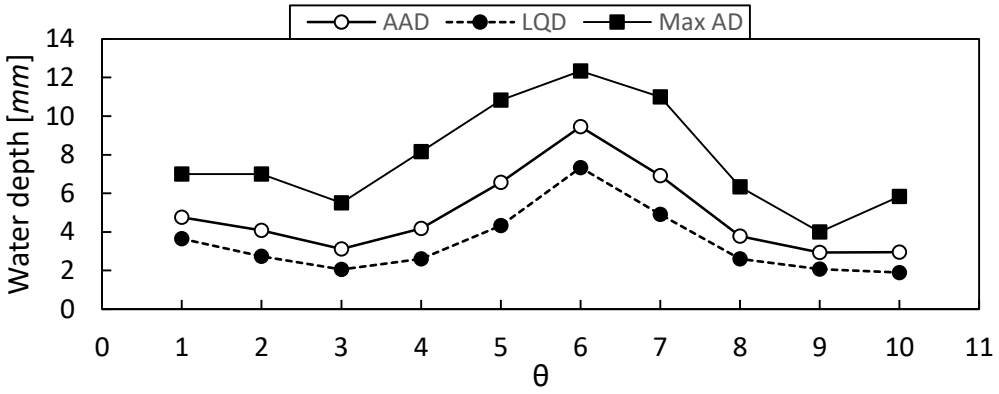

Figure F9: Zone C2 Powasave sprinkler AAD, LQD and max AD in circumferential direction